Scattering properties of quantum degenerate atomic gases

-

Streueigenschaften von quanten-entarteten atomaren Gasen

Diplomarbeit
von

Alexander Janisch

30. September 2008 – 30. September 2009

| Hauptberichter: | Prof. Dr. sci. nat. Hans-Peter Büchler |
| Mitberichter: | Prof. Dr. rer. nat. Ulrich Weiß |

ii

Alexander Janisch
Gaisburgstrae 16
70182 Stuttgart

Hiermit erkläre ich an Eides statt, dass ich die von mir vorgelegte Arbeit selbstständig verfasst habe, dass ich die verwendeten Quellen, Internet-Quellen und Hilfsmittel vollständig angegeben habe und dass ich die Stellen der Arbeit – einschließlich Tabellen, Karten und Abbildungen –, die anderen Werken oder dem Internet im Wortlaut oder dem Sinn nach entnommen sind, auf jeden Fall unter Angabe der Quelle als Entlehnung kenntlich gemacht habe.

Stuttgart, den 25. September 2009

(Unterschrift)

_____

Alexander Janisch

Contents

Contents

1. Introduction

In recent years, there have been lots of interests in strongly correlated bosonic and fermionic systems. There are many such quantum systems, which show particular behaviour. For example superconductors are characterized by exactly zero electrical resistance and the exclusion of the interior magnetic field.

Many of these systems can be described by the Bose Hubbard or the Hubbard model, which are the simplest models, where one can investigate quantum phases, e.g. the Mott-insulator or the superfluid phase [1], [2], [3] and [4].

In 1998 Dieter Jaksch *et al.* [5] proposed to apply the Bose Hubbard model onto ultra-cold boson atoms, trapped in optical lattices. They showed, that the dynamics of such systems is well described by the Bose Hubbard Hamiltonian. These dynamics are similar to the dynamics of electrons in the periodic structure of a crystalline solid state. Therefore the band theory also applies onto ultra-cold atoms in optical lattices. As a result, optical lattices link atomic physics and quantum optics with solid state physics.

Ultra-cold atoms in optical lattices can be used as a testbed for modern condensed matter theories. These systems' big advantage is their high tunability. By adjusting the laser beams' intensities, one is able to change the interaction matrix element U and the hopping rate J, which are the only two parameters of the Bose Hubbard Hamiltonian. Besides, it is also possible to realize one- and two-dimensional systems by turning off the hopping along one or two directions, by increase the laser intensity in these directions. Other advantages of optical lattices are the absence of defects and lattice vibrations, where atoms could undergo scattering.

Novel and exotic many body quantum phases have been predicted and are now to be realized in such quantum systems in experiments.

This diploma work gives a overview over the scattering properties of quantum degenerate gases, trapped in optical lattices and introduces a novel method to create artificial interactions. The interaction of such a gas are usually dominated by two particle collisions, due to the low density and the short ranged interaction potential acting between the particles. In the following the main emphasis is on these two particle scattering processes. First, we give a summary of basic concepts of quantum scattering theory, tuning the s-wave scattering length with Feshbach resonances [6] and optical lattices [7]. Second, we give a short introduction of the Bose Hubbard model applied on ultra-cold boson gases in optical lattices, introduced by Jaksch *et al.* [5]. Than, we will recapitulate the two particle problem of the Bose Hubbard Hamiltonian, first investigated by Winkler *et al.* [8]. Afterwards we work out, how the change of the scattering length by a Feshbach resonance influences the on-site interactions in an optical lattice. Finally we propose a model system, which allows to implement particular artificial nearest interactions to the recent system.

1. Introduction

We assume the occurrence of novel and exotic quantum phases, e.g. a checkerboard supersolid phase [9].

2. Basics Concepts

2.1. Scattering theory

In the following the basic concepts of scattering theory, with main emphasis on interaction in ultra-cold quantum degenerate dilute gases, will be reviewed. The two-particle problem can be reduced to an effective one particle problem by introducing center-of-mass and relative coordinates

$$\text{relative coordinate:} \qquad \boldsymbol{r} := \boldsymbol{r}_2 - \boldsymbol{r}_1 \qquad (2.1)$$

$$\text{center of mass-motion coordinate:} \qquad \boldsymbol{R} := \frac{m_1\boldsymbol{r}_1 + m_2\boldsymbol{r}_2}{m_1 + m_2} \qquad (2.2)$$

$$\text{reduced mass:} \qquad \mu := \frac{m_1 m_2}{m_1 + m_2}. \qquad (2.3)$$
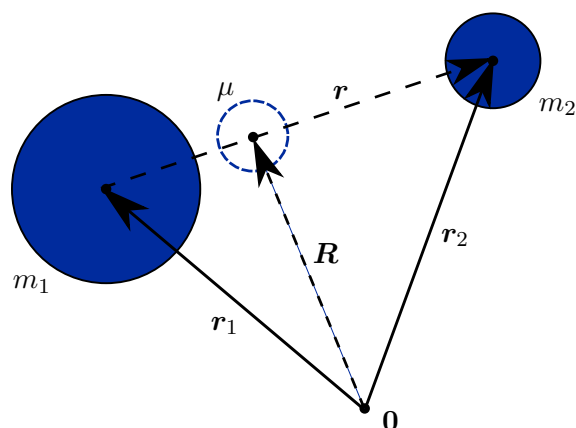
Figure 2.1.: **Center of mass system**

The equation of motion for the effective one particle problem is given by

$$\mu\ddot{r} = \frac{\mathrm{d}}{\mathrm{d}\boldsymbol{r}}V(\boldsymbol{r}), \qquad (2.4)$$

with $V(\boldsymbol{r})$ the interaction potential between the two particles.

2.1.1. Quantum scattering theory

Scattering between particles of the atomic regime has to be discussed different from classical scattering theory. Due to the Heisenberg uncertainty principle, position and

momentum of particles cannot be measured precisely at the same time. There is no concept of a trajectory like in classical theories, and thus quantum scattering has to be described with the tools of quantum mechanics. The kinetics of the scattering process are characterized by the initial wave vector $\boldsymbol{k}_0 = \boldsymbol{p}_0/\hbar = p_0/\hbar\boldsymbol{e}_x$ and the corresponding energy $E_0 = \hbar^2\boldsymbol{k}_0^2/2m$. Particles, represented by a wave packet, interact with a target, represented by an interaction potential. The particles wave packet is given by

$$\Psi\left(\boldsymbol{r}, t\right) = \int \frac{\mathrm{d}^3\boldsymbol{k}}{2\pi}\hat{\psi}\left(\boldsymbol{k}\right)\mathrm{e}^{\mathrm{i}\left(\boldsymbol{k}\boldsymbol{r}-\omega(\boldsymbol{k})t\right)} \tag{2.5}$$

with $\hat{\psi}\left(\boldsymbol{k}\right)$ the amplitude and $\omega(\boldsymbol{k}) = \hbar\left|\boldsymbol{k}\right|^2/2m$ the free dispersion relation. Since wave packets are linear super-positions of plane waves, the calculations can be performed for one wavelength. In the following only elastic scattering at a spherical symmetric potential is assumed. The scattering process can be divided into three parts. Long before the scattering the particle is in large distance and out of the influence of the target. The wave-packet is a solution of the free Hamilton operator

$$\hat{\mathrm{H}}_0\phi_0\left(\boldsymbol{r}\right) = -\frac{\hbar^2}{2m}\nabla^2\phi_0\left(\boldsymbol{r}\right) = E_0\phi_0\left(\boldsymbol{r}\right), \tag{2.6}$$

When the particle comes into the range of the interaction potential, one has to solve the Schrödinger equation

$$\left[-\frac{\hbar^2}{2m}\nabla^2 + V\left(\boldsymbol{r}\right)\right]\phi\left(\boldsymbol{r}\right) = E_0\phi\left(\boldsymbol{r}\right). \tag{2.7}$$

Parts of the incoming wave-packet are scattered, but there are also parts going through unaffected. Therefore the resulting solution consists of an unscattered and a scattered part.

$$\phi\left(\boldsymbol{r}\right) = \phi_0\left(\boldsymbol{r}\right) + \phi_s\left(\boldsymbol{r}\right), \tag{2.8}$$

with $\phi_0\left(\boldsymbol{r}\right) = \mathrm{e}^{\mathrm{i}k_0x}$ is the incident plane wave and $\phi_s\left(\boldsymbol{r}\right)$ the scattered outgoing part. In the far field $\left(\boldsymbol{r} \to \infty\right)$ reduces to a spherical wave of the form

$$\phi_s\left(\boldsymbol{r}\right) \sim f\left(\vartheta\right)\frac{\mathrm{e}^{\mathrm{i}\boldsymbol{k}\boldsymbol{r}}}{r}, \tag{2.9}$$

with $f\left(\vartheta\right)$ the scattering amplitude, where ϑ is the angle between $\boldsymbol{k}_0$ and $\boldsymbol{k}$ [fig. 2.2]. $f\left(\vartheta\right)$ contains all information about the interaction potential.

Long after the scattering and in large distance to the target again, $\phi\left(\boldsymbol{r}\right)$ has to be an eigenfunction of the free Hamilton operator again.

2.1.2. Integral representation of the scattering problem and Lippmann-Schwinger-equation

To determine $\phi\left(\boldsymbol{r}\right)$ and $f\left(\vartheta\right)$ it is necessary to solve equation (2.7) or

$$\left[\frac{\hbar^2}{2m}\nabla^2 + E_0\right]\phi\left(\boldsymbol{r}\right) = V\left(\boldsymbol{r}\right)\phi\left(\boldsymbol{r}\right) \tag{2.10}$$
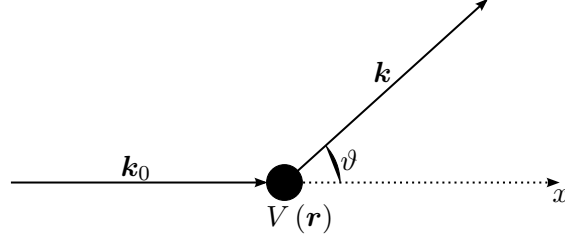
Figure 2.2.: An incident plane wave with wavevector $\boldsymbol{k}_0 = k_0 \boldsymbol{e}_x$ is scattered by the potential $V(\boldsymbol{r})$. The scattered wave has the wavevector $\boldsymbol{k}$ and the scattering amplitude $f(\vartheta)$

respectively. With the Green's function formalism one obtains the Lippmann-Schwinger-equation[1]

$$\phi(\boldsymbol{r}) = \phi_0(\boldsymbol{r}) + \int \mathrm{d}^3 r' \, G(\boldsymbol{r} - \boldsymbol{r}') \, V(\boldsymbol{r}') \, \phi(\boldsymbol{r}') , \qquad (2.11)$$

with $G(\boldsymbol{r} - \boldsymbol{r}')$ the Green's function defined by

$$\left[\frac{\hbar^2}{2m} \Delta_r + E_0 \right] G(\boldsymbol{r} - \boldsymbol{r}') = \delta(\boldsymbol{r} - \boldsymbol{r}') . \qquad (2.12)$$

The Green's function can be determined by Fourier transformation

$$G(\boldsymbol{r} - \boldsymbol{r}') = \frac{1}{(2\pi)^3} \int \mathrm{d}^3 q \, \mathrm{e}^{\mathrm{i}\boldsymbol{q}\boldsymbol{r}} G(\boldsymbol{q}) \qquad (2.13)$$

$$\delta(\boldsymbol{r} - \boldsymbol{r}') = \frac{1}{(2\pi)^3} \int \mathrm{d}^3 q \, \mathrm{e}^{\mathrm{i}\boldsymbol{q}\boldsymbol{r}} . \qquad (2.14)$$

Inserting this in equation (2.12) and transposing, leads to

$$\int \mathrm{d}^3 q \, \mathrm{e}^{\mathrm{i}\boldsymbol{q}\boldsymbol{r}} \left\{ G(\boldsymbol{q}) \left[E_0(\boldsymbol{k}_0) - \epsilon(\boldsymbol{q}) \right] - 1 \right\} = 0 \qquad (2.15)$$

with $\epsilon(\boldsymbol{q}) = \frac{\hbar^2 q^2}{2m}$ a particle's dispersion relation in free space. Inverse transformation of $G(\boldsymbol{q})$ yields

$$G(\boldsymbol{r} - \boldsymbol{r}') = \frac{1}{(2\pi)^3} \int \mathrm{d}^3 q \frac{\mathrm{e}^{\mathrm{i}q(\boldsymbol{r}-\boldsymbol{r}')}}{E_0(\boldsymbol{k}_0) - \epsilon(\boldsymbol{q})} = -\frac{m \mathrm{e}^{\pm \mathrm{i}k_0 |\boldsymbol{r}-\boldsymbol{r}'|}}{2\pi \hbar^2 |\boldsymbol{r} - \boldsymbol{r}'|} , \qquad (2.16)$$

two linear independent solutions, but since the scattered solution has to be an outgoing wave, only the solution with the positive exponent is physically reasonable. The solution with the minus would represent an incoming wave. Inserting the physical solution in (2.11) leads to the solution

$$\phi(\boldsymbol{r}) = \phi_0(\boldsymbol{r}) - \int \mathrm{d}^3 r \frac{m \mathrm{e}^{+\mathrm{i}k_0 |\boldsymbol{r}-\boldsymbol{r}'|}}{2\pi \hbar^2 |\boldsymbol{r} - \boldsymbol{r}'|} V(\boldsymbol{r}') \, \phi(\boldsymbol{r}') . \qquad (2.17)$$

---

[1]Derivation in [A]

In the limit $r' \gg r$ the following approximations can be performed:

$$\frac{1}{|\boldsymbol{r} - \boldsymbol{r}'|} \approx \frac{1}{r} \tag{2.18}$$

$$|\boldsymbol{r} - \boldsymbol{r}'| \approx \sqrt{r'^2 + r^2 - 2\boldsymbol{r} \cdot \boldsymbol{r}'} \approx r \left(1 - \frac{2\boldsymbol{r} \cdot \boldsymbol{r}'}{r^2}\right)^{1/2}$$

$$\approx r - \frac{2\boldsymbol{r} \cdot \boldsymbol{r}'}{r} \approx r - e_{\boldsymbol{r}} \cdot \boldsymbol{r}' \tag{2.19}$$

This leads to the asymptotic solution:

$$\phi(\boldsymbol{r}) = \phi_0(\boldsymbol{r}) - \frac{\mathrm{e}^{\mathrm{i}k_0 r}}{r} \frac{m}{2\pi\hbar^2} \int \mathrm{d}^3\boldsymbol{r} \ \mathrm{e}^{-\mathrm{i}k_0(\boldsymbol{r}' \cdot e_r)} V(\boldsymbol{r}') \phi(\boldsymbol{r}') . \tag{2.20}$$

In comparison to equation (2.8) the prefactor of the second term can be identified as the scattering amplitude.

$$f(\vartheta) = -\frac{m}{2\pi\hbar^2} \int \mathrm{d}^3\boldsymbol{r}' \ \mathrm{e}^{-\mathrm{i}k(\boldsymbol{r}' \cdot e_r)} V(\boldsymbol{r}') \phi(\boldsymbol{r}') \tag{2.21}$$

2.1.3. Born expansion and Born approximation

The formal solution (2.17) can be found with the iterative ansatz called Born expansion.

$$\phi(\boldsymbol{r}) = \sum_{n=0}^{\infty} \phi^{(n)}(\boldsymbol{r}) \tag{2.22}$$

with $\phi^{(0)}(\boldsymbol{r}) = \mathrm{e}^{\mathrm{i}kx}$ and $\phi^{(n+1)}(\boldsymbol{r}) = -\frac{m}{2\pi\hbar^2} \int \mathrm{d}^3\boldsymbol{r} \ \frac{\mathrm{e}^{\mathrm{i}k|\boldsymbol{r}-\boldsymbol{r}'|}}{|\boldsymbol{r}-\boldsymbol{r}'|} V(\boldsymbol{r}') \phi^{(n)}(\boldsymbol{r}')$. Expanding up to the first order in $V(\boldsymbol{r}')$ is called the first Born approximation:

$$\phi^{(1)}(\boldsymbol{r}) = \mathrm{e}^{\mathrm{i}kx} - \frac{m}{2\pi\hbar^2} \int \mathrm{d}^3\boldsymbol{r} \ \mathrm{e}^{\mathrm{i}k\boldsymbol{r}'(e_r - e_x)} V(\boldsymbol{r}') \tag{2.23}$$

2.1.4. Partial wave method

For a spherically symmetric interaction potential the Hamilton operator of the system $\hat{H} = -\frac{\hbar^2}{2m}\nabla^2 + V(\boldsymbol{r})$ commutes with $\hat{L}^2$ and $\hat{L}_x$, where $\hat{L}$ is the angular momentum operator. Therefore the solution of the system can be expanded in angular momentum eigenfunctions with azimuthal symmetry, the spherical harmonics

$$Y_{\ell 0}(\vartheta) = \sqrt{\frac{2\ell + 1}{4\pi}} P_\ell(\cos\vartheta) , \tag{2.24}$$

from which follows the expanded solution

$$\phi(\boldsymbol{r}) = \sum_{\ell=0}^{\infty} \frac{u_\ell(\boldsymbol{r})}{r} P_\ell(\cos\vartheta) . \tag{2.25}$$

Inserting this expansion in the Schrödinger equation (2.7) yields the following differential equation for the expansion coefficient $u_\ell(\boldsymbol{r})$:

$$u_\ell''(\boldsymbol{r}) + \left[\frac{2m}{\hbar^2}E_0 - \frac{2m}{\hbar^2}V(\boldsymbol{r}) - \frac{\ell(\ell+1)}{r^2}\right]u_\ell(\boldsymbol{r}) = 0 \tag{2.26}$$

In the special case $V = 0$, equation (2.26) is similiar to the spherical Bessel differential equation and the solution is given by

$$u_\ell^{(0)}(\boldsymbol{r}) = \mathrm{i}^\ell(2\ell+1)\,r j_\ell(kr), \tag{2.27}$$

where $j_\ell(z) = (-z)^\ell\left(\frac{1}{z}\frac{\mathrm{d}}{\mathrm{d}z}\right)^\ell\frac{\sin z}{z}$ is the Bessel function, whose asymptotic behaviour for $kr \gg \ell$ is

$$u_\ell(\boldsymbol{r}) \sim \frac{1}{k}\mathrm{i}^\ell(2\ell+1)\sin\left(kr - \frac{\ell\pi}{2}\right). \tag{2.28}$$

In the limit $kr \to \infty$ the solution of the scattering problem has to be also a solution of the free Schrödinger equation and since $V(\boldsymbol{r})$ is short ranged, its influence leads to a phase shift in the free solution only

$$u_\ell(\boldsymbol{r}) \sim \alpha_\ell \sin\left(kr - \frac{\ell\pi}{2} + \delta_\ell\right). \tag{2.29}$$

δ_ℓ is called the scattering phase of the ℓth partial wave and is characteristic for the interaction potential $V(\boldsymbol{r})$. It is a function of $\boldsymbol{k}$ and thus a function of the energy.

With equation (2.29) and by keeping in mind, that only the outgoing part of the solution is affected by the interaction potential, ansatz (2.25) can be rewritten:

$$\phi(\boldsymbol{r}) \sim \left\{\frac{\mathrm{e}^{\mathrm{i}kr}}{r}\left[\frac{1}{k}\sum_\ell\frac{\mathrm{i}^l}{2\mathrm{i}}(2l+1)\,\mathrm{e}^{-\mathrm{i}\frac{\ell\pi}{2}}P_\ell(\cos\vartheta) + f(\vartheta)\right]\right.$$
$$\left.+ \frac{\mathrm{e}^{-\mathrm{i}kr}}{r}\frac{1}{k}\sum_\ell\frac{\mathrm{i}^\ell}{2\mathrm{i}}(2\ell+1)\,\mathrm{e}^{\mathrm{i}\frac{\ell\pi}{2}}P_\ell(\cos\vartheta)\right\} \tag{2.30}$$

with $f(\vartheta) = \frac{1}{2\mathrm{i}k}\sum_\ell(2\ell+1)\left(\mathrm{e}^{\mathrm{i}2\delta_\ell}-1\right)P_\ell(\cos\vartheta)$ the scattering amplitude. At low momenta the scattering phase behave as $\delta^\ell \sim k^{(2\ell+1)}$, therefore at low temperatures only s-wave scattering plays a role.

In fact, a good assumption for ultra-cold bosonic quantum gases is to truncate the series (2.30) after the first term ($\ell = 0$) and to consider only s-wave scattering with

$$f_0(\vartheta) = f_s(\vartheta) = \frac{1}{2\mathrm{i}k}\left(\mathrm{e}^{\mathrm{i}2\delta_0}-1\right) = \frac{1}{k(\cot\delta_0 - \mathrm{i})}. \tag{2.31}$$
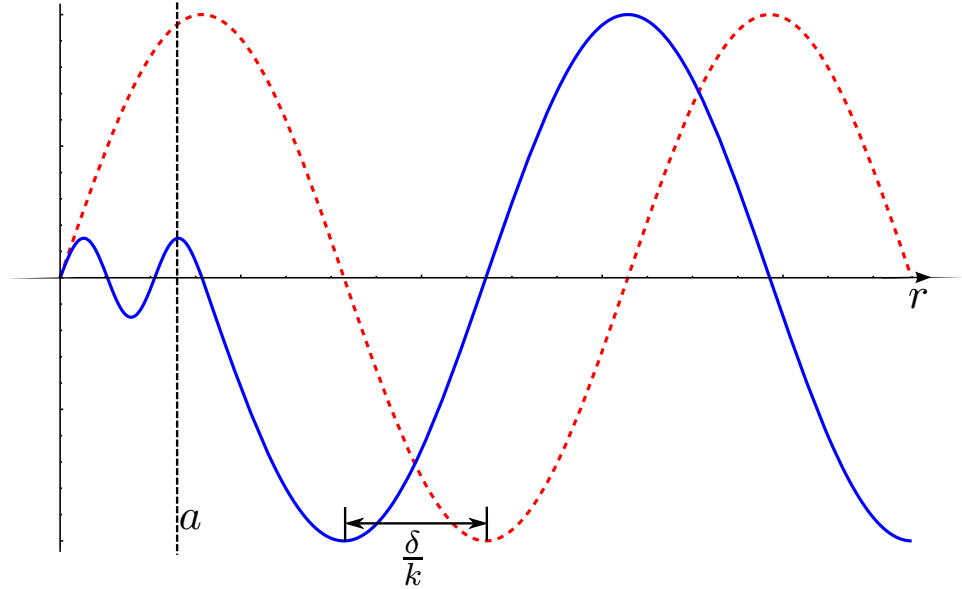
Figure 2.3.: **Scattering phase**: The red dashed curve shows the free solution ($V(\boldsymbol{r}) = 0$). The blue curve is the solution for a square interaction potential. Asymptotically it must have the same structure as the free solution (red curve). The phase shift $\frac{\delta}{k}$ provides for a continuous connection condition at the edge of the potential.

2.1.5. s-wave scattering length

For a square potential

$$V(\boldsymbol{r}) = \begin{cases} -V_0 & \text{if } \boldsymbol{r} < a, \\ 0 & \text{if } \boldsymbol{r} > a, \end{cases} \tag{2.32}$$

the scattering phase of the s-wave is

$$\delta_0 = \arctan\left(\frac{k}{k_0}\tan(k_0 a)\right) - ka \approx \frac{k}{k_0}\tan(k_0 a) - ka, \tag{2.33}$$

with $k = \hbar^{-1}\sqrt{2mE}$ and $k_0 = \hbar^{-1}\sqrt{2m(E + V_0)}$. Now the scattering length a_{s} is defined by

$$a_{\mathrm{s}} = a\left(1 - \frac{\tan(k_0 a)}{k_0 a}\right), \tag{2.34}$$

and the s-wave scattering phase can be expressed as

$$\delta_0 \approx -k a_{\mathrm{s}}. \tag{2.35}$$

which measures the strength of the interaction on large length scales, because the low energy scattering should not depend on the details of the potential $V(\boldsymbol{r})$.

With a expansion of the factor $k \cot \delta_0$ in small k in equation (2.31)

$$k \cot \delta_0 = -\frac{1}{a_\mathrm{s}} + \frac{1}{2} r_0 k^2, \tag{2.36}$$

a direct relation between the scattering amplitude and the s-wave scattering length can be found:

$$f_s(\vartheta) = \frac{1}{k(\cot \delta_0 - \mathrm{i})} \approx \frac{1}{-\frac{1}{a_\mathrm{s}} - \mathrm{i}k + r_0 k^2} \approx -a_\mathrm{s}, \tag{2.37}$$

for $k \ll 1/a_\mathrm{s}$. r_0 is called the effectiv range of the potential. At very low temperatures the scattering strength between two particles depends only on the s-wave scattering length a_s. Therefore the microscopic interaction potential $V(\boldsymbol{r})$ can be substituted by a suitable pseudo potential, which has the same scattering properties.

$$U_p(\boldsymbol{r}) = \frac{4\pi\hbar^2 a_\mathrm{s}}{2m} \delta(\boldsymbol{r}) \frac{\partial}{\partial r} \cdot r. \tag{2.38}$$

Now the Schrödinger equation

$$\left[\hat{\mathrm{H}}_0 + U(\boldsymbol{r})\right] \phi(\boldsymbol{r}) = E_0 \phi(\boldsymbol{r}) \tag{2.39}$$

is solved by the wave function

$$\phi(\boldsymbol{r}) = \mathrm{e}^{\mathrm{i}\boldsymbol{k}\cdot\boldsymbol{r}} - \frac{1}{\frac{1}{a_\mathrm{s}} + \mathrm{i}k} \frac{\mathrm{e}^{\mathrm{i}kr}}{r} \overset{k\to\infty}{\sim} 1 - \frac{a_\mathrm{s}}{r}. \tag{2.40}$$

2.2. Feshbach resonance

With the knowledge that the scattering amplitude $f(\vartheta)$ is related to the scattering length a_s, it is now desirable to have control over this parameter. By using Feshbach resonances this can be achieved. The control over the scattering length enables many new and interesting experiments with ultra-cold atoms [10]. Coherent formation of molecules in ^{85}Rb is possible [11], as much as forming strong interaction between fermionic atoms like ^{6}Li [12].

A Feshbach resonance is a multi-channel[2] resonance, which can be tuned via an external field, e.g. magnetic field. The resonance occurs if the overall energy of the incoming particles is in proximity to a bound state of a closed channel.

In ultra-cold collision theory, the involved channels are usually different hyperfine molecular potentials. Figure (2.4) shows the molecular potentials for two fictitious atoms, both with nuclear spin $I = 3/2$, electron spin $s = 1/2$ and an electronic angular momentum

---

[2]If a collision process is allowed by all conservation laws, the corresponding channel is called *open* and *closed* if not, where a channel is a possible mode depending on the two colliding particles' internal properties, e.g. the magnetic momentum.
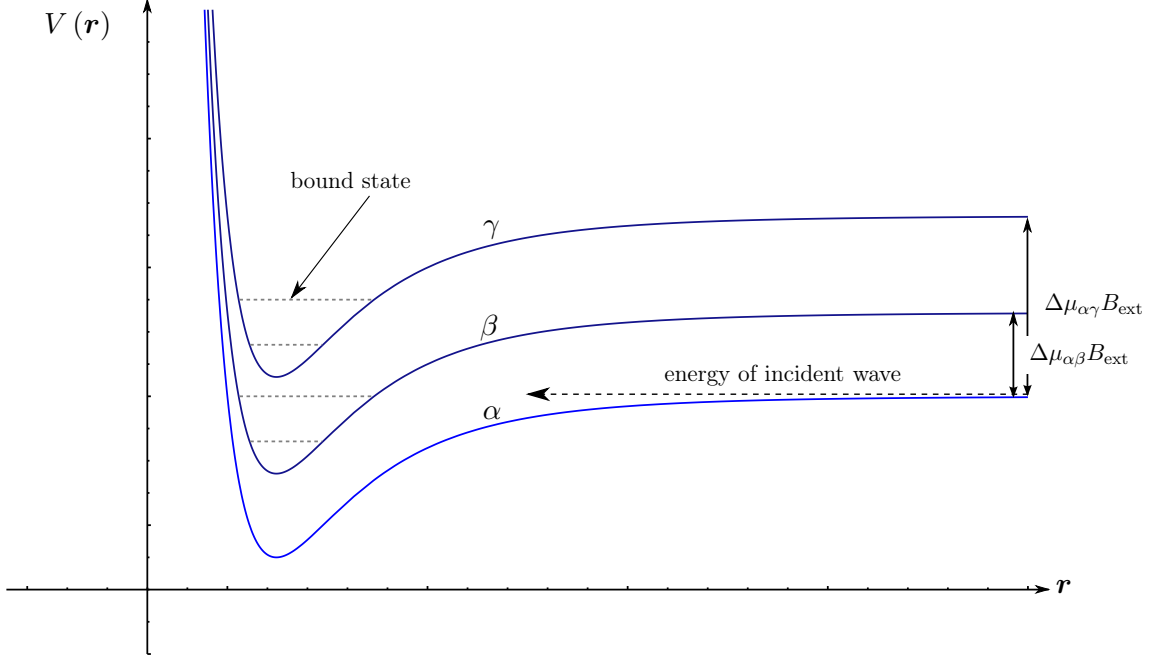
Figure 2.4.: A magnetic field shifts the molecular potentials of the different channels with respect to each other by the energy $E = \Delta\mu B_{\text{ext}}$. A Feshbach resonance occurs, if a bound state of one of the closed channels' potentials comes into resonance with the energy of the incident wave.

$\ell = 0$. This allows for a total angular momentum of $f = 1$ or $f = 2$. The channels are $\alpha = 1 + 1$, $\beta = 1 + 2$ and $\gamma = 2 + 2$. For two atoms colliding in channel α, the other channels are closed. The energy level of the molecular potentials can be shifted by applying an external magnetic field, that allows to bring a bound state of β or γ in resonance with the overall energy of the colliding particles. The difference between the channel's threshold energies is

$$\Delta E = \Delta\mu_{\alpha\beta}B_{\text{ext}}, \tag{2.41}$$

where $\Delta\mu_{\alpha\beta}$ is the difference between the magnetic momenta of the channels α and β and B_{ext} ist the external magnetic field. Because of the coupling caused by the hyperfine interaction, the atoms can go through a Landau-Zener type transition from one channel to another, and form a quasi-bound metastable state. This affects the scattering length a_{s} dramatically. Close to the Feshbach resonance, it can approximately be written as

$$a_{\text{Fb}} = a_{\text{bg}} \left(1 - \frac{\Delta B}{B_{\text{ext}} - B_{\text{res}}}\right), \tag{2.42}$$

with a_{bg} the background scattering length, B_{res} the resonant field and ΔB its width [6]. With a sufficiently broad Feshbach resonance, it is possible to tune the scattering length
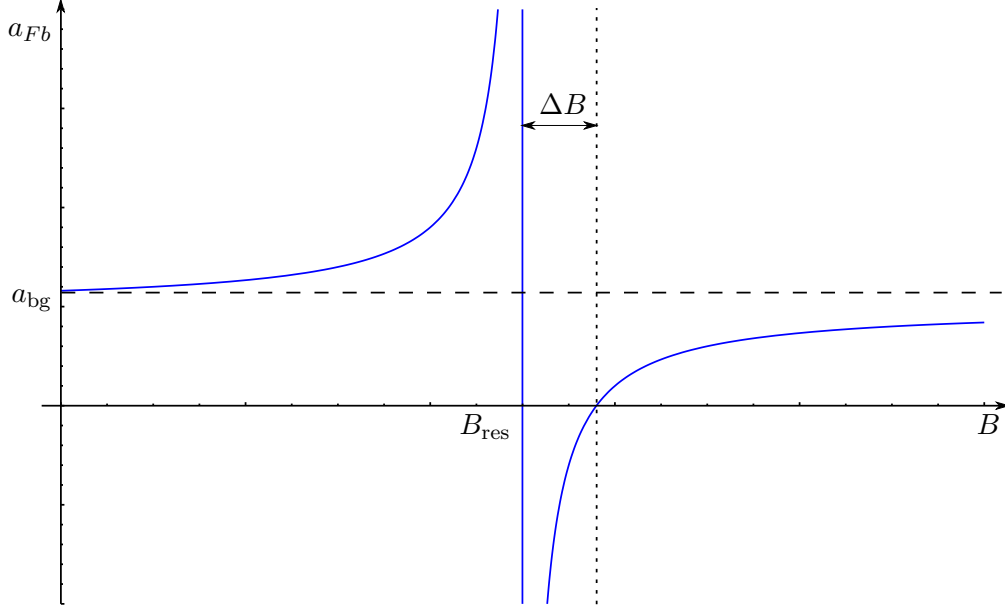
Figure 2.5.: The behaviour of the scattering length a_{Fb} close to the resonant magnetic field B_r according to equation (2.42).

to any desired value between $-\infty$ and $+\infty$.

In the following a more detailed approach to capture the influence of a Feshbach resonance on the scattering length will be discussed. As mentioned before, a Feshbach resonance is a multi-channel resonance. The wave function $\psi(\boldsymbol{x}, \boldsymbol{y})$ describes the two colliding particles in the open channel with position $\boldsymbol{x}$ and $\boldsymbol{y}$. $\phi(\boldsymbol{z})$ describes the closed channel and can be considered as a molecular state, characterized by a bare detuning ν_0. They are coupled to each other with a coupling parameter g. The Schrödinger equation of the system has the form

$$\left[E - \hat{\mathrm{H}}_0^{xy}\right] \psi(\boldsymbol{x}, \boldsymbol{y}) = g \int \mathrm{d}\boldsymbol{z} \; \alpha(\boldsymbol{r}) \phi(\boldsymbol{z}) \delta(\boldsymbol{z} - \boldsymbol{R}) \tag{2.43}$$

$$\left[E - \nu_0 - \hat{\mathrm{H}}_0^{m}\right] \phi(\boldsymbol{z}) = g \int \mathrm{d}\boldsymbol{x}\mathrm{d}\boldsymbol{y} \; \alpha(\boldsymbol{r}) \psi(\boldsymbol{x}, \boldsymbol{y}) \delta(\boldsymbol{z} - \boldsymbol{R}), \tag{2.44}$$

with $\boldsymbol{r}$ and $\boldsymbol{R}$ the relative and center of mass coordinates respectively (2.1, 2.2) and $\hat{\mathrm{H}}_0^{xy}$ and $\hat{\mathrm{H}}_0^{m}$ the Hamiltonians of the un-coupled system

$$\hat{\mathrm{H}}_0^{xy} = -\frac{\hbar^2}{2m_x}\Delta_{\boldsymbol{x}} - \frac{\hbar^2}{2m_y}\Delta_{\boldsymbol{y}} + V_x(\boldsymbol{x}) + V_y(\boldsymbol{y}) \tag{2.45}$$

$$\hat{\mathrm{H}}_0^{m} = -\frac{\hbar^2}{2(m_x + m_y)}\Delta_{\boldsymbol{z}} + V_m(\boldsymbol{z}). \tag{2.46}$$

2. Basics Concepts

For a realistic system of a ultra cold gas, the coupling function is well described by a δ-function $\alpha(\boldsymbol{r}) = \delta(\boldsymbol{r})$, but such a singular coupling will give rise to a divergence. Therefore, we will apply a regularization, which will not affect the final results.

$$\alpha(\boldsymbol{r}) = \frac{1}{(2\Lambda^2\pi)^{3/2}} e^{-\boldsymbol{r}^2/2\Lambda^2}, \tag{2.47}$$

with $\Lambda \to 0$.

As the the coupling function only depends on the relative coordinte $\boldsymbol{r}$, the system separates in relative and center of mass motion

$$\psi(\boldsymbol{x}, \boldsymbol{y}) = e^{i\boldsymbol{K}\cdot\boldsymbol{R}} \psi(\boldsymbol{r}) \tag{2.48}$$

$$\phi(\boldsymbol{z}) = e^{i\boldsymbol{K}\cdot\boldsymbol{z}} \chi, \tag{2.49}$$

with the total momentum of the system $\boldsymbol{K} = \boldsymbol{k}_x + \boldsymbol{k}_y$.

The Schrödinger equation system reduces to

$$\left[E + \frac{\hbar^2}{2\mu}\Delta_{\boldsymbol{r}} - E_{\boldsymbol{K}}\right] \psi(\boldsymbol{r}) = g\alpha(\boldsymbol{r})\chi \tag{2.50}$$

$$[E - \nu_0 - E^m(\boldsymbol{K})]\chi = g\int d\boldsymbol{r}\,\alpha(\boldsymbol{r})\psi(\boldsymbol{r}) \tag{2.51}$$

where $E_{bmK} = \hbar^2\boldsymbol{K}^2/2(m_x + m_y)$ is the energy of center of mass motion. Equation (2.50) can be solved with the Green's function formalism similar to (2.13). The solution for the atomic wave function is

$$\begin{aligned}\psi(\boldsymbol{r}) &= \psi_0(\boldsymbol{r}) + g\chi\int d\boldsymbol{r}'\alpha(\boldsymbol{r})\,G_{\boldsymbol{K}}(E, \boldsymbol{r} - \boldsymbol{r}') \\ &\sim \psi_0(\boldsymbol{r}) + f(\boldsymbol{k})\frac{e^{ikr}}{r}\end{aligned} \tag{2.52}$$

with the free solution $\psi_0(\boldsymbol{r}) = \exp(i\boldsymbol{k}_0\cdot\boldsymbol{r})$ and the Green's functions

$$G_{\boldsymbol{K}}(E, \boldsymbol{k}) = \frac{1}{E - \epsilon(\boldsymbol{k}) - E_{\boldsymbol{K}} + i\eta} \tag{2.53}$$

and

$$G_{\boldsymbol{K}}(E, \boldsymbol{r}) = -\frac{\mu}{2\pi\hbar^2}\frac{e^{ikr}}{r} \tag{2.54}$$

respectively. The momentum $\boldsymbol{k}$ is related to the energy $E = \epsilon(\boldsymbol{k}) + E_{\boldsymbol{K}}$ with the dispersion relation for a free particle $\epsilon(\boldsymbol{k}) = \hbar^2\boldsymbol{k}^2/2\mu$. With equation (2.52) and (2.54) the scattering amplitude $f(\boldsymbol{k})$ can be identified with

$$f(\boldsymbol{k}) = -\frac{\mu}{2\pi\hbar^2}g\chi. \tag{2.55}$$

Inserting this in equation (2.51) yields a self-consistency equation for χ

$$[E - \nu_0 - E^m(\boldsymbol{K})]\chi = g + g^2 G_{\boldsymbol{K}}(E, 0)\chi \tag{2.56}$$

The regularization (2.47) is applied on the Greens's function $G_{\boldsymbol{K}}(E, 0)$ and is evaluated in the limit $\Lambda \to 0$

$$G_{\boldsymbol{K}}(E, 0) = \int \mathrm{d}\boldsymbol{r}\mathrm{d}\boldsymbol{r}' \; \alpha(\boldsymbol{r})G_{\boldsymbol{K}}(E, \boldsymbol{r} - \boldsymbol{r}')\alpha(\boldsymbol{r}') = -\frac{2\mu}{\hbar^2}\left[\frac{1}{4\pi^{3/2}\Lambda} + \frac{\mathrm{i}k}{4\pi}\right]. \qquad (2.57)$$

The first term accounts for a shift in the energy of the molecular state, due to the coupling to the atomic state. As a consequence, the bare detuning ν_0 has to be renormalized to a physical detuning

$$\nu = \nu_0 - \frac{g^2\mu}{2\hbar^2\pi^{3/2}\Lambda}. \qquad (2.58)$$

Inserting this in the solution of equation (2.56) leads to the final result for the scattering amplitude

$$f(\boldsymbol{k}) = -\frac{\mu}{2\pi\hbar^2}\frac{g^2}{\epsilon(\boldsymbol{k}) - \nu + \frac{\mu g^2}{2\pi\hbar^2}\mathrm{i}k}. \qquad (2.59)$$

Comparison with equation (2.37)

$$f(\boldsymbol{k}) = -\frac{1}{\frac{1}{a_\mathrm{s}} + \mathrm{i}k + r_b k^2}, \qquad \text{(eq:scats)}$$

yields the scattering length

$$a_\mathrm{s} = -\frac{\mu g^2}{2\pi\hbar^2\nu} \qquad (2.60)$$

and additionally the effective range of the Feshbach resonance

$$r_b = \frac{\pi\hbar^4}{\mu^2 g^2}. \qquad (2.61)$$

2.3. Optical Lattice

A system of cold atoms trapped in an optical lattice provides a very powerful and versatile tool to investigate quantum mechanical effects at the macroscopic scale and quantum many body physics in an engineered quantum system [7]. The lattice parameters can be varied in a wide range. This system allows for the realization of bosonic and fermionic Hubbard models [5], and offers the possibility for the experimental study of strongly correlated systems.

An optical lattice is generated by six pairwise, in the simplest case mutually, counter-propagating laser beams, which form due to interference a standing wave with period $\lambda/2$, in which atoms can be trapped. By choosing an interference angle less than $\vartheta = 180°$ for the two laser beams, one can adjust the period of the lattice to lower value.

The laser beams induce an AC Stark shift in the atoms. The Hamilton operator for the
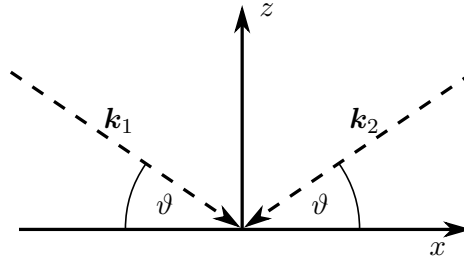

Figure 2.6.: Two laser beams intersecting unter an angle 2ϑ. Adjusting the angel ϑ allows to vary the lattice spacing a: $\boldsymbol{k}_x = \cos(\vartheta\,|\boldsymbol{k}|) = \cos(\vartheta\,\omega/c)$

interaction between atoms and light is

$$\hat{\mathrm{H}}_{dp} - -\mathbf{d}\boldsymbol{E}\left(\boldsymbol{r},t\right), \tag{2.62}$$

with $\mathbf{d}$ the dipole moment operator of the atoms and $\boldsymbol{E}\left(\boldsymbol{r},t\right)$ the laser light's electric field

$$\boldsymbol{E}\left(\boldsymbol{r},t\right) = \boldsymbol{E}_\omega \mathrm{e}^{\mathrm{i}\omega t} + \boldsymbol{E}_\omega^* \mathrm{e}^{-\mathrm{i}\omega t}, \tag{2.63}$$

with ω and $\boldsymbol{E}_\omega$ the laser's frequency and polarity respectively.

One atom is assumed to be a two level state system, with $|g\rangle$ the ground state, and $|e\rangle$ the excited state. The corresponding energies are E_g and E_e respectively. The Rabi frequency between the two state is

$$\Omega = \frac{|\langle e|\mathbf{d}\boldsymbol{E}_\omega|g\rangle|}{\hbar}, \tag{2.64}$$

and the detuning of the laser beams is

$$\Delta = \omega - \frac{E_e - E_g}{\hbar} \tag{2.65}$$

The Hamilton operator of the two level system is

$$\hat{H} = \begin{pmatrix} E_g & 2\hbar\Omega\cos(\omega t) \\ 2\hbar\Omega\cos(\omega t) & E_e \end{pmatrix} \tag{2.66}$$

and can be simplified with the help of the rotating frame and the rotating wave approximation

$$\hat{H} = \frac{\hbar}{2}\begin{pmatrix} \Delta & 2\Omega\left(1 + \mathrm{e}^{-2\mathrm{i}\omega t}\right) \\ 2\Omega\left(1 + \mathrm{e}^{2\mathrm{i}\omega t}\right) & -\Delta \end{pmatrix} \approx \frac{\hbar}{2}\begin{pmatrix} \Delta & \Omega \\ \Omega & -\Delta \end{pmatrix}. \tag{2.67}$$

The two state transform to

$$|g\rangle \rightarrow \quad |g\rangle \tag{2.68}$$

$$|e\rangle \rightarrow \quad \mathrm{e}^{\mathrm{i}\omega t}\,|e\rangle. \tag{2.69}$$

With far detuning the excited state is adiabatically eliminated and the AC Stark shift causes an energy shift in the ground state, which can be determine with second order perpetuation theory:

$$\Delta E_g = \frac{\hbar^2\Omega^2}{\hbar\Delta} = -\frac{|\langle e|\boldsymbol{d}\,\boldsymbol{\varepsilon}|g\rangle|^2}{E_e - E_g - \hbar\omega}\,|\boldsymbol{E}_\omega|^2 = -\alpha(\omega)\,|\boldsymbol{E}_\omega|^2, \tag{2.70}$$

with ε the laser light polarity and $\alpha(\omega)$ the dynamical polarizability of the atom. By adjusting the detuning, the force affecting the atoms can be tuned. A blue detuned laser beam, i.e. $\Delta > 0$, will push the atoms away. The atoms seek for a low field, i.e. an intensity minimum. In contrast, a red detuned laser beam, i.e. $\Delta < 0$, will attract them, the atoms seek for a high field, i.e. an intensity maximum.

If spontaneous emission is considered, i.e. the energy of the excited state has a finite imaginary part $(E_e \rightarrow E_e - 1/2\,\hbar\Gamma_e\mathrm{i}$, the ground state is getting unstable and has a finite lifetime. This changes the shift in the ground state energy

$$\Delta E_g = \frac{\hbar\Omega^2}{\Delta + \mathrm{i}\frac{\Gamma_e}{2}} = \underbrace{\frac{\hbar\Omega^2\Delta}{\Delta^2 + \left(\frac{\Gamma_e}{2}\right)^2}}_{\Delta E:\,\text{Stark shift}} - \mathrm{i}\underbrace{\frac{1/2\Gamma_e\hbar\Omega^2}{\Delta^2 + \left(\frac{\Gamma_e}{2}\right)^2}}_{\frac{\hbar}{2}\Gamma_g = \Delta E_g\frac{\Gamma_e}{\Delta}}. \tag{2.71}$$

The first term denotes the shift of the energy and the second term the decay rate of the ground state because of the spontaneous emission. For a stable optical lattice a constant energy shift and stable ground state is necessary. The spontaneous emission can be suppressed with a high detuning:

$$\Delta \gg \Gamma_e \Rightarrow \Gamma_g = \frac{2}{\hbar}\Delta E\frac{\Gamma_e}{\Delta} \ll 1, \tag{2.72}$$

and high laser intensity, i.e. high Rabi frequency, accounts for a constant stark shift ΔE. The electric field for two laser beams in one dimension is

$$\boldsymbol{E}(\boldsymbol{r}, t) = \boldsymbol{E}_\omega\left[\cos(k_x x)\mathrm{e}^{-\mathrm{i}k_z z}\mathrm{e}^{-\mathrm{i}\omega t} + \cos(k_x x)\mathrm{e}^{\mathrm{i}k_z z}\mathrm{e}^{\mathrm{i}\omega t}\right] \tag{2.73}$$
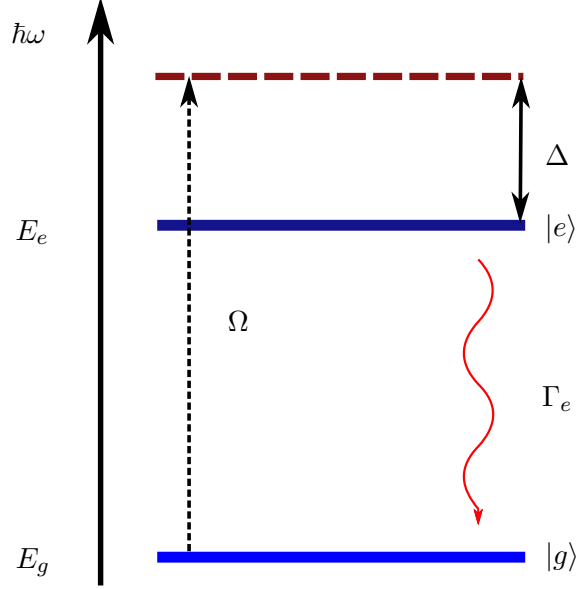
Figure 2.7.: Assumed two level system of states in an atom. Ω is the Rabi frequency between the states, Δ the detuning of the laser beam and Γ_e is the spontaneous decay rate of the excited state to the ground state.

with $k_x = \cos(\vartheta k_i)$ as shown in figure (2.6) and k_i the wave-vectors of the two laser beams. This can be generalized for six laser beams in three dimensions.

$$\boldsymbol{E}\left(\boldsymbol{r}, t\right) = \sum_i \boldsymbol{E}^i_{\omega_i} \cos\left(\boldsymbol{k}_i \cdot \boldsymbol{r}\right) \mathrm{e}^{-\mathrm{i}\omega_i t} + \mathrm{c.c.}. \tag{2.74}$$

The laser beams cause a conservative periodic potential

$$\Delta E = -\alpha(\omega) \left|\boldsymbol{E}\left(\boldsymbol{r}, t\right)\right|^2 = V_{0x} \cos^2\left(k_x x\right) \tag{2.75}$$

for one dimension or

$$\Delta E = V_0\left(\boldsymbol{x}\right) = \sum_i V_{0i} \cos^2\left(\boldsymbol{k}_i \cdot \boldsymbol{r}\right) \tag{2.76}$$

for three dimensions, respectively, with V_i the depth of the potential and $|k|_i = \omega_i/c = 2\pi/\lambda$ denoting the lattice spacing $|a|_i = \lambda/2 = \pi/|k|_i$, which is variable at will. A natural measure of energy in an optical lattice is the recoil energy $E_\mathrm{r} = \hbar^2 k^2/2m$.
Six equal laser beams generate a homogeneous three dimensional cubic optical lattice. A two dimensional lattice is generated by four lasers with high and two with low intensity. The according lattice consists of potential tubes in the direction of the weak lasers.

2.4. Periodic potential

An optical lattice presents a periodic potential as shown in section [2.3] and is often called crystal of light because it is similar to crystals from solid state theory. The simplest optical lattice is the three dimensional (3D) cubic lattice, therefore the following will be treated with main emphasis on the simple cubic lattice.

Crystals are generally described with a Bravais lattice, which is an infinite set of points, generated by a set of discrete translation operations described by a Bravais vector

$$\boldsymbol{R} = n_1 \boldsymbol{a}_1 + n_2 \boldsymbol{a}_2 + n_3 \boldsymbol{a}_3, \tag{2.77}$$

with $(\boldsymbol{a}_1, \boldsymbol{a}_2, \boldsymbol{a}_3)$ the basis vectors of the primitive unit cell, and n_1, n_2 and n_3 integer numbers. For the 3D cubic optical lattice is $|\boldsymbol{a}_1| = |\boldsymbol{a}_2| = |\boldsymbol{a}_3| = a = \lambda/2$.
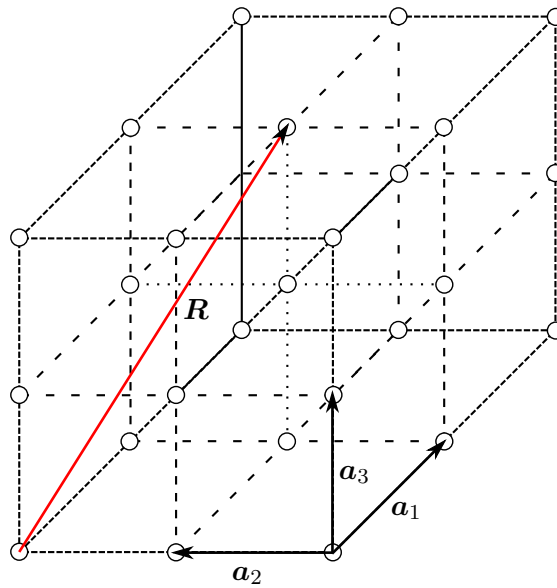
Figure 2.8.: Bravais vector $\boldsymbol{R} = n_1 \boldsymbol{a}_1 + n_2 \boldsymbol{a}_2 + n_3 \boldsymbol{a}_3$ in a three dimensional cubic lattice. $n_1 = 1$, $n_2 = -1$ and $n_3 = 2$

Corresponding to the Bravais lattice the reciprocal lattice is defined, which consists of all wave-vectors $\boldsymbol{q}$ generating plane waves $e^{i\boldsymbol{q}\cdot\boldsymbol{r}}$ with the same periodicity as the Bravais lattice.

$$e^{i\boldsymbol{q}\cdot(\boldsymbol{r}+\boldsymbol{R})} = e^{i\boldsymbol{q}\cdot\boldsymbol{r}}. \tag{2.78}$$

The reciprocal unit cell is spanned by the three primitive reciprocal vectors

$$\boldsymbol{b1} = 2\pi \frac{\boldsymbol{a}_2 \times \boldsymbol{a}_3}{\boldsymbol{a}_1 \cdot (\boldsymbol{a}_2 \times \boldsymbol{a}_3)} \tag{2.79}$$

$$\boldsymbol{b2} = 2\pi \frac{\boldsymbol{a}_3 \times \boldsymbol{a}_1}{\boldsymbol{a}_1 \cdot (\boldsymbol{a}_2 \times \boldsymbol{a}_3)} \tag{2.80}$$

$$\boldsymbol{b3} = 2\pi \frac{\boldsymbol{a}_1 \times \boldsymbol{a}_2}{\boldsymbol{a}_1 \cdot (\boldsymbol{a}_2 \times \boldsymbol{a}_3)}. \tag{2.81}$$

They obey the relation $\boldsymbol{b}_i \cdot \boldsymbol{a}_j = \delta_{ij}$. Hence every linear combination of $\boldsymbol{b}_i$

$$\boldsymbol{q} = q_1\boldsymbol{b}_1 + q_2\boldsymbol{b}_2 + q_3\boldsymbol{b}_3, \tag{2.82}$$

with q_i integer numbers, is a wave vector of the reciprocal lattice and generates a plane wave with the same periodicity as the corresponding Bravais lattice.

The primitive unit cell of the reciprocal lattice is called the first Brillouin zone. Its volume is given by

$$v_0 = \frac{(2\pi)^3}{V}, \tag{2.83}$$

with $V = \boldsymbol{a}_1 \cdot (\boldsymbol{a}_2 \times \boldsymbol{a}_3)$ the volume of the unit cell of the Bravais lattice. The reciprocal lattice of the simple cubic lattice, is a simple cubic lattice again. Therefore the first Brillouin zone is a cube with the volume $v_0 = (2\pi/a)^3$, i.e. $\boldsymbol{q} \in K = \left[-\frac{\pi}{a}; \frac{\pi}{a}\right]$.

2.5. Bloch waves

The dynamics of a single particle in a periodic potential $V(\boldsymbol{r}) = V(\boldsymbol{r} + \boldsymbol{R})$, e.g. an optical lattice is described by the Schrödinger equation

$$\left[-\frac{\hbar^2}{2m}\nabla^2 + V(\boldsymbol{r})\right]\phi_{n\boldsymbol{q}}(\boldsymbol{r}) = \left[-\frac{\hbar^2}{2m}\nabla^2 + V(\boldsymbol{r}+\boldsymbol{R})\right]\phi_{n\boldsymbol{q}}(\boldsymbol{r}) = \varepsilon_{\boldsymbol{q}}\phi_{n\boldsymbol{q}}(\boldsymbol{r}) \qquad (2.84)$$

Its energy eigenstates are Bloch waves, where n is the band index, and $\boldsymbol{q}$ is the quasi-momentum within the first Brillouin zone. Bloch waves are the product of plane waves and a periodic function $u_{n\boldsymbol{q}}(\boldsymbol{r})$, which has the same periodicity as the potential.

$$\phi_{n\boldsymbol{q}}(\boldsymbol{r}) = u_{n\boldsymbol{q}}(\boldsymbol{r})\,\mathrm{e}^{\mathrm{i}\boldsymbol{q}\cdot\boldsymbol{r}}, \qquad (2.85)$$

with

$$u_{n\boldsymbol{q}}(\boldsymbol{r}) = u_{n\boldsymbol{q}}(\boldsymbol{r} + \boldsymbol{R}). \qquad (2.86)$$

From the equations (2.86) follows:

$$\phi_{n\boldsymbol{q}}(\boldsymbol{r} + \boldsymbol{R}) = \mathrm{e}^{\mathrm{i}\boldsymbol{q}\cdot\boldsymbol{R}}\phi_{n\boldsymbol{q}}(\boldsymbol{r}), \qquad (2.87)$$

with $\boldsymbol{q}$ the quasi-momentum within the first Brillouin zone ($\boldsymbol{q} \in K = \left[-\frac{\pi}{a}; \frac{\pi}{a}\right]$). Because of the phase factor $\mathrm{e}^{\mathrm{i}\boldsymbol{q}\cdot\boldsymbol{R}}$, Bloch waves are extended over the whole lattice. Therefore they are not a appropriate basis to describe well localized particles.

2.6. Wannier basis

An appropriate basis to describe well localized particles in a periodic potential is the Wannier basis. It is the corresponding basis of the Bloch basis [sec. 2.5] in position space, therefore they are connected via Fourier transformation.

$$w_{in}(\boldsymbol{r} - \boldsymbol{R}_i) = \frac{1}{\sqrt{N}}\sum_{\boldsymbol{q}}\mathrm{e}^{\mathrm{i}\boldsymbol{q}\cdot\boldsymbol{R}_i}\phi_{n\boldsymbol{q}}(\boldsymbol{r}). \qquad (2.88)$$

A Wannier function is well localized to lattice sites $\boldsymbol{R}_i$, but is not related to a certain energy value, since it is a superposition of Bloch waves, which are the energy eigenstates in a periodic potential (2.84). It depends only on the difference $\boldsymbol{r} - \boldsymbol{R}_i$. The Wannier basis is an orthonormal basis, i.e. Wannier functions of different lattice sites are mutually orthogonal. The reverse transformation is

$$\phi_{n\boldsymbol{q}}(\boldsymbol{r}) = \frac{1}{\sqrt{N}}\sum_{\boldsymbol{R}_i}\mathrm{e}^{\mathrm{i}\boldsymbol{q}\cdot\boldsymbol{R}_i}w_{in}(\boldsymbol{r} - \boldsymbol{R}_i). \qquad (2.89)$$

For deep lattices and low particle energies the sinusoidal potential of each single lattice site can be approximated by a harmonic potential, whose eigenfunctions are the Hermite functions

$$\Phi_n(x) = \left(\frac{m\omega}{\pi\hbar}\right)^{1/4}\frac{1}{\sqrt{2^n n!}}H_n\left(\sqrt{\frac{m\omega}{\hbar}}x\right)\mathrm{e}^{-\frac{1}{2}\frac{m\omega}{\hbar}x^2}, \qquad (2.90)$$

with $H_n(x) = (-1)^n \mathrm{e}^{x^2} \frac{\mathrm{d}}{\mathrm{d}x^n} \mathrm{e}^{-x^2}$ the Hermite polynoms. The Hermite function of zeroth order is a good approximation for the near-field behaviour of the Wannier function in the lowest Bloch band.
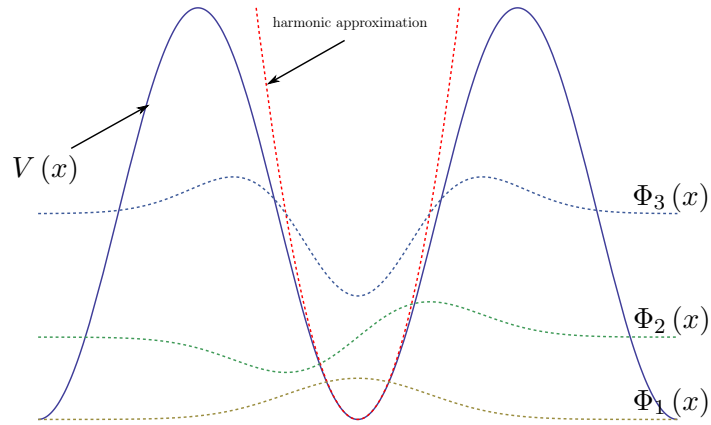
It must be pointed out, that the long range behaviour of the Wannier functions is not well described by the Hermite functions, as they rather exhibits an exponential deacay

$$w(\boldsymbol{r}) \xrightarrow[\boldsymbol{r} \to \infty]{} \mathrm{e}^{-|\boldsymbol{r}|/l}, \tag{2.91}$$

with l a characteristic length.

Additionally, Wannier functions are not ambiguous, as the Bloch waves can be multiplied with an arbitrary phase.

2.7. Bose Hubbard model

In 1998 Dieter Jaksch et al. suggested to described the dynamics of an ultra-cold dilute gas of bosonic atoms in an optical lattice by the Bose Hubbard model [5]. The Hamilton operator of bosons in an optical lattice is in second quantization

$$
\hat{H} = \int d^3x \ \psi^\dagger(\boldsymbol{x}) \left(-\frac{\hbar^2}{2m}\nabla^2 + V_0(\boldsymbol{x}) + V_T(\boldsymbol{x}) \right) \psi(\boldsymbol{x})
$$
$$
+ \frac{1}{2}\frac{4\pi a_s \hbar^2}{m} \int d^3x \ \psi^\dagger(\boldsymbol{x})\psi^\dagger(\boldsymbol{x})\psi(\boldsymbol{x})\psi(\boldsymbol{x}),
\tag{2.92}
$$

with $\psi^\dagger(\boldsymbol{x})$ and $\psi(\boldsymbol{x})$ the boson field creation and annihilation operator respectively, $V_0(\boldsymbol{x})$ the potential of the optical lattice and $V_T(\boldsymbol{x})$ an additional external (slowly varying) trapping potential, e.g. magnetic trap. In the simplest case, a three dimensional cubic lattice, the potential of the optical lattice has the form of equation (2.76): $V_0(\boldsymbol{x}) = \sum_i V_{0i}\cos^2(\boldsymbol{k}_i \cdot \boldsymbol{r})$, with $a = \lambda/2 = \pi/|\boldsymbol{k}_i|$ the lattice spacing. $U_p = 2\pi a_s \hbar^2 m^{-1}$ is the pseudo potential, introduced in [sec. 2.1.5] with equation (2.38), denoting the interaction between the atoms.

In an optical lattice the energy eigenstates of the Hamilton operator (2.92) for a single atom are Bloch waves. This gives rise to a description by an appropriate superposition of these Bloch waves or by a set of Wannier functions

$$
\psi(\boldsymbol{x}) = \sum_{ni} b_{ni} w_{ni}(\boldsymbol{x} - \boldsymbol{x}_i) = \frac{1}{\sqrt{N}} \sum_{\boldsymbol{q}\in K} \phi_{n\boldsymbol{q}}(\boldsymbol{x}) a_{n\boldsymbol{q}}.
\tag{2.93}
$$

with the annihilation and creation operators b_i and $b_i^\dagger$ of bosonic particles on lattice site i, and the corresponding operators a_k and $a_k^\dagger$ annihilating and creating respectively an atoms in the state k. Both obey the canonical commutation relation $\left[b_{\boldsymbol{i}}, b_{\boldsymbol{j}}^\dagger \right] = \delta_{\boldsymbol{ij}}$ and $\left[a_{\boldsymbol{q}}, a_{\boldsymbol{l}}^\dagger \right] = \delta_{\boldsymbol{ql}}$ respectively. They are connected with the Fourier transformation

$$
b_{n\boldsymbol{i}}^\dagger = \frac{1}{\sqrt{N}} \sum_{\boldsymbol{q}\in K} a_{\boldsymbol{q}n}^\dagger e^{i\boldsymbol{q}\cdot\boldsymbol{R}_i}
\tag{2.94}
$$

Inserting the expressions (2.93) and (2.94) into the Hamiltonian (2.92) yields

$$
\hat{H} = \sum_{n\boldsymbol{q}\in K} \varepsilon_n(\boldsymbol{q}) a_{\boldsymbol{q}n}^\dagger a_{\boldsymbol{q}n} + \frac{U_p}{2} \sum_{\substack{nn' \\ mm'}} \sum_{\substack{ii' \\ jj'}} \int d^3x \ w_n^*(\boldsymbol{x} - \boldsymbol{x}_i) \times
$$
$$
\times w_n(\boldsymbol{x} - \boldsymbol{x}_{i'}) w_n^*(\boldsymbol{x} - \boldsymbol{x}_j) w_n(\boldsymbol{x} - \boldsymbol{x}_{j'}) b_{n\boldsymbol{i}}^\dagger b_{m\boldsymbol{j}}^\dagger b_{n'\boldsymbol{i'}} b_{m'\boldsymbol{j'}},
\tag{2.95}
$$

with $\varepsilon_n(\boldsymbol{q})$ the Bloch band's dispersion relations.

For ultra-cold gases with weak interaction energies ($U \ll 2\sqrt{E_r V_0}$), it is assumed that the system's dynamics is confined to the lowest Bloch band. Furthermore for deep optical lattices the Wannier function are decreasing rapidly, hence the overlap of functions on

neighbouring sites is negligible. With the help this approximations the Hamiltonian (2.95) simplifies to

$$\hat{H} = -J \sum_{<i,j>} b_i^\dagger b_j + \sum_i \epsilon_i \hat{n}_i + \frac{U}{2} \sum_i \hat{n}_i (\hat{n}_i - 1), \tag{2.96}$$

with $\hat{n}_i = b_i^\dagger b_i$ the occupation number operator for lattice site i. The dispersion relation is given by

$$\varepsilon_0(\boldsymbol{q}) = 2J \sum_i^d [1 - \cos(\boldsymbol{q} \cdot \boldsymbol{a}_i)], \tag{2.97}$$

with the hopping rate between neighbouring lattice sites i and j, which can be determined with semi-classical methods.

$$J = \frac{4}{\sqrt{\pi}} \sqrt{E_r V_0} \left(\frac{V_0}{E_r}\right)^{1/4} e^{-2\sqrt{V_0/E_r}}. \tag{2.98}$$

The strength of the interaction of two particles on the same lattice is denoted by

$$U = a_{\mathrm{s}} \frac{4\pi\hbar^2}{m} \int \mathrm{d}^3 x \ |w(\boldsymbol{x})|^4. \tag{2.99}$$

Due to the small overlap of neighbouring Wannier functions, next nearest neighbour hopping and nearest neighbour interaction can be neglected.
The energy offset of each lattice site

$$\epsilon_i = \int \mathrm{d}^3 x \ V_T(\boldsymbol{x}) |w(\boldsymbol{x} - \boldsymbol{x}_i)|^2 \tag{2.100}$$

is caused by the optional additional external trap.
The Bose Hubbard model describes the competition between the parameter J, which indicates the delocalization of atoms over the lattice and the parameter U, which indicates the disfavour to have two or more particles on one lattice site. The ratio between these two parameters

$$\frac{U}{J} \sim \frac{a_{\mathrm{s}}}{a} \exp\left(2\sqrt{V_0/E_r}\right) \tag{2.101}$$

can be changed by varying the dimensionless lattice depth V_0/E_r. It increases exponentially with V_0. By varying the ratio U/J at integer filling one can find a superfluid - Mott-insulator quantum phase transition [5].

3. Two particle interaction properties in an optical lattice

In the following we will discuss the interaction properties of ultra-cold quantum degenerate dilute gases in optical lattices. Due to its low density, the interactions are dominated by two particle scattering processes. These processes and their special characteristics, due to the periodic structure of the lattice, has been investigated by K. Winkler et al. [8] and they predicted and observed bound atom pairs, despite the repulsive interaction and showed that this result is a consequence of the periodic structure and the absence of dissipation.

We will continue this investigation and extend it by introducing Feshbach resonances to tune the interaction between two particles. These Feshbach resonances are well captured by a two channel system, with an open and a closed channel. As a consequence, we will obtain different additional bound states of atom pairs. After this, we will introduced a model system, which gives rise to an effective nearest neighbour interaction of ultra-cold atoms trapped in optical lattices. We consider a second order process, which is a result of a resonant coupling to a molecular state, living on a second detuned lattice. New scattering properties and bound states are expected.

3.1. Repulsively bound atom pairs in an optical lattice[1]

In 2006 the groups of Prof. Grimm and Zoller from the University Innsbruck investigated the two particle scattering properties in an optical lattice, which are primarily responsible for the interactions in an ultra-cold dilute gas. The predicted repulsively bound atom pairs, due to the periodic structure of the lattice and the absence of dissipation. These bound states are eigenstates of the Bose Hubbard Hamiltonian (2.96) with two atoms present on the lattice. It is convenient to study the two particle problem within the first quantization formalism. The two particle wave function is denoted by $\psi(\boldsymbol{x}, \boldsymbol{y})$, with $\boldsymbol{x} = \sum_{i=1}^{d} x_i \boldsymbol{a}_i$ and $\boldsymbol{y} = \sum_{i=1}^{d} y_i \boldsymbol{a}_i$ denoting the particles' position in an d-dimensional cubic optical lattice, spanned by the primitive lattice vectors $\boldsymbol{a}_i$. Then the Hamiltonian (2.96) reduces to

$$\hat{H}_{\text{TP}} = \hat{H}_{\text{kin}} + \hat{H}_{\text{int}} = -J\left[\tilde{\Delta}_{\boldsymbol{x}}^0 + \tilde{\Delta}_{\boldsymbol{y}}^0\right] + U\delta_{\boldsymbol{x},\boldsymbol{y}}, \tag{3.1}$$

with $\tilde{\Delta}^{\boldsymbol{Q}}$ the discrete lattice derivative

$$\tilde{\Delta}_{\boldsymbol{x}}^{\boldsymbol{Q}}\psi(\boldsymbol{x}) = \sum_{i=1}^{d} \cos\frac{Q_i a}{2}\left[\psi(\boldsymbol{x} + \boldsymbol{a}_i) + \psi(\boldsymbol{x} - \boldsymbol{a}_i) - 2\psi(\boldsymbol{x})\right] \tag{3.2}$$

---

[1] [8]

3. Two particle interaction properties in an optical lattice

with $\boldsymbol{Q}$ an arbitrary vector. To solve the Schrödinger equation $\hat{\mathrm{H}}_{\mathrm{TP}}\psi\left(\boldsymbol{x},\boldsymbol{y}\right)=E\left(\boldsymbol{x},\boldsymbol{y}\right)$ it is reasonable to transform to relative and center of mass motion coordinates, introduced in [sec. 2.1]. The relative cooridnate $\boldsymbol{r}=\boldsymbol{x}-\boldsymbol{y}$ is described by the same lattice as $\boldsymbol{x}$, but the center of mass coordinate $\boldsymbol{R}=(\boldsymbol{x}+\boldsymbol{y})/2$ is described by a similar lattice with the same symmetry but half lattice spacing. With the new coordinates the two particle wave function can be rewritten as $\psi\left(\boldsymbol{x},\boldsymbol{y}\right)=\exp\left(\mathrm{i}\boldsymbol{Q}\cdot\boldsymbol{R}\right)\psi\left(\boldsymbol{r}\right)$, with a performed variable separation in $\boldsymbol{R}$ and $\boldsymbol{r}$ and with $\boldsymbol{Q}$ the quasi momentum of the center of mass motion. Then the kinetic energy reduces to

$$\hat{\mathrm{H}}_{\mathrm{kin}}\psi\left(\boldsymbol{x},\boldsymbol{y}\right)=\left[-2J\tilde{\Delta}_{\boldsymbol{r}}^{\boldsymbol{Q}}+4J\sum_{i=1}^{d}\left(1-\cos\frac{Q_{i}a}{2}\right)\right]\mathrm{e}^{\mathrm{i}\boldsymbol{Q}\cdot\boldsymbol{R}}\psi\left(\boldsymbol{r}\right).\tag{3.3}$$

The energy of the center of mass motion can be separated and the Schrödinger equation reduces to a problem for the relative coordinate only.

$$\left[-2J\tilde{\Delta}_{\boldsymbol{r}}^{\boldsymbol{Q}}+U\delta_{\boldsymbol{r},\boldsymbol{0}}\right]\psi\left(\boldsymbol{r}\right)=E\psi\left(\boldsymbol{r}\right).\tag{3.4}$$

This equation can be solved with the Green's function formalism, similar to [sec. 2.1.2]. The Green's function is defined by the equation

$$\left[E-\hat{\mathrm{H}}_{0}\right]G_{\boldsymbol{Q}}(E,\boldsymbol{r})=\delta_{\boldsymbol{r},\boldsymbol{0}},\tag{3.5}$$

with $\hat{\mathrm{H}}_{0}=-2J\tilde{\Delta}_{\boldsymbol{r}}^{\boldsymbol{Q}}$. It can be determined with Fourier transformation

$$G_{\boldsymbol{Q}}(E,\boldsymbol{r})=\frac{1}{v_{0}}\sum_{\boldsymbol{q}\in K}G_{\boldsymbol{Q}}(\boldsymbol{q})\mathrm{e}^{\mathrm{i}\boldsymbol{q}\cdot\boldsymbol{r}}\tag{3.6}$$

$$\delta_{\boldsymbol{r},\boldsymbol{0}}=\frac{1}{v_{0}}\sum_{\boldsymbol{q}\in K}\mathrm{e}^{\mathrm{i}\boldsymbol{q}\cdot\boldsymbol{r}},\tag{3.7}$$

with $K=\left[-\frac{\pi}{a};\frac{\pi}{a}\right]$ the first Brillouin zone and v_{0} its volume.

Inserting this in equation (3.5) and transpose yields

$$\frac{1}{v_{0}}\sum_{\boldsymbol{q}\in K}\mathrm{e}^{\mathrm{i}\boldsymbol{q}\cdot\boldsymbol{r}}\left\{G_{\boldsymbol{Q}}\left[E-\varepsilon_{\boldsymbol{Q}}(\boldsymbol{q})\right]-1\right\}=0\tag{3.8}$$

from which follows

$$G_{\boldsymbol{Q}}(E,\boldsymbol{q})=\frac{1}{E-\varepsilon_{\boldsymbol{Q}}(\boldsymbol{q})+\mathrm{i}\eta},\tag{3.9}$$

with $\varepsilon_{\boldsymbol{Q}}(\boldsymbol{q})$ the disperion relation of a particle in a d-dimensional optical lattice.

$$\varepsilon_{\boldsymbol{Q}}(\boldsymbol{q})=4J\sum_{i=1}^{d}\cos\frac{Q_{i}a}{2}\left[1-\cos\left(q_{i}a\right)\right].\tag{3.10}$$

There are two classes of solutions of equation (3.3), scattering states and bound states.
Scattering states: The scattering states obey the Lippmann-Schwinger equation, similiar
to the free particle in [sec. 2.1.2] obeying the equation (2.11).

$$\psi_E(\boldsymbol{r}) = \psi_E^0(\boldsymbol{r}) + \sum_{\boldsymbol{r}'} G_{\boldsymbol{Q}}(E, \boldsymbol{r} - \boldsymbol{r}')V(\boldsymbol{r}')\psi_E(\boldsymbol{r}'), \tag{3.11}$$

with $\psi_E^0(\boldsymbol{r}) = \exp(\mathrm{i}\boldsymbol{q}_0 \cdot \boldsymbol{r})$ the incident wave and eigenstate of $\hat{\mathrm{H}}_0$ with the energy $E = \varepsilon_{\boldsymbol{Q}}(\boldsymbol{q}_0)$. Due to the short range interacion potential $V(\boldsymbol{r}') = U\delta_{\boldsymbol{r}',\boldsymbol{0}}$, the Lippmann-Schwinger equation (3.11) can be solved exactly

$$\psi_E(\boldsymbol{r}) = \psi_E^0(\boldsymbol{r}) + \frac{U}{1 - \alpha_0\left(\frac{E}{2J}\right)\frac{U}{2J}}G_{\boldsymbol{Q}}(E, \boldsymbol{r}), \tag{3.12}$$

with

$$\alpha_0\left(\frac{E}{2J}\right) = \int \frac{\mathrm{d}\boldsymbol{q}}{v_0} \frac{1}{\frac{E}{2J} - 2\sum_{i=1}^d \cos\frac{Q_i a}{2}\left[1 - \cos(q_i a)\right]}. \tag{3.13}$$

It is interesting to analyse this solution for incoming plane waves at the limit of small
momenta, i.e. at the center of the Brillouin zone $\boldsymbol{q}_0 \to 0$, and at the limit of high
momenta, i.e. at the edge of the Brillouin zone $\boldsymbol{q}_0 \to \pi/a$.
For $\boldsymbol{q}_0 \to 0$, $\boldsymbol{Q} \to 0$ and $E \to 0$ the solution (3.12) reduces in the limit $\boldsymbol{r} \to \infty$ to

$$\psi_E(\boldsymbol{r}) \sim \psi_E^0(\boldsymbol{r}) + f(\boldsymbol{q}, \boldsymbol{q}_0)\frac{\mathrm{e}^{\mathrm{i}qr}}{r}, \tag{3.14}$$

with the scattering amplitude

$$f(\boldsymbol{q}, \boldsymbol{q}_0) = -\frac{1}{4\pi}\frac{\frac{U}{2J}}{1 - \alpha_0(0)\frac{U}{2J}}a. \tag{3.15}$$

For particles with momentum $\boldsymbol{q}_0 \to \pi/a$ and energy $E \approx 24J$ (in 3D), the solution has
the same form as (3.14), but with the scattering amplitude

$$f(\boldsymbol{q}, \boldsymbol{q}_0) = -\frac{1}{4\pi}\frac{\frac{U}{2J}}{1 - \alpha_0(12)\frac{U}{2J}}a, \tag{3.16}$$

with $\alpha_0(12) = -\alpha_0(0) \approx 0.25$. For both limits, a divergence in the scattering amplitude
at certain interaction energies U can be found. In the limit of small momentum $\boldsymbol{q}_0 \to 0$
the divergence occurs at an attractive interaction energy $U_{c1} = -2J/|\alpha_0(0)| < 0$ and
describes a change of sign of the scattering amplitude $f(\boldsymbol{q}, \boldsymbol{q}_0)$ from minus to plus. The
resonance can be associated with a bound state of atoms, previously predicted by [13].
For a high momentum the divergence occurs at repulsive interaction energy $U_{c2} = 2J/|\alpha_0(0)| > 0$ and describes a change of sign of the scattering amplitude $f(\boldsymbol{q}, \boldsymbol{q}')$ from
plus to minus. The divergence of the scattering amplitude can again be associated with a
bound state of atoms, which will be analysed in detail in the next section. In three dimen-
sions, resonant scattering always occurs for interaction energies $U < U_{c1}$ and $U > U_{c2}$,

in one or two dimensions, there is no such constraint.

Bound states: In the following the focus will is on bound states $\psi_{\boldsymbol{Q}}^{\mathrm{BS}}$ with repulsive interaction $U > 0$. To find the wave funcion $\psi_{\boldsymbol{Q}}^{\mathrm{BS}}(\boldsymbol{r})$ of the bound state, one can use again the Green's function $G_{\boldsymbol{Q}}(E, \boldsymbol{r})$. Equation (3.5) can be rewritten in the form

$$\left[E - \hat{\mathrm{H}}_0\right] G_{\boldsymbol{Q}}(E, \boldsymbol{r}) = \frac{1}{G_{\boldsymbol{Q}}(E, \boldsymbol{0})} \delta_{\boldsymbol{r},\boldsymbol{0}} G_{\boldsymbol{Q}}(E, \boldsymbol{r}). \tag{3.17}$$

$\psi_{\boldsymbol{Q}}^{\mathrm{BS}}(\boldsymbol{r}) = G_{\boldsymbol{Q}}(E, \boldsymbol{r})$ is a solution of the Schrödinger equation, if the self-consistency relation is satisfied

$$G_{\boldsymbol{Q}}(E, \boldsymbol{0}) = \int \frac{\mathrm{d}\boldsymbol{q}}{v_0} \frac{1}{E - 4J \sum_{i=1}^{d} \cos \frac{Q_i a}{2} \left[1 - \cos\left(q_i a\right)\right]} = \frac{1}{U}, \tag{3.18}$$

which determines the energy E_{BS} of the bound two particle state. The wave function $\psi_{\boldsymbol{Q}}^{\mathrm{BS}}(\boldsymbol{r})$ traveling through the lattice with the center of mass momentum $\boldsymbol{Q}$ and a given momentum distribution is

$$\psi_{\boldsymbol{Q}}^{\mathrm{BS}}(\boldsymbol{q}) = \frac{1}{E_{\mathrm{BS}} - \varepsilon_{\boldsymbol{Q}}(\boldsymbol{q})}. \tag{3.19}$$

In one dimension the self-consistency relation (3.18) can be solved analytically and yields the solution ($\boldsymbol{Q} = 0$)

$$E_{\mathrm{BS}} = 2J \left[\sqrt{4 + \left(\frac{U}{2J}\right)^2} + 2\right]. \tag{3.20}$$

In contrast to the 3D situation, in 1D the bound state exists for arbitrary small repulsive interaction $U > 0$.

For a finite center of mass momentum $\boldsymbol{Q}$ the hopping matrix element J reduces to $J_Q \to J \cos \frac{Qa}{2}$. Inserting in the equations above provides a new energy of the bound state

$$E(Q) = 2J \left[\sqrt{4 \left(\cos \frac{Qa}{2}\right)^2 + \left(\frac{U}{2J}\right)^2} + 2\right]. \tag{3.21}$$

In the limit of large interaction energies U an expansion in Q yields

$$E(Q) \sim 4J + U + \frac{4J^2}{U} \left(1 + \cos Qa\right). \tag{3.22}$$

Therefore the hopping rate of the bound two particle state reduces to J^2/U, as it is expected from perturbation theory.

These bound states were observed in an experiment with ^{87}Rb atoms in a cubic 3D optical lattice performed by the group of Prof. Grimm in Innsbruck.

3.2. Feshbach resonances in optical lattices

In the preceding chapter the interaction properties of two atoms in an optical lattice were discussed. As a consequence of the periodic structure of the lattice and the absence of dissipation, repulsively bound atom pairs occur. Their energy strongly depends on the interaction strength between the atoms. As shown in [sec. 2.7] the interaction of two slow atoms in an optical lattice is described by the paramter

$$U = \frac{4\pi a_{\mathrm{s}} \hbar^2}{m} \int \mathrm{d}^3 x \ |w(\boldsymbol{x})|^4, \tag{2.99}$$

which depends on the s-wave scattering length a_{s}. To have control over the energy of the bound states, it is necessary to tune the interaction strength. This can be achieved with the help of a Feshbach resonance, described in [sec. 2.2]. In the following the influence of a Feshbach resonance on the interaction of atoms in an optical lattice will be discussed. The system's dynamic is assumed to be confined to the lowest Bloch band and can be described by the Hamitlonian

$$\begin{aligned} \hat{\mathrm{H}} = &- J \sum_{<i,j>} \hat{b}_i^\dagger \hat{b}_j + \frac{U}{2} \sum_i \hat{n}_i (\hat{n} - 1) \\ &+ g \sum_i \left(\hat{b}_i \hat{b}_i \hat{m}_i^\dagger + \hat{b}_i^\dagger \hat{b}_i^\dagger \hat{m}_i \right) - \nu \sum_i \hat{m}_i^\dagger \hat{m}_i, \end{aligned} \tag{3.23}$$

where $\hat{b}_i$ $(\hat{b}_i^\dagger)$ and $\hat{m}_{ij}$ $(\hat{m}_{ij}^\dagger)$ are the bosonice annihilation (creation) operators of the atomic and molecular channel. The parameter g denotes the coupling strength and ν the detuning between the two channels. The problem can again be solved in the first quantization formalism and is described by the Schrödinger equation

$$\left[E + 2J\tilde{\Delta}_{\boldsymbol{r}} \right] \psi(\boldsymbol{r}) = U\delta_{\boldsymbol{r},\boldsymbol{0}} + g\chi\delta_{\boldsymbol{r},\boldsymbol{0}} \tag{3.24}$$

$$\left[E - \nu \right] \chi = g\psi(\boldsymbol{r})\delta_{\boldsymbol{r},\boldsymbol{0}}, \tag{3.25}$$

with $\psi(\boldsymbol{r})$ describing the two particle atomic state, with the relative coordinate $\boldsymbol{r}$ between the particle and χ describing the molecular state. The general solution of the differential equation (3.24) is

$$\psi(\boldsymbol{r}) = \psi_0(\boldsymbol{r}) + G(\boldsymbol{r})U\psi(\boldsymbol{0}) + g\chi G(\boldsymbol{r}) \tag{3.26}$$

where $\psi_0(\boldsymbol{r}) = \exp(i\boldsymbol{q}_0 \cdot \boldsymbol{a})$ is the homogeneous and $G(\boldsymbol{r})U\psi(\boldsymbol{0}) + g\chi G(\boldsymbol{r})$ the inhomogeneous solution. With equation (3.26) one obtains for $\psi(\boldsymbol{0})$

$$\psi(\boldsymbol{0}) = \frac{1 + g\chi G(\boldsymbol{0})}{1 - G(\boldsymbol{0})U}. \tag{3.27}$$

Inserting this in equation (3.25) gives rise to a self-consistency equation for the molecular state

$$\chi = \frac{\frac{g}{1 - G(\boldsymbol{0})U}}{E - \nu - \frac{g^2 G(\boldsymbol{0})}{1 - G(\boldsymbol{0})U}}. \tag{3.28}$$

3. Two particle interaction properties in an optical lattice

The final result for $\psi(\mathbf{r})^2$ is

$$\psi(\mathbf{r}) = \mathrm{e}^{\mathrm{i}\mathbf{q}_0 \cdot \mathbf{r}} + \frac{U}{1 - G(\mathbf{0})U} G(\mathbf{r}) + \frac{\frac{g^2}{(1-G(\mathbf{0})U)^2}}{E - \nu - \frac{g^2 G(\mathbf{0})}{1-G(\mathbf{0})U}} G(\mathbf{r}). \tag{3.29}$$

with the scattering amplitude

$$f(\mathbf{q}, \mathbf{q}_0) = \frac{U}{1 - G(\mathbf{0})U} + \frac{\frac{g^2}{(1-G(\mathbf{0},\mathbf{Q})U)^2}}{E - \nu - \frac{g^2 G(\mathbf{0})}{1-G(\mathbf{0})U}}, \tag{3.30}$$

which consists of, additionally to the known scattering amplitude (3.15), a coupling and detuning dependend term. From this term follow two additional bound states, which are determined by the equation

$$E - \nu - \frac{g^2 G(\mathbf{0})}{1 - G(\mathbf{0})U} = 0. \tag{3.31}$$

or

$$\frac{1}{G(\mathbf{0})} = U + \frac{g^2}{E - \nu}, \tag{3.32}$$

respectively. On the left hand side of the equation is the reciprocal Green's function, which for large energies can be approximated by the function $E + \xi$. The larger the energy, the smaller is the error ξ. For energies $E < 12J$ the reciprocal Green's function has a gap, depending on the center-of-mass motion quasi-momentum $\mathbf{Q}$. The width of the gap is $\Delta W = 4J \sum_{i=1}^{d} \cos \frac{Q_i a}{2} (1 - \cos q_i a)$, i.e. for a quasi-momentum of $\mathbf{Q} = 0$ the width is $\Delta W = 24J$ and for a quasi-momentum of $\mathbf{Q} = \left| \frac{\pi}{a} \right|$ the width is $\Delta W = 0$. The behaviour of the reciprocal Green's function is illustrated in detail in [C].

On the right hand side of the equation is a function in E which is a hyperbola. The on-site repulsion parameter U shifts the curve on the y-axis and the detuning ν is the pole of the hyperbola and shifts the curve on the energy-axis. The points of intersection of the reciprocal Green's function and the hyperbola determine the energies of the bound states. For a quasi-momentum of $\mathbf{Q} = \left| \frac{\pi}{a} \right|$ there are always two bound states, since the reciprocal Green's function is a gapless linear function with a slope $m \neq 0$ [fig. 3.1a]. If the detuning ν is smaller than the width ΔW of the gap, and is U smaller than the value of the reciprocal Green's function at the border of the gap, then there are no bound states [fig. 3.1b]. In [fig. 3.1c] and [fig. 3.1d] there are examples shown, with one and two bound states, respectively.

Figure [fig. 3.2] shows the energies of bound states of two atoms depending on the center-of-mass quasi-momentum of the two atoms. The interaction U and the detuning ν are choosen, that there are always two bound states. They are both located above the continuum of scattering states (green dashed curves).

---

[2] A detailed derivation in [B.6]

$Q = \frac{\pi}{a}$

-12   12 $\frac{E}{J}$

(a) Points of intersection of the reciprocal Green's function $\frac{J}{G(0)}$ with center-of-mass quasi-momentum $Q = \frac{\pi}{a}$ and the hyperbola function. There are always two bound states.

$Q = 0$

-12   12 $\frac{E}{J}$

(b) Points of intersection of the reciprocal Green's function $\frac{J}{G(0)}$ with center-of-mass quasi-momentum $Q = 0$ and the hyperbola function. In this situation there are no bound states.

$Q = 0$

-12   12 $\frac{E}{J}$

(c) Example with only one bound state.

$Q = 0$

-12   12 $\frac{E}{J}$

(d) Example with two bound states, due to sufficiently large U and ν.

Figure 3.1.

For stronger interactions the dynamic cannot be confined to the lowest Bloch band anymore. Higher Bloch bands have to be involved in the calculations.

In an optical lattice the atomic and molecular channel are well described by Bloch waves

$$\psi^x_{n\boldsymbol{q}_x}(\boldsymbol{x}) = \frac{1}{\sqrt{N}} \mathrm{e}^{\mathrm{i}\boldsymbol{x}\cdot\boldsymbol{q}_x} u^x_{n\boldsymbol{q}_x}(\boldsymbol{x}) \tag{3.33}$$

$$\psi^y_{n\boldsymbol{q}_y}(\boldsymbol{y}) = \frac{1}{\sqrt{N}} \mathrm{e}^{\mathrm{i}\boldsymbol{y}\cdot\boldsymbol{q}_y} u^y_{n\boldsymbol{q}_y}(\boldsymbol{y}) \tag{3.34}$$

$$\phi_{n\boldsymbol{Q}}(\boldsymbol{z}) = \frac{1}{\sqrt{N}} \mathrm{e}^{\mathrm{i}\boldsymbol{z}\cdot\boldsymbol{Q}} u^m_{n\boldsymbol{Q}}(\boldsymbol{z}), \tag{3.35}$$

with $\boldsymbol{x}$, $\boldsymbol{y}$ and $\boldsymbol{z}$ the atoms' and molecule's position respectively, N the number of lattice sites and index n is denoting the Bloch band. The quasi-momenta are denoted by $\boldsymbol{q_x}$, $\boldsymbol{q_y}$ and $\boldsymbol{Q}$ and $u^\beta_{n\boldsymbol{q}}(\boldsymbol{x}) = u^\beta_{n\boldsymbol{q}}(\boldsymbol{x} + \boldsymbol{R})$ (eq. 2.86) periodic functions, which obey the Bloch theorem and the normalization condition $\int_{v_0} \mathrm{d}\boldsymbol{x} \left| u^\beta_{n\boldsymbol{q}}(\boldsymbol{x}) \right|^2 = 1$. Due to the discrete translation invariance, the total quasi-momentum $\boldsymbol{Q} = \boldsymbol{q}_x + \boldsymbol{q}_y + \boldsymbol{Q}_j$ is conserved. $\boldsymbol{Q}_j$ is a reciprocal lattice vector, which may provide a projection of the sum $\boldsymbol{q}_x + \boldsymbol{q}_y$ into the
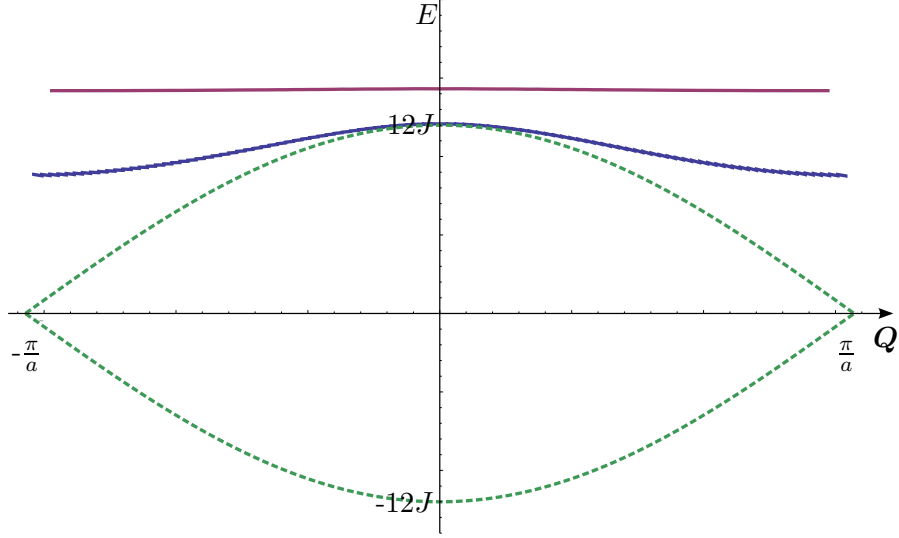
35

Figure 3.2.: Repulsivley bound atom pairs with on-site interaction U and Feshbach resonance. The figure shows a situation with two bound states for every center-of-mass quasi-momentum, due to sufficient parameters U, ν and g. They are located above the continuum of scattering states (green dashed curves).

first Brillouin zone, if necessary. The general solution with fixed total quasi-momentum $\boldsymbol{Q}$ can therefore be written as

$$\psi(\boldsymbol{x}, \boldsymbol{y}) = \frac{1}{\sqrt{V}} \sum_{nm} \sum_{\boldsymbol{k}} \varphi^{nm}(\boldsymbol{k}) \psi^x_{n\boldsymbol{q}_x}(\boldsymbol{x}) \psi^y_{m\boldsymbol{q}_y}(\boldsymbol{y}) \tag{3.36}$$

$$\phi(\boldsymbol{z}) = \sum_{s} \chi^s \phi^m_s(\boldsymbol{z}) \tag{3.37}$$

$$\tag{3.38}$$

with $\boldsymbol{q}_x = \boldsymbol{k}$ and $\boldsymbol{q}_y = \boldsymbol{Q} - \boldsymbol{q}_x + \boldsymbol{Q}_j$. With n, m and s indicating the Bloch bands and $\varphi^{nm}(\boldsymbol{k})$ and χ^s are the expansion coefficients of the Bloch basis. In the following, we will assume that the on-site repulsion U in the atomic channel is a result of a wide Feshbach resonance and will therefore be replace by a coupling to a second molecular channel and all in all third channel.

$$\breve{\phi}_{n\boldsymbol{Q}}(\boldsymbol{z}) = \frac{1}{\sqrt{N}} e^{i\boldsymbol{z}\cdot\boldsymbol{Q}} u_{n\boldsymbol{Q}}(\boldsymbol{z}), \tag{3.39}$$

from which follows a third wave function

$$\breve{\phi}(\boldsymbol{z}) = \sum_{t} \eta^t \breve{\phi}^m_t(\boldsymbol{z}), \tag{3.40}$$

with $\breve{\phi}(\boldsymbol{z})$ the wave function of the second molecular channel, t indicating the Bloch bands and η^t the expansion coefficient of the Bloch basis. Then the normalization of the

wave functions is

$$\sum_{nm} \int_{v_0} \frac{\mathrm{d}\boldsymbol{k}}{(2\pi)^3} \left|\varphi^{nm}(\boldsymbol{k})\right|^2 + \sum_s |\chi^s|^2 + \sum_t \left|\eta^t\right|^2 = 1. \tag{3.41}$$

Inserting equations (3.36, 3.37 and 3.40) in the system of exact Schrödinger equations leads to a system of equations for the amplitudes of the wave functions.

$$\left[E - E_{nm}(\boldsymbol{k}, \boldsymbol{Q})\right] \varphi^{nm}(\boldsymbol{k}) = g \sum_s \tilde{g}_s^{nm}(\boldsymbol{k})\chi^s + \breve{g} \sum_t \tilde{g}_t^{nm}(\boldsymbol{k})\eta^t \tag{3.42}$$

$$\left[E - \nu_0 - E_s^{mol}(\boldsymbol{Q})\right] \chi^s = g \sum_{nm} \frac{1}{V} \sum_{\boldsymbol{k}} \tilde{g}_{nm}^s(\boldsymbol{k})\varphi^{nm} \tag{3.43}$$

$$\left[E - \breve{\nu}_0 - E_s^{mol}(\boldsymbol{Q})\right] \eta^s = \breve{g} \sum_{nm} \frac{1}{V} \sum_{\boldsymbol{k}} \tilde{g}_{nm}^s(\boldsymbol{k})\varphi^{nm}, \tag{3.44}$$

with ν_0 and $\breve{\nu}_0$ the bare detuning of the molecular channels, $E_{nm}(\boldsymbol{k}, \boldsymbol{Q})$ the dispersion relation of the atoms in the Bloch bands n and m, $E_s^{mol}(\boldsymbol{Q})$ and $E_t^{mol}(\boldsymbol{Q})$ the molecules' dispersion relation in the Bloch bands s and t, respectively. The coupling parameter is

$$\frac{g}{\sqrt{V}} \tilde{g}_{s(t)}^{nm}(\boldsymbol{k}) = g \int \mathrm{d}\boldsymbol{x}\mathrm{d}\boldsymbol{y} \left[\psi_{n\boldsymbol{q}_x}^x(\boldsymbol{x})\psi_{m\boldsymbol{q}_y}^y(\boldsymbol{y})\right]^* \alpha(\boldsymbol{r})\phi_{s\boldsymbol{Q}}(\boldsymbol{R}), \tag{3.45}$$

with $\alpha(\boldsymbol{r})$ the regularized coupling function (2.47) and the convenient notation $\tilde{g}_s^{nm}(\boldsymbol{k}) = [\tilde{g}_{nm}^s(\boldsymbol{k})]^*$.

For an incoming wave $\varphi_0^{nm}(\boldsymbol{k}) = V\delta_{nk}\delta_{ml}\delta_{\boldsymbol{qk}}$ at the momentum $\boldsymbol{q}$ in the k,l-band at the energy $E_0 = E_{kl}(\boldsymbol{q}, \boldsymbol{Q})$ the formal solution can be expressed in terms of a resolvent formalism

$$\varphi^{nm}(\boldsymbol{k}) = \varphi_0^{nm}(\boldsymbol{q}) + \frac{\lambda_{kl}^{nm}(\boldsymbol{k}, \boldsymbol{q})}{E - E_{nm}(\boldsymbol{k}, \boldsymbol{Q}) + \mathrm{i}\eta} \tag{3.46}$$

$$\chi^s = R_{kl}^s(\boldsymbol{q}) \tag{3.47}$$

$$\eta^t = S_{kl}^t(\boldsymbol{q}), \tag{3.48}$$

with $\lambda_{kl}^{nm}(\boldsymbol{k}, \boldsymbol{q})$ determining the scattering amplitude and $R_{kl}^s(\boldsymbol{q})$, as well as $S_{kl}^t(\boldsymbol{q})$, are describing a molecular wave function in the s-band and t-band respectively, in momentum space. The atoms, which are forming the molecule, are coming from the k and l-band of the atomic channel. These resolvents are determined by following set of equations

$$\lambda_{kl}^{nm}(\boldsymbol{k}, \boldsymbol{q}) - g \sum_s \tilde{g}_s^{nm}(\boldsymbol{k})R_{kl}^s(\boldsymbol{q}) - \breve{g} \sum_t \tilde{g}_t^{nm}(\boldsymbol{k})S_{kl}^t(\boldsymbol{q}) = 0 \tag{3.49}$$

$$\left[E - \nu_0 - E_s^{mol}(\boldsymbol{Q})\right] R_{kl}^s(\boldsymbol{q}) - g \sum_{nm} \frac{1}{V} \sum_{\boldsymbol{k}} \frac{\tilde{g}_{nm}^s(\boldsymbol{k})\lambda_{kl}^{nm}(\boldsymbol{k}, \boldsymbol{q})}{E - E_{nm}(\boldsymbol{k}, \boldsymbol{Q}) + \mathrm{i}\eta} = g\tilde{g}_{kl}^s(\boldsymbol{q}) \tag{3.50}$$

$$\left[E - \breve{\nu}_0 - E_t^{mol}(\boldsymbol{Q})\right] S_{kl}^t(\boldsymbol{q}) - \breve{g} \sum_{nm} \frac{1}{V} \sum_{\boldsymbol{k}} \frac{\tilde{g}_{nm}^t(\boldsymbol{k})\lambda_{kl}^{nm}(\boldsymbol{k}, \boldsymbol{q})}{E - E_{nm}(\boldsymbol{k}, \boldsymbol{Q}) + \mathrm{i}\eta} = \breve{g}\tilde{g}_{kl}^t(\boldsymbol{q}). \tag{3.51}$$

3. Two particle interaction properties in an optical lattice

By inserting equation (3.46) in equations (3.47) and (3.48) the dependence of the bare detunings ν_0 and $\breve{\nu}_0$ can be expressed in terms of the physical detuning ν and $\breve{\nu}$, and the system reduces to the simple equations

$$\left[E - \nu - E_s^{\mathrm{mol}}(\boldsymbol{Q})\right] R_{kl}^s(\boldsymbol{q}) - g^2 \sum_{s'} \chi_{s'}^s R_{kl}^{s'}(\boldsymbol{q}) - g\breve{g} \sum_{t'} \tau_{t'}^s S_{kl}^{t'}(\boldsymbol{q}) = g\tilde{g}_{kl}^s(\boldsymbol{q}) \qquad (3.52)$$

$$\left[E - \breve{\nu} - E_s^{\mathrm{mol}}(\boldsymbol{Q})\right] S_{kl}^t(\boldsymbol{q}) - \breve{g}^2 \sum_{s'} \eta_{t'}^t S_{kl}^{t'}(\boldsymbol{q}) - g\breve{g} \sum_{s'} \tau_{s'}^t R_{kl}^{s'}(\boldsymbol{q}) = \breve{g}\tilde{g}_{kl}^t(\boldsymbol{q}). \qquad (3.53)$$

The matrices $\chi_{s'}^s$, $\eta_{t'}^t$ and $\tau_{t'}^s$ are describe the shift of the closed channels, due to the change in dispersion relation of the particle in the open channel. They have the form

$$\chi_{s'}^s = \sum_{nm} \int \frac{\mathrm{d}\boldsymbol{k}}{(2\pi)^3} \left[\frac{\tilde{g}_{nm}^s(\boldsymbol{k})\tilde{g}_{s'}^{nm}(\boldsymbol{k})}{E - E_{nm}(\boldsymbol{k},\boldsymbol{Q}) + \mathrm{i}\eta} + \frac{\hat{g}_{nm}^s(\boldsymbol{k})\hat{g}_{s'}^{nm}(\boldsymbol{k})}{\hat{E}_{nm}(\boldsymbol{k},\boldsymbol{Q})}\right] \qquad (3.54)$$

$$\eta_{t'}^t = \sum_{nm} \int \frac{\mathrm{d}\boldsymbol{k}}{(2\pi)^3} \left[\frac{\tilde{g}_{nm}^t(\boldsymbol{k})\tilde{g}_{t'}^{nm}(\boldsymbol{k})}{E - E_{nm}(\boldsymbol{k},\boldsymbol{Q}) + \mathrm{i}\eta} + \frac{\hat{g}_{nm}^t(\boldsymbol{k})\hat{g}_{t'}^{nm}(\boldsymbol{k})}{\hat{E}_{nm}(\boldsymbol{k},\boldsymbol{Q})}\right] \qquad (3.55)$$

$$\tau_{t'}^s = \sum_{nm} \int \frac{\mathrm{d}\boldsymbol{k}}{(2\pi)^3} \left[\frac{\tilde{g}_{nm}^s(\boldsymbol{k})\tilde{g}_{t'}^{nm}(\boldsymbol{k})}{E - E_{nm}(\boldsymbol{k},\boldsymbol{Q}) + \mathrm{i}\eta} + \frac{\hat{g}_{nm}^s(\boldsymbol{k})\hat{g}_{t'}^{nm}(\boldsymbol{k})}{\hat{E}_{nm}(\boldsymbol{k},\boldsymbol{Q})}\right]. \qquad (3.56)$$

Considering the regularization (2.47) again, one obtains that these expressions remain finite in the limit $\Lambda \to 0$. Therefore the theory is renormalized properly. The variables $\hat{E}_{nm}$ and $\hat{g}_s^{nm}$ are given by the free system in absence of the optical lattice and determine the shift of the physical detunings ν and $\breve{\nu}$

$$\nu = \nu_0 + g^2 \sum_{nm} \int \frac{\mathrm{d}\boldsymbol{k}}{(2\pi)^3} \frac{\hat{g}_{nm}^s(\boldsymbol{k})\hat{g}_{s'}^{nm}(\boldsymbol{k})}{\hat{E}_{nm}(\boldsymbol{k},\boldsymbol{Q})} R_{kl}^{s'}(\boldsymbol{q}) \qquad (3.57)$$

$$+ g\breve{g} \sum_{nm} \int \frac{\mathrm{d}\boldsymbol{k}}{(2\pi)^3} \frac{\hat{g}_{nm}^s(\boldsymbol{k})\hat{g}_{t'}^{nm}(\boldsymbol{k})}{\hat{E}_{nm}(\boldsymbol{k},\boldsymbol{Q})} S_{kl}^{t'}(\boldsymbol{q}) \qquad (3.58)$$

$$\breve{\nu} = \breve{\nu}_0 + g^2 \sum_{nm} \int \frac{\mathrm{d}\boldsymbol{k}}{(2\pi)^3} \frac{\hat{g}_{nm}^t(\boldsymbol{k})\hat{g}_{t'}^{nm}(\boldsymbol{k})}{\hat{E}_{nm}(\boldsymbol{k},\boldsymbol{Q})} S_{kl}^{t'}(\boldsymbol{q}) \qquad (3.59)$$

$$+ g\breve{g} \sum_{nm} \int \frac{\mathrm{d}\boldsymbol{k}}{(2\pi)^3} \frac{\hat{g}_{nm}^t(\boldsymbol{k})\hat{g}_{s'}^{nm}(\boldsymbol{k})}{\hat{E}_{nm}(\boldsymbol{k},\boldsymbol{Q})} R_{kl}^{s'}(\boldsymbol{q}). \qquad (3.60)$$

With an exact ansatz for the Bloch waves (3.33-3.35) and numerical calculations the matrices (3.54-3.56) can be determined. One obtains an equations system for the molecular wave functions $R_{kl}^s(\boldsymbol{q})$ and $S_{kl}^t(\boldsymbol{q})$. The poles of the determinant of the homogeneous equation system determine the energies of the bound states of atoms pairs.

For ultra-cold gases with weak interactions one can restrict the calculations to the lowest Bloch band, which simplifies the calculations enormously. As mentioned above, the on-site repulsion of two particles was replaced by a wide Feshbach resonance, formally obtained in the limit $\breve{g} \to \infty$ and $\breve{\nu} \to \infty$ with a fixed ratio $\breve{g}^2/\breve{\nu}$. Therefore, it is a valid approximation to replace $\breve{g}^2/[E - \breve{\nu} - E_s^{\mathrm{mol}}] \sim \breve{g}^2/\breve{\nu}$, which is directly related with the background scattering length

$$\frac{\breve{g}^2}{\breve{\nu}} = -a_{\mathrm{bg}} \frac{2\pi\hbar^2}{\mu}. \qquad (3.61)$$

and therefore with the on-site interaction (2.99).

$$U = a_{\text{bg}} \frac{2\pi\hbar^2}{\mu} \int \mathrm{d}\boldsymbol{z} \, |w_0^x(\boldsymbol{z})|^2 \, |w_0^y(\boldsymbol{z})|^2 = -\frac{\breve{g}^2}{\breve{\nu}} \int \mathrm{d}\boldsymbol{z} \, |w_0^x(\boldsymbol{z})|^2 \, |w_0^y(\boldsymbol{z})|^2 \qquad (3.62)$$

with $w_0^\alpha(\boldsymbol{z})$ the Wannier functions of the particles in the lowest Bloch band.

3.3. Artificial nearest neighbour interaction in the Bose Hubbard model

In the following, we suggest a model system which provides for an artificial nearest neighbour interaction between atoms in an optical lattice. The dynamics of ultra-cold atoms, trapped in an optical lattice is well described by the Bose Hubbard model, which usually does not consider nearest neighbour interaction, due to the rapid decrease of the atoms wave functions [sec. 2.5 and 2.7].

We consider a second order process, which allows atoms on neighbouring lattice site to lower their energy, due to a resonant coupling to a molecular state, living on a second optical lattice, shifted by half the lattice spacing [fig. 3.3]. The consequence is a effective nearest neighbour interaction. The coupling can be associated with an artificial Feshbach resonance between two atoms on neighbouring lattice sites.
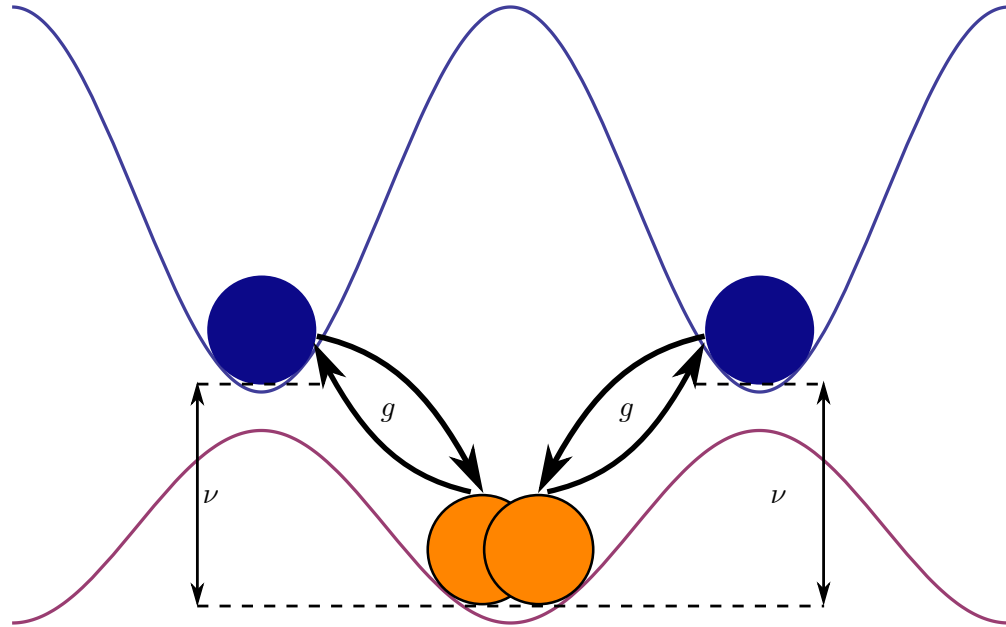
Figure 3.3.: Two atoms on neighbouring lattice sites, are coupled (coupling parameter g) to a molecular state with a detuning ν, living on a second overlaid and shifted lattice.

The Hamiltonian describing the system is

$$
\begin{aligned}
\hat{\mathrm{H}} = & -J \sum_{<i,j>} \hat{b}_i^\dagger \hat{b}_j + \frac{U}{2} \sum_i \hat{n}_i \left(\hat{n}_i - 1 \right) \\
& + g \sum_{<i,j>} \left(\hat{b}_i \hat{b}_j \hat{m}_{<i,j>}^\dagger + \hat{b}_i^\dagger \hat{b}_j^\dagger \hat{m}_{<i,j>} \right) - \nu \sum_{<i,j>} \hat{m}_{<i,j>}^\dagger \hat{m}_{<i,j>},
\end{aligned}
\tag{3.63}
$$

with g the coupling parameter, ν the detuning of the molecular state and $\hat{m}_{<i,j>}$ ($\hat{m}^{\dagger}_{<i,j>}$) the annihilation (creation) operator of the molecular state between neighbouring lattice i and j. Since the system's interactions properties are dominated by two particle interactions, it is interesting to investigate the two particle problem of this Hamiltonian. As already mentioned in [sec. 3.1], it is convenient to perform the calculations in the first quantization formalism. The two particle atomic state is called the open channel and is denoted by the wave function $\psi(\boldsymbol{x}, \boldsymbol{y})$, where $\boldsymbol{x} = \sum_i^d x_i \boldsymbol{a}_i$ and $\boldsymbol{y} = \sum_i^d y_i \boldsymbol{a}_i$ are the position of the particles in the optical lattice, spanned by the primitive vector $\boldsymbol{a}_i$. The molecular state is the closed channel, an is denoted by the wave function $\phi(\boldsymbol{z})$, where $\boldsymbol{z}$ is the position of the to molecule coupled atoms in the second optical lattice. Then the Schrödinger equation is

$$\left\{ -J \left[\tilde{\Delta}^{\boldsymbol{0}}_{\boldsymbol{x}} + \tilde{\Delta}^{\boldsymbol{0}}_{\boldsymbol{y}} \right] + U \delta_{\boldsymbol{x},\boldsymbol{y}} \right\} \psi(\boldsymbol{x}, \boldsymbol{y})$$
$$+ g \sum_{\boldsymbol{x},\boldsymbol{y}} \left(\delta_{\boldsymbol{x},\boldsymbol{y}+\boldsymbol{a}} + \delta_{\boldsymbol{x},\boldsymbol{y}-\boldsymbol{a}} \right) \phi(\boldsymbol{z}) = E \psi(\boldsymbol{x}, \boldsymbol{y}) \tag{3.64}$$

$$\nu \phi(\boldsymbol{z}) + g \sum_{\boldsymbol{x},\boldsymbol{y}} \left(\delta_{\boldsymbol{x},\boldsymbol{y}+\boldsymbol{a}} + \delta_{\boldsymbol{x},\boldsymbol{y}-\boldsymbol{a}} \right) \psi(\boldsymbol{x}, \boldsymbol{y}) = E \phi(\boldsymbol{z}), \tag{3.65}$$

with $\boldsymbol{a} = x_1 \boldsymbol{a}_1 + y \boldsymbol{a}_2 + z \boldsymbol{a}_3$ a lattice vector. It is reasonable to introduced relative (2.1) and center of mass coordinates (2.2). Then the atomic and molecular wave functions reduce to

$$\psi(\boldsymbol{x}, \boldsymbol{y}) = \mathrm{e}^{\mathrm{i}\boldsymbol{Q}\cdot\boldsymbol{R}} \psi(\boldsymbol{r}) \tag{3.66}$$

$$\phi(\boldsymbol{z}) = \mathrm{e}^{\mathrm{i}\boldsymbol{Q}\cdot\boldsymbol{R}} \chi. \tag{3.67}$$

The energy of the center of mass motion is a constant, therefore the system reduces to a problem for the relative coordinate only. With the new coordinates the Schrödinger equation system is

$$\left[E + 2J\tilde{\Delta}^{\boldsymbol{Q}}_{\boldsymbol{r}} \right] \psi(\boldsymbol{r}) = U \delta_{\boldsymbol{r},\boldsymbol{0}} + g\chi \sum_{\boldsymbol{r}} \left(\delta_{\boldsymbol{r},\boldsymbol{a}} + \delta_{\boldsymbol{r},-\boldsymbol{a}} \right) \tag{3.68}$$

$$\left[E - \nu \right] \chi = g \sum_{\boldsymbol{r}} \psi(\boldsymbol{r}) \left(\delta_{\boldsymbol{r},\boldsymbol{a}} + \delta_{\boldsymbol{r},-\boldsymbol{a}} \right). \tag{3.69}$$

At first, it is reasonable to solve the problem for the special case $U = 0$. The solution for equation (3.68) with $U = 0$ is

$$\psi(\boldsymbol{r}) = \psi_0(\boldsymbol{r}) + g\chi \left[G(\boldsymbol{r} - \boldsymbol{a}) + G(\boldsymbol{r} + \boldsymbol{a}) \right], \tag{3.70}$$

where $\psi_0(\boldsymbol{r}) = \exp\left(\mathrm{i} \boldsymbol{q}_0 \cdot \boldsymbol{a} \right)$ is the homogeneous and $g\chi \left[G(\boldsymbol{r} - \boldsymbol{a}) + G(\boldsymbol{r} + \boldsymbol{a}) \right]$ the inhomogeneous solution. Equation (3.69) yields a solution for χ

$$\chi = \frac{2g \sum_i^d \cos\left(q_{0i} a \right)}{E - \nu - 2g^2 \left[G(\boldsymbol{0}) + G(2\boldsymbol{a}) \right]}. \tag{3.71}$$

3. Two particle interaction properties in an optical lattice

Therefore the final result[3] for the atomic wave function $\psi(\boldsymbol{r})$ is

$$\psi(\boldsymbol{r}) = \mathrm{e}^{\mathrm{i}\boldsymbol{q}_0 \cdot \boldsymbol{r}} + \frac{4g^2 \sum_i^d \cos(q_{0i}a)}{E - \nu - 2g^2 \left[G(\boldsymbol{0}) + G(2\boldsymbol{a}) \right]} G(\boldsymbol{r}), \tag{3.72}$$

with the scattering amplitude

$$f(\boldsymbol{q}, \boldsymbol{q}_0) = \frac{4g^2 \sum_i^d \cos(q_{0i}a)}{E - \nu - 2g^2 \left[G(\boldsymbol{0}) + G(2\boldsymbol{a}) \right]} \tag{3.73}$$

Determining the poles of the scattering amplitude gives rise to localized bound states of atom pairs.

$$E - \nu - 2g^2 \left[G(\boldsymbol{0}) + G(2\boldsymbol{a}) \right] = 0 \tag{3.74}$$

The Green's function

$$G(\boldsymbol{r}) = \int \frac{\mathrm{d}\boldsymbol{q}}{v_0} \frac{\mathrm{e}^{\mathrm{i}\boldsymbol{q}\cdot\boldsymbol{r}}}{E - 4J \sum_i^d \cos\frac{Q_i a}{2} \left[1 - \cos(q_i a) \right] + \mathrm{i}\eta} \tag{3.75}$$

depends on the energy E and is not solvable analytically. The function

$$\tilde{G}(E) := \left[G(\boldsymbol{0}) + G(2\boldsymbol{a}) \right] = \int \frac{\mathrm{d}\boldsymbol{q}}{v_0} \frac{1 + \mathrm{e}^{2\mathrm{i}\boldsymbol{q}\cdot\boldsymbol{a}}}{E - 4J \sum_i^d \cos\frac{Q_i a}{2} \left[1 - \cos(q_i a) \right] + \mathrm{i}\eta}$$

$$= \int \frac{\mathrm{d}\boldsymbol{q}}{v_0} \frac{2 \sum_i \cos^2(q_i a)}{E - 4J \sum_i^d \cos\frac{Q_i a}{2} \left[1 - \cos(q_i a) \right] + \mathrm{i}\eta} \tag{3.76}$$

makes most of the problems, because it can not be solved analytically. Therefore we introduce the dimensionless energy $\gamma = E/2J$ and obtain

$$\alpha(\gamma) = \frac{\tilde{G}(E)}{2J} = \int \frac{\mathrm{d}\boldsymbol{q}}{v_0} \frac{2 \sum_i \cos^2(q_i a)}{\gamma - 2 \sum_i^d \cos\frac{Q_i a}{2} \left[1 - \cos(q_i a) \right] + \mathrm{i}\eta}. \tag{3.77}$$

We calculate the function $\alpha(\gamma)$ for a constant quasi-momentum $\boldsymbol{Q}$ and search the intersection with the function $\beta(\gamma) = \gamma/4g^2 - \tilde{\nu}/4g^2$, with a given coupling constant g and reduced detuning $\tilde{\nu} = \nu/2J$. By performing this step for all quasi-momentum $\boldsymbol{Q}$ within the first Brillouin zone, we can determine the Bloch bands of bound atom pairs.

As shown in [fig 3.4], $\alpha(\gamma)$ takes a constant value as it converges to the edges of the scattering band. This gives rise to the possibility, that it intersects only once with $\beta(\gamma)$ or not even, depending on the detuning $\tilde{\nu}$ and on the coupling g^2, giving the slope for $\beta(\gamma)$. This is only the case in three dimensions. In one and two dimensions $\alpha(\gamma)$ diverges, due to the characteristics of the dispersions realtion $\varepsilon_{\boldsymbol{Q}}(\boldsymbol{q})$. In one dimension the integral diverges with $1/q$ and in two dimension it diverges logarithmically. Therefore we can find two, one or even no Bloch band of bound atom pairs. The last case is rather improbable, as the slope of $\beta(\gamma)$ is usually very flat.

---

[3]A more detailed calculation can be found in the appendix [B.4].

In the limit of a wide resonant coupling, i.e. $g \to \infty$, $\nu \to \infty$ and $g^2/\nu \to$ const., the scattering amplitude reduces to

$$f(\boldsymbol{q}, \boldsymbol{q}_0) = \frac{-\frac{4g^2}{\nu} \sum_i^d \cos(q_{0i}a)}{1 + \frac{2g^2}{\nu} [G(\boldsymbol{0}) + G(2\boldsymbol{a})]}. \tag{3.78}$$

The comparison with the scattering amplitude of the two particle problem with nearest neighbour interaction only [B.3] gives rise to an effective nearest neighbour interaction parameter

$$V_{\text{eff}} = -\frac{4g^2}{\nu}. \tag{3.79}$$

In this case, $\beta(\gamma)$ looses its dependency of γ and its slope.

$$1 + \frac{2g^2}{\nu}[G(\boldsymbol{0}) + G(2\boldsymbol{a})] \Longrightarrow \frac{\tilde{\nu}}{4g^2} - \alpha(\gamma) = 0 \tag{3.80}$$

As a consequence, only one bound state occurs.

The statement of equation (3.79) can be confirmed with second order perturbation theory. The terms in the Hamiltonian (3.63), describing the coupling to the molecular states and their detuning, can be interpreted as a disturbance. We calculate the matrix element

$$\left\langle a \middle| \hat{H} \middle| b \right\rangle = E\delta_{a,b} + \left\langle a \middle| \hat{H}_1 \middle| b \right\rangle + \frac{1}{2} \sum_k \left\langle a \middle| \hat{H}_1 \middle| k \right\rangle \left\langle k \middle| \hat{H}_1 \middle| b \right\rangle \left[\frac{1}{E_a - \nu} + \frac{1}{E_b - \nu} \right], \tag{3.81}$$

with

$$\hat{H}_1 = g \sum_{<\alpha,\beta>} \left(b_\alpha b_\beta m^\dagger_{<\alpha,\beta>} + b^\dagger_\alpha b^\dagger_\beta m_{<\alpha,\beta>} \right), \tag{3.82}$$

and the states $|a\rangle = b^\dagger_i b^\dagger_j |0\rangle$, $|b\rangle = b^\dagger_s b^\dagger_t |0\rangle$ and $|k\rangle = m^\dagger_{<m,n>} |0\rangle$. The term $\left\langle a \middle| \hat{H}_1 \middle| b \right\rangle$ is solved easily

$$\left\langle a \middle| \hat{H}_1 \middle| b \right\rangle = \langle 0 | b_i b_i | g \sum_{<\alpha,\beta>} \left(b_\alpha b_\beta m^\dagger_{<\alpha,\beta>} + b^\dagger_\alpha b^\dagger_\beta m_{<\alpha,\beta>} \right) |b^\dagger_s b^\dagger_t |0\rangle = 0. \tag{3.83}$$

We obtain for the matrix element

$$\begin{aligned} \left\langle a \middle| \hat{H}_1 \middle| k \right\rangle &= \langle 0 | b_i b_j | g \sum_{<\alpha,\beta>} \left(b_\alpha b_\beta m^\dagger_{<\alpha,\beta>} + b^\dagger_\alpha b^\dagger_\beta m_{<\alpha,\beta>} \right) |m^\dagger_{<m,n>} |0\rangle \\ &= \langle 0 | b_i b_j | g \sum_{<\alpha,\beta>} b_i b_j b^\dagger_\alpha b^\dagger_\beta m_{<\alpha,\beta>} |m^\dagger_{<m,n>} |0\rangle \\ &= \langle 0 | b_i b_j | g \; (\delta_{im}\delta_{jn} + \delta_{in}\delta_{jm}) \, b^\dagger_m b^\dagger_n m_{<m,n>} m^\dagger_{<m,n>} |0\rangle = 2g \end{aligned} \tag{3.84}$$

By inserting this in equation (3.81), we obtain in the limit of a wide resonant

$$\left\langle i \middle| \hat{H} \middle| j \right\rangle = E - \frac{4g^2}{\nu}, \tag{3.85}$$

3. Two particle interaction properties in an optical lattice

(a) A negative detuning yields a repulsive nearest neighbour interaction.

(b) A positive detuning yields an attractive nearest neighbour interaction.
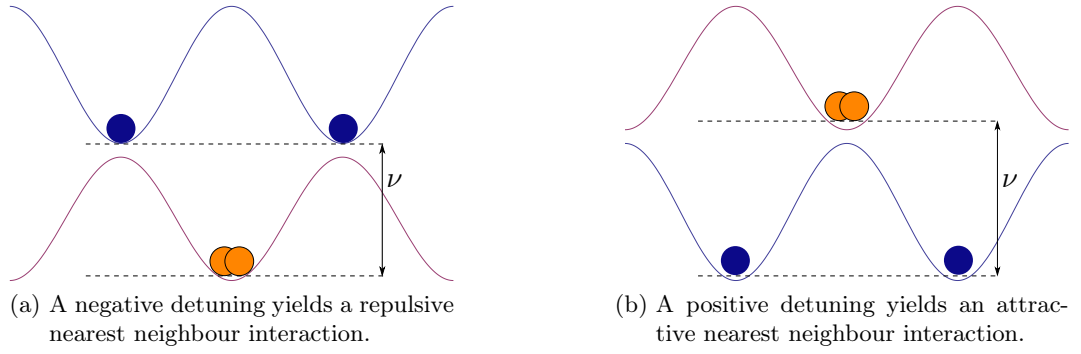
which is obviously the same result as in (3.79).

The sign of the effective nearest neighbour interaction is determined by the sign of the detuning. A positiv detuning gives rise to an attractive nearest neighbour interaction and vice versa a negative detuning gives rise to an repulsive nearest neighbour interaction.

$$V_{eff} = -\frac{4g^2}{\nu} \left\{ \begin{array}{l} < 0 \text{ for } \nu > 0 \\ > 0 \text{ for } \nu < 0. \end{array} \right. \tag{3.86}$$

In case of negative detuning ν, the detuning has to be large, as the real ground state of the system is the molecular state. For a small detuning the atoms can collapse into the molecular state (This circumstance is used in [sec. 4]), as for a large detuning the atoms cannot loose their energy, hence the molecular state is only virtual occupied intermediated state, the atoms transit in a second order process.
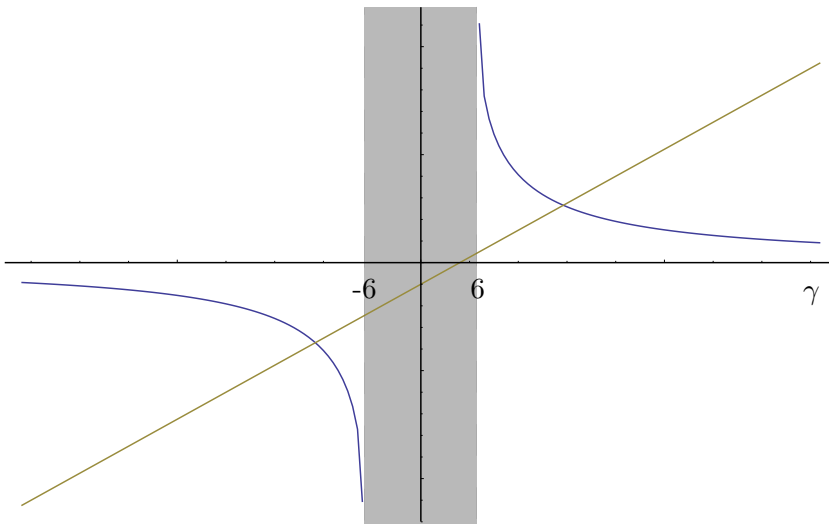
Figure 3.4.: The figure shows the behaviour of equation (3.74) for a center of mass quasi-momentum of $\boldsymbol{Q} = 0$. The blue curve shows the function $\alpha(\gamma)$, with no values within the scattering band within $-6 < \gamma < 6$. At the edges of the scattering band, the function converges in 3D to a constant value, but in 1D and 2D it diverges. The orange curve is the function $\beta(\gamma)$. The cross point of both function determine the energies of the bound states.
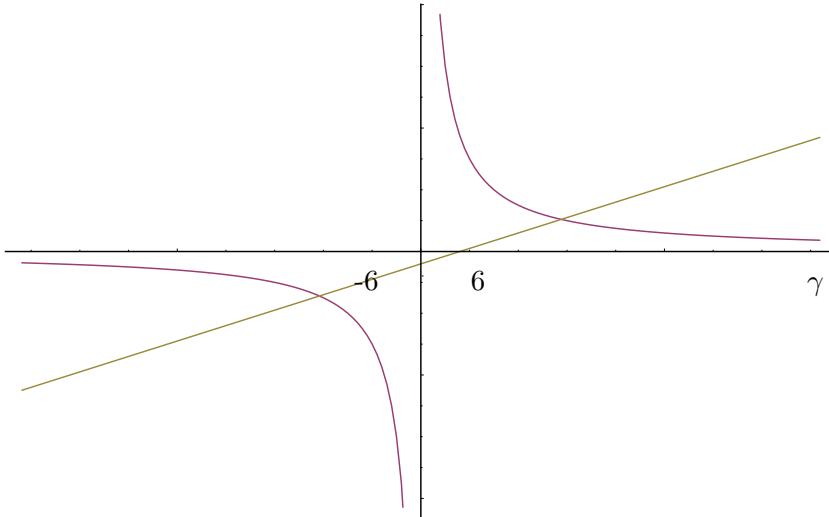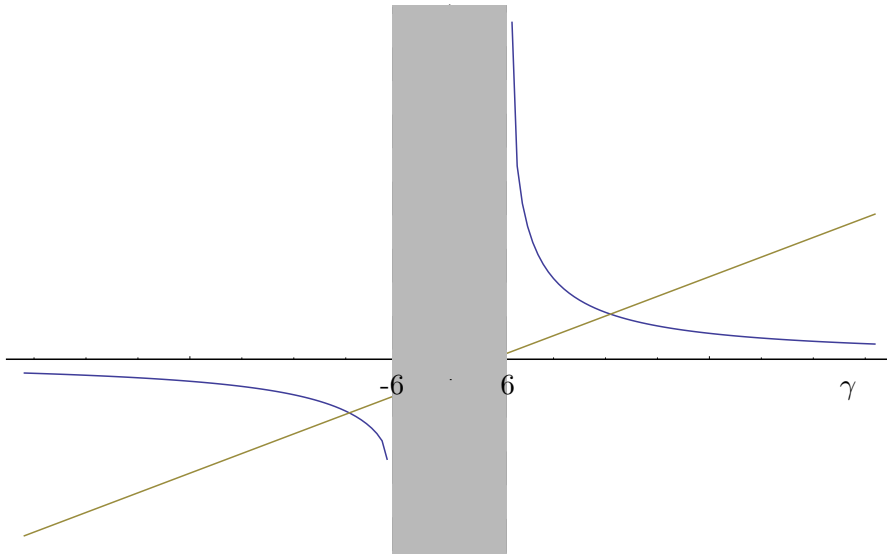

Figure 3.5.: The figure shows the behaviour of equation (3.74) for a center of mass quasi-momentum of $\boldsymbol{Q} = \pi/a$. Here the width of the scattering band is zero and the function $\alpha(\gamma)$ diverges for $\gamma \to 0^{\pm}$.
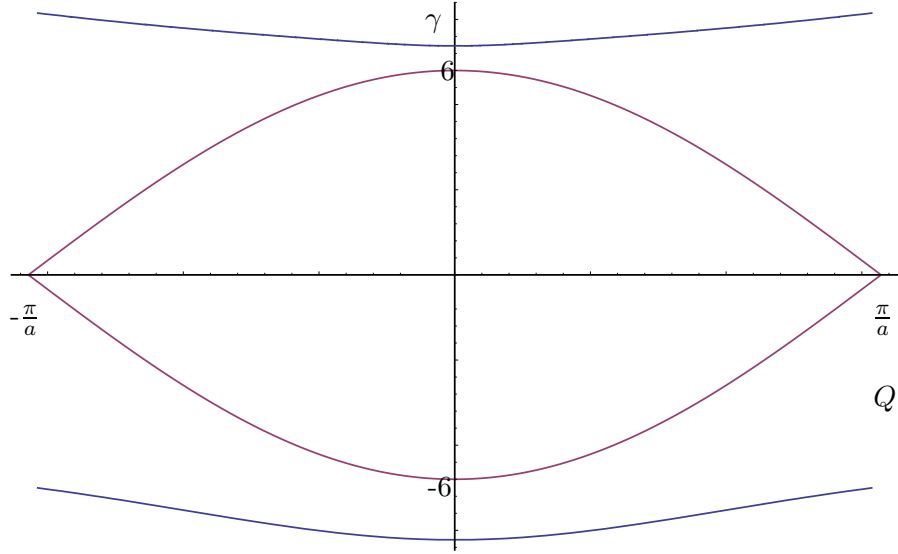
3. Two particle interaction properties in an optical lattice
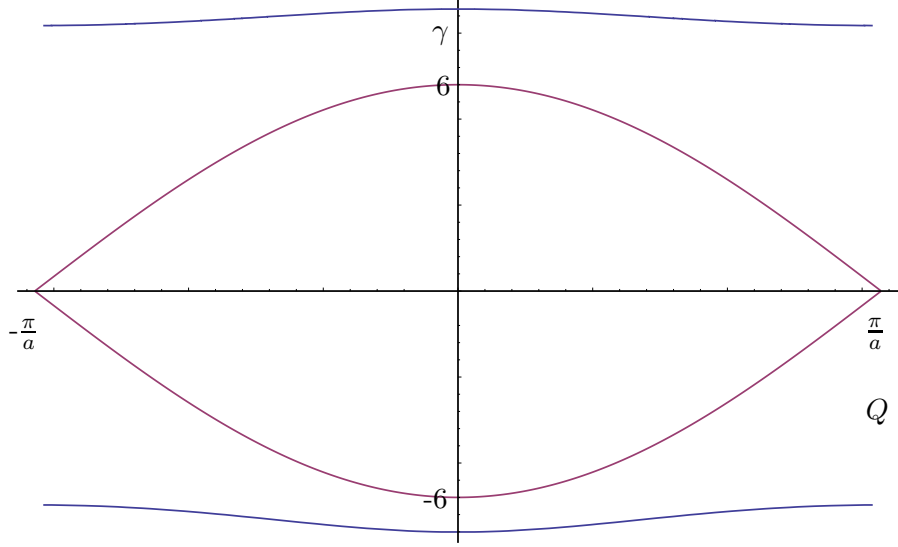
Figure 3.6.: This figure (blue curve) show the Bloch band of bound atom pairs only with artificial nearest neighbour interaction, above the scattering continuum, indicated by the purple graph.

In the case of $U \neq 0$ the solution of equation (3.68) is

$$\psi(\boldsymbol{r}) = \psi_0(\boldsymbol{r}) + G(\boldsymbol{r})U\psi(\boldsymbol{0}) + g\chi\left[G(\boldsymbol{r}-\boldsymbol{a}) + G(\boldsymbol{r}+\boldsymbol{a})\right], \tag{3.87}$$

where $\psi_0(\boldsymbol{r}) = \exp\left(\mathrm{i}\boldsymbol{q}_0 \cdot \boldsymbol{a}\right)$ is the homogeneous and $G(\boldsymbol{r})U\psi(\boldsymbol{0}) + g\chi\left[G(\boldsymbol{r}-\boldsymbol{a}) + G(\boldsymbol{r}+\boldsymbol{a})\right]$ the inhomogeneous solution. The wave function χ of the molculare state is

$$\chi = \frac{2g\sum_i^d \cos\left(q_{0i}a\right) + \frac{2gG(\boldsymbol{0})U}{1-G(\boldsymbol{0})U}}{E - \nu - 2g^2\left[G(2\boldsymbol{a}) + G(\boldsymbol{0})\right] - \frac{2g^2G(\boldsymbol{a})}{1-G(\boldsymbol{0})U}}. \tag{3.88}$$

The final result[4] for the two particle wave function $\psi(\boldsymbol{r})$ is

$$\psi(\boldsymbol{r}) = \mathrm{e}^{\mathrm{i}\boldsymbol{q}_0 \cdot \boldsymbol{r}} + \frac{U}{1-G(\boldsymbol{0})U}G(\boldsymbol{r}) +$$

$$+ \left[\frac{UG(\boldsymbol{a})}{1-G(\boldsymbol{0})U} + 1\right]\frac{4g^2\sum_i^d \cos\left(q_{0i}a\right) + \frac{4g^2G(\boldsymbol{0})U}{1-G(\boldsymbol{0})U}}{E - \nu - 2g^2\left[G(2\boldsymbol{a}) + G(\boldsymbol{0})\right] - \frac{2g^2G(\boldsymbol{a})}{1-G(\boldsymbol{0})U}}G(\boldsymbol{r}), \tag{3.89}$$

with the scattering amplitude

$$f(\boldsymbol{q},\boldsymbol{q}') = \frac{U}{1-G(\boldsymbol{0})U} + \left[\frac{UG(\boldsymbol{a})}{1-G(\boldsymbol{0})U} + 1\right]\frac{4g^2\sum_i^d \cos\left(q_{0i}a\right) + \frac{4g^2G(\boldsymbol{0})U}{1-G(\boldsymbol{0})U}}{E - \nu - 2g^2\left[G(2\boldsymbol{a}) + G(\boldsymbol{0})\right] - \frac{2g^2G(\boldsymbol{a})}{1-G(\boldsymbol{0})U}}. \tag{3.90}$$

---

[4] A more detailed calculation can be found in the appendix [B.7].

The energies of the bound states have changed, due to the additional on-site interaction. The condition is now

$$E - \nu - 2g^2 \left[G(2\boldsymbol{a}) + G(\boldsymbol{0}) \right] - \frac{2g^2 G(\boldsymbol{a})}{1 - G(\boldsymbol{0})U} = 0, \tag{3.91}$$

with the additional term $2g^2 G(\boldsymbol{a})/(1 - G(\boldsymbol{0})U)$, which leads to an shift of the energies of the bound states.

Figure 3.7.: The figure shows the behaviour of equation (3.91) for a center of mass quasi-momentum of $\boldsymbol{Q} = 0$. Here is the width of the scattering band $-6 < \gamma < 6$ and the function $\alpha(\gamma) - 2g^2 G(\boldsymbol{a})/(1 - G(\boldsymbol{0})U)$ converges for $\gamma \to \pm 6$ to a constant value. Due to the on-site interaction, the curve is shifted to the top.

Figure 3.8.: This figure (blue curve) shows the Bloch band of bound atom pairs with on-site interaction U and artificial nearest neighbour interaction, above the scattering continuum, indicated by the purple graph.

3.3.1. Proposal for an experimental setup

We propose an experimental setup with ^{87}Sr [fig. 3.11] atoms in two different states trapped in two independent optical lattices. The Sr atoms are prepared in the $^3P_1$ state and trapped in an optical lattice with a lattice constant of 532 nm. They are coupled to the $^1S_0$ state, which is trapped in an optical lattice with a constant of 376.2 nm. The lattices are generated by laser beams with a wavelength of 1064 nm (A) and 532 nm (B), respectively.
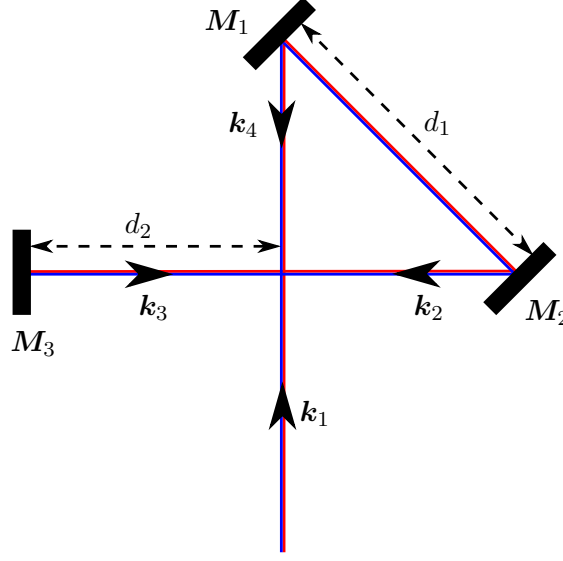
Figure 3.9.: This figure shows the optical path of the laser beams, which generate the two independent optical lattice, needed for an experiment.

It intersects the position of the atom cloud four times. The incoming beam with a wave vector $\boldsymbol{k}_{\alpha 1}$ (with α indicating the laser beam A or B) is intersects the atom cloud, is then reflected by the mirror $\boldsymbol{M}_1$, and after travelling an effective distance d_1 (possible phase shifts from the mirrors are included) it is reflected by the mirror $\boldsymbol{M}_2$ and returns to the cloud with a wave vector $\boldsymbol{k}_{\alpha 2}$. Behind the cloud the beam is reflected again by the mirror $\boldsymbol{M}_3$ and returns again with the wave vector $\boldsymbol{k}_{\alpha 3} = -\boldsymbol{k}_{\alpha 2}$. After passing the mirrors $\boldsymbol{M}_2$ and $\boldsymbol{M}_1$ again, it intersects the atom cloud a fourth time with the $\boldsymbol{k}_{\alpha 4} = -\boldsymbol{k}_{\alpha 1}$. The total electric field for this two dimensional lattice is given by $\mathrm{Re}\left[\boldsymbol{E}_\alpha(x,y)\mathrm{e}^{\mathrm{i}\omega t}\right]$, where

$$
\begin{aligned}
\boldsymbol{E}_\alpha(x,y) =& E_{\alpha 1}\mathrm{e}^{\mathrm{i}\boldsymbol{k}_{\alpha 1}\cdot\boldsymbol{r}}\hat{e}_{\alpha 1} + E_{\alpha 2}\mathrm{e}^{\mathrm{i}\left(d_1\frac{2\pi}{\lambda_\alpha}+\boldsymbol{k}_{\alpha 2}\cdot\boldsymbol{r}\right)}\hat{e}_{\alpha 2} \\
&+E_{\alpha 3}\mathrm{e}^{\mathrm{i}\left(d_1\frac{2\pi}{\lambda_\alpha}+\boldsymbol{k}_{\alpha 3}\cdot\boldsymbol{r}+d_2\frac{4\pi}{\lambda_\alpha}\right)}\hat{e}_{\alpha 3} + E_{\alpha 4}\mathrm{e}^{\mathrm{i}\left(d_1\frac{4\pi}{\lambda_\alpha}+\boldsymbol{k}_{\alpha 4}\cdot\boldsymbol{r}+d_2\frac{4\pi}{\lambda_\alpha}\right)}\hat{e}_{\alpha 4},
\end{aligned}
\tag{3.92}
$$

with $\boldsymbol{r} = x\boldsymbol{e}_x + y\boldsymbol{e}_y$ and $\hat{e}_{\alpha i}$ the polarization vectors. The lattices are topologically stable to vibrational motion of the mirrors, as the beams retrace the same path and there are only two independent phases between the the four beams of a wave length. Variations in d_1 and d_2 result in a simple translation of the lattices. We consider the ideal situation of four equal beam intensities ($E_{\alpha i} = E_\alpha$). The polarization vectors of the laser beam with the wave length $\lambda_A =$1054 are all in-the-plane, $\hat{e}_{A1} = \hat{e}_{A4} = \boldsymbol{e}_y$ and $\hat{e}_{A2} = \hat{e}_{A3} = \boldsymbol{e}_x$. The resulting electric field is given by

$$
\boldsymbol{E}_A(x,y) = E_A\left[\left(\mathrm{e}^{\mathrm{i}kx} + \mathrm{e}^{\mathrm{i}\frac{2\pi}{\lambda_A}(2d_1+2d_2-x)}\right)\boldsymbol{e}_y + \left(\mathrm{e}^{\mathrm{i}\frac{2\pi}{\lambda_A}(-y+d_1)} + \mathrm{e}^{\mathrm{i}\frac{2\pi}{\lambda_A}(d_1+2d_2+y)}\right)\boldsymbol{e}_x\right].
\tag{3.93}
$$

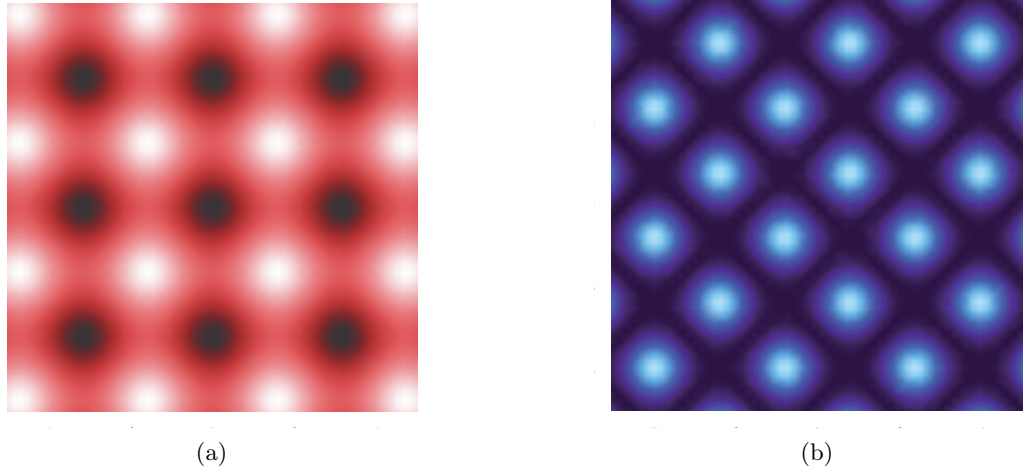The resulting optical lattice pattern is shown in [fig. 3.10a].

(a)

(b)

Figure 3.10.: Intensities patterns for in-plane and out-of-plane polarizations. Due to the smaller wave length λ_B, the sites of lattice B fit perfect between the sites of lattice A. The lattice spacings are a_A =532 nm and a_B =376.2 nm.

The polarization vectors of the second laser beam B are out of plane, i.e. $\hat{e}_{Bi} = \mathbf{z}$. The electric field is given by

$$\boldsymbol{E}_B(x,y) = E_B \left(e^{i\frac{2\pi}{\lambda_B}x} + e^{i\frac{2\pi}{\lambda_B}(2d_1+d_2-x)} + e^{i\frac{2\pi}{\lambda_B}(-y+d_1)} + e^{i\frac{2\pi}{\lambda_B}(d_1+d_2+y)} \right), \qquad (3.94)$$

and the optical lattice pattern is shown in [fig. 3.10b]. The lattice spacing of lattice A is $a_A = \lambda_A/2$ and of lattice B is $a_B = \lambda_B/\sqrt{2} = \lambda_A/2\sqrt{2}$. The relative position of the two lattices can be shifted by a polarization dependend wave plate. The coupling between the two states can be achieved by a stimulated Raman passagem (STIRAP).
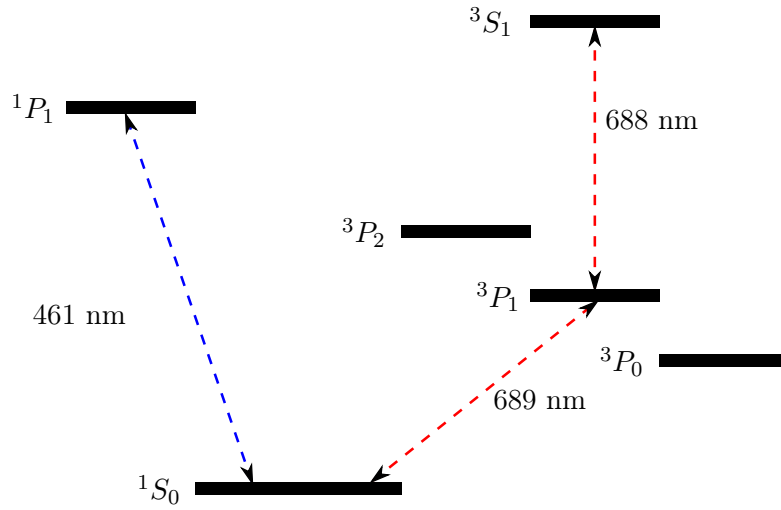
Figure 3.11.: Energy levels of ^{87}Sr of interest.

3. Two particle interaction properties in an optical lattice

4. Many body physics

Up to now, we have investigated the two particle interactions of atoms in an ultra-cold dilute gases in an optical lattice. The properties of the two particle problem of the standard Bose Hubbard Hamiltonian (2.96) were summarized, and the influence of a Feshbach resonance, allowing the tuning of the on-site interaction parameter, was analysed. After that, we suggested a model system, which gave rise to an artificial nearest neighbour interaction and hence extended the Bose Hubbard model by an additional nearest neighbour interaction term.

The next step is to apply this novel and particular nearest neighbour interaction onto many body problems and analyse whether new quantum phase of an ultra-cold quantum gases are possible.

As shown by mean field calculations [5], the quantum phases of an ultra-cold gas in an three-dimensional optical lattice, described by the Bose Hubbard Modell, are a Mott-insulator and a superfluid phase. A strong interaction parameter, compared to the kinectic energy of the atoms, yields a localized particle wave funciton, which is conditional for the Mott-insulator phase. The superfluid phase is characterized by its macroscopic wavefunction and off-diagonal longrange order.

In 2004 Sengupta *et al.* [14] investigated the extended Bose Hubbard model on a d-dimensional hypercubic lattice with repulsive on-site and nearest neighbour interaction. They analysed the stability of crystalline and supersolid orders of bosons. A supersolid phase exhibits, additionally to the off-diagonal longrange order, diagonal longrange order. They showed under which conditions checkerboard super solids are unstable and how they can be stabilized with large but infinte on-site and nearest neighbour energies. Their exact arguments are supported by quantum Monte Carlo simulations of a two dimensional extended Bose Hubbard model.

In the zero-hopping limit and at half-filling $\rho = 1/2$ the potential energy ($U, V > 0$) is minimized by the crystal state with one sublattice occupied (ckeckerboard pattern). In the presence of a small hopping, $J \ll U, V$ the state remains stable, due to a gap. The energy gain per boson is $\Delta E \approx zJ^2/[(z-1)V]$, with $z = 2d$ the coordinance. Introducing holes or doping the $\rho = 1/2$ crystal leads to an instability and to a planar domain wall formation. A hole doping might lead to a phase seperation between the commensurate crystal at $\rho = 1/2$ and a uniform superfluid with $\rho < 1/2$. Doping with additional bosons can lead to again to a planar domain wall ($U = zV \gg J > 0$) which destabilise the checkerboard crystal order or a superfluid on top of a density-wave background and hence a supersolid ($zV \gtrsim U$). At a filling density $\rho = 1$ can either be a uniform Mott insulator phase with boson per lattice site ($U > zV$), or an orderd solid with two bosons per site on one sublattice ($U < zV$). Figure [fig. 4.1] shows a sketch of the phase diagram for the two-dimensional extended Bose Hubbard model with on-site and nearest
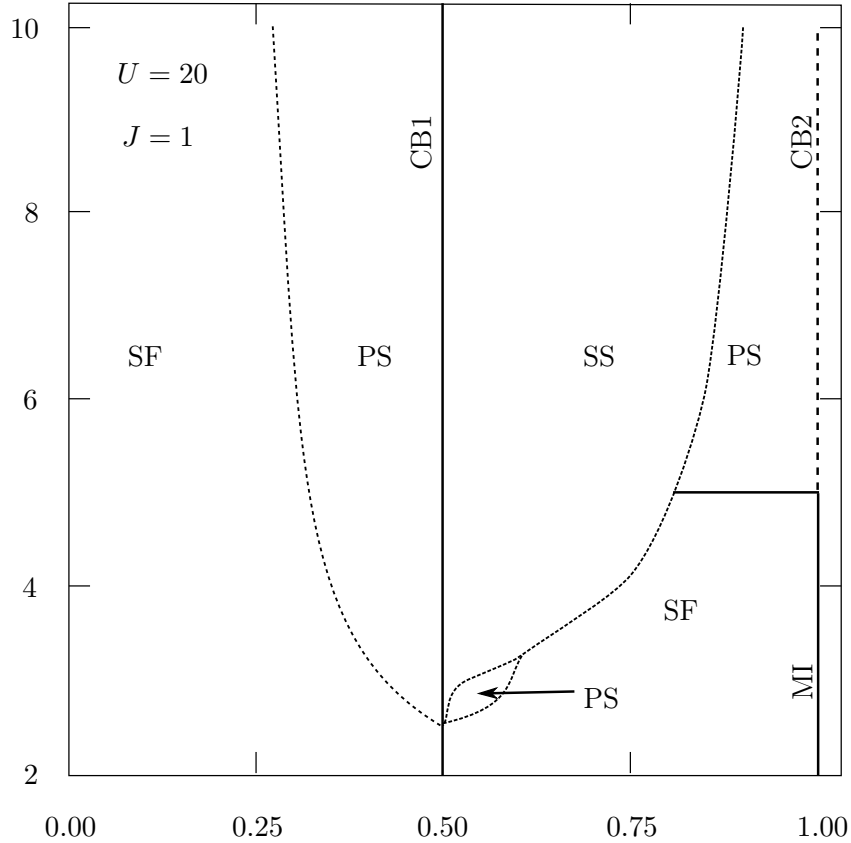
Figure 4.1.: the ground state phase diagram of the two-dimensional extended Bose Hubbard model in the $V - \rho$ plane for $U/J - 20$ and densities $0 \leq \rho \leq 1$. The figure shows superfluid (SF) phases, checkerboard solids formed by single bosons (CB1) and pairs of bosons (CB2), a Mott-insulating phase (MI), phase separation (PS) and a supersolid phase (SS).

neighbour interaction, based on the data of [14].

In this chapter we will apply our results of the previous chapter on a ultra-cold bosonic quantum gas in an two-dimensional optical lattice and analyse if we get the same results with the particular nearest neighbour interactions introduced in [sec. 3.3]. We use the same system geometry as in [sec. 3.3]. Bosonic atoms in an optical lattice (in the following Σ_1) are coupled to a molecular state, living on a second optical lattice (Σ_2), shifted about half the lattice spacing of lattice Σ_1 and rotated about an angle of 45 degrees.

We choose a large negative detuning ν of the molecular state and a large coupling g, so the system merges to a molecular Bose-Einstein condensate. The system's dynamic can
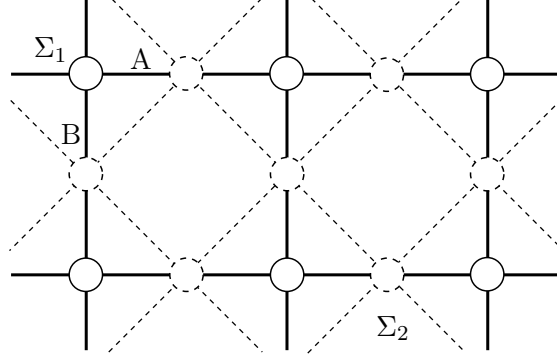
Figure 4.2.: The Figure shows the both optical lattice Σ_1 and Σ_2 (dashed lines). The horizontal links of lattice Σ_1 are indicated as A, the vertical as B.

be described by the Hamiltonian (3.63)

$$
\begin{aligned}
\hat{H} = & - J \sum_{<i,j>} \hat{b}_i^\dagger \hat{b}_j + \frac{U}{2} \sum_i \hat{n}_i \left(\hat{n}_i - 1 \right) \\
& + g \sum_{<i,j>} \left(\hat{b}_i \hat{b}_j \hat{m}_{<i,j>}^\dagger + \hat{b}_i^\dagger \hat{b}_j^\dagger \hat{m}_{<i,j>} \right) - \nu \sum_{<i,j>} \hat{m}_{<i,j>}^\dagger \hat{m}_{<i,j>},
\end{aligned}
\tag{3.63}
$$

or if we want to described the molecules directly, with the Hamiltonian

$$
\begin{aligned}
\hat{H} = & - J_{\mathrm{M}} \sum_{<m,n>} \hat{m}_m^\dagger \hat{m}_n - J_{\mathrm{M}} \sum_{<<m,n>>} \hat{m}_m^\dagger \hat{m}_n + \frac{U_{\mathrm{M}}}{2} \sum_m \hat{n}_m \left(\hat{n}_m + 1 \right) \\
& + \frac{V_{\mathrm{M}}}{2} \sum_{<m,n>} \hat{n}_m \hat{n}_n + \frac{V_{\mathrm{M}}}{2} \sum_{<<m,n>>} \hat{n}_m \hat{n}_n,
\end{aligned}
\tag{4.1}
$$

where $<< m,n >>$ is the sum over the next-nearest neighbours, which are connected by a lattice site of Σ_1 and with $\hat{n}_m = \hat{m}_m \hat{m}_m^\dagger$ the occupation operator of molecules at the site m on the second optical lattice. The properties of the particular nearest neighbour and next-nearest neighbour interactions are results of the system's geometry. They occur if two molecular state coupled to two two-particle states, but sharing one lattice site of Σ_1. The interaction of a molecule on a link A [fig. 4.2] with a molecule about the corner on a link B lead to a nearest neighbour interaction. Two molecules on neighbouring links A or B, respectively lead to a next-nearest neighbour interaction.
The interaction is a result of the coupling between the molecular and two-particle atomic states. A molecule, living in Σ_2 is coupled to two adjacent lattice sites of Σ_1. If there is a molecule on the neighbouring or next-neighbouring lattice site, then both are interacting.

The interaction strength is calculated with perturbation theory. We assume a molecular state $|m_{<i,j>}\rangle$, which is perturbed by the coupling to a two-particle atomic state $|b_i b_j\rangle$.
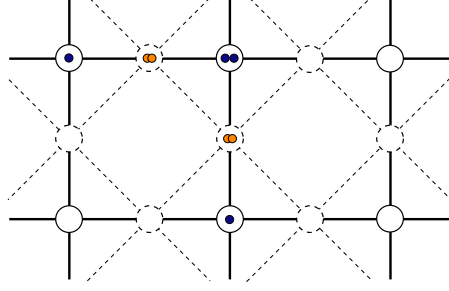
(a) Nearest neighbour interaction. The molecules live on neighbouring lattice site in Σ_2. They are coupled to two-particle states, living in Σ_1, which share one lattice site. The two particles on this lattice interact with the energy U.
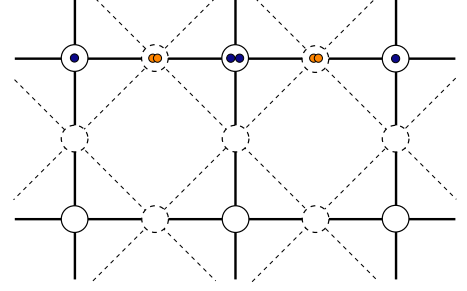
(b) Next-nearest neighbour interaction. The molecules live on opposite site of a square in the lattice Σ_2, but due to the coupling to the two-particle states, sharing a site of Σ_1 at the center of the square, the two molecule are interacting.

Figure 4.3.

Therefore the eigenstate of the perturbed system is

$$
\begin{aligned}
\left|m^*_{<i,j>}\right\rangle &= |m_{<i,j>}\rangle + \lambda^* \left|m^{(1)}_{<i,j>}\right\rangle \\
&= |m_{<i,j>}\rangle + \frac{\left\langle b_i b_j \left|\hat{H}_{\text{int}}\right| m_{<i,j>}\right\rangle}{E_m - \nu} |b_i b_j\rangle \\
&= |m_{<i,j>}\rangle - \frac{2g}{\nu} |b_i b_j\rangle ,
\end{aligned} \tag{4.2}
$$

a series of eigenstates of the non-perturbed systems of molecular and atomic states. We calculate the matrix element $\left\langle m^*_{<i,j>} m^*_{<s,t>} \left|U^*\right| m^*_{<i,j>} m^*_{<s,t>}\right\rangle$, with $U^* = \frac{U}{2} \sum_\alpha n_\alpha (n_\alpha - 1)$,
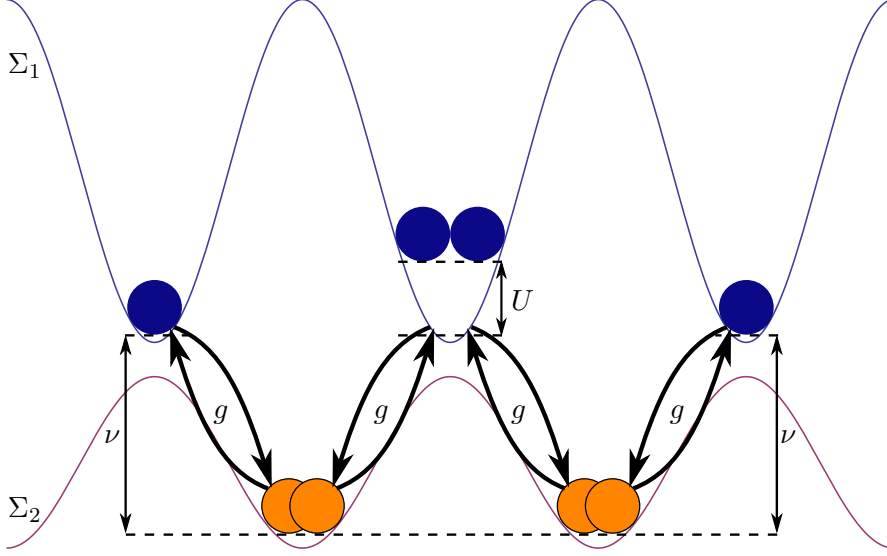
Figure 4.4.: The molecular states in lattice Σ_2 are coupled to two-particle atomic states in the other lattice Σ_1. The parameter g denotes the coupling strength and ν the detuning. One atom of each fragmented molecule share the same site in Σ_1. As the interaction strength of two atoms on the same lattice site is U, the two molecule are interacting indirectly.

to determine the nearest neighbour and next-nearest neighbour interaction strength.

$$
\left\langle m^*_{<i,j>} m^*_{<s,t>} \middle| U^* \middle| m^*_{<i,j>} m^*_{<s,t>} \right\rangle =
$$

$$
\begin{aligned}
& \langle m_{<i,j>} m_{<s,t>} | U^* | m_{<i,j>} m_{<s,t>} \rangle \\
& + \left\langle m_{<i,j>} b_s b_t \middle| \frac{4g^2}{\nu^2} U^* \middle| b_s b_t m_{<i,j>} \right\rangle \\
& + \left\langle b_i b_j m_{<s,t>} \middle| \frac{4g^2}{\nu^2} U^* \middle| m_{<s,t>} b_i b_j \right\rangle \\
& + \left\langle b_i b_j b_s b_t \middle| 16 \frac{g^4}{\nu^4} U^* \middle| b_s b_t b_i b_j \right\rangle \\
= & \left\langle b_i b_j b_s b_t \middle| 16 \frac{g^4}{\nu^4} \frac{U}{2} \sum_\alpha n_\alpha (n_\alpha - 1) \middle| b_s b_t b_i b_j \right\rangle \\
= & \left\langle b_i b_j b_s b_t \middle| 16 \frac{g^4}{\nu^4} \frac{U}{2} \sum_\alpha b_\alpha^\dagger b_\alpha^\dagger b_\alpha b_\alpha \middle| b_s b_t b_i b_j \right\rangle .
\end{aligned}
\tag{4.3}
$$

$$
\tag{4.4}
$$

The first three terms of (4.3) vanish and only the fourth term makes a contribution. Due to the particular coupling properties, the indices of the atoms are partially specified with $j = i + 1$ and $t = s + 1$. Since we want to determine nearest and next-nearest neighbour

interaction, we have to choose the indices $s = j$, from which follows $t = j + 1 = i + 2$. As a result of (4.4), we obtain

$$
\begin{aligned}
V_{\mathrm{M}} &= \left\langle b_i b_j b_j b_{j+1} \left| 16 \frac{g^4}{\nu^4} \frac{U}{2} \sum_\alpha b_\alpha^\dagger b_\alpha^\dagger b_\alpha b_\alpha \right| b_j b_{j+1} b_i b_j \right\rangle \\
&= \left\langle 0 \left| b_i b_j b_j b_{j+1} 16 \frac{g^4}{\nu^4} \frac{U}{2} \sum_\alpha \delta_{\alpha,j} b_\alpha^\dagger b_\alpha^\dagger b_\alpha b_\alpha b_j^\dagger b_{j+1}^\dagger b_i^\dagger b_j^\dagger \right| 0 \right\rangle \\
&= \frac{8 g^4 U}{\nu}.
\end{aligned}
\tag{4.5}
$$

The on-site interaction of the molecules can be determined similarly. It is a result of two molecules on the same lattice site of Σ_2 coupled to two-particle atomic states on the same adjacent sites of lattice Σ_1. To determine the on-site interaction of two molecules, we
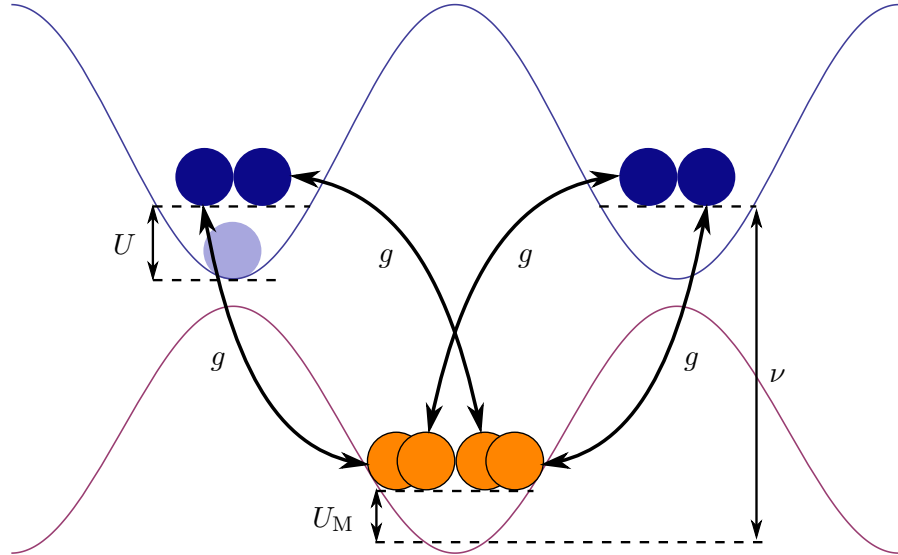

Figure 4.5.: The molecular states in lattice Σ_2 are coupled to two-particle atomic states in the other lattice Σ_1. The two atoms of each fragmented molecule share the same neighbouring lattice sites in Σ_1. As the interaction strength of two atoms on the same lattice site is U, the two molecule are interacting indirectly, via lattice Σ_1.

have to calculate the matrix-element $\left\langle m^*_{<i,j>} m^*_{<i,j>} \left| U^* \right| m^*_{<i,j>} m^*_{<i,j>} \right\rangle$, where we can

use directly the result of equation (4.4)

$$
\begin{aligned}
U_{\mathrm{M}} &= \left\langle b_i b_j b_i b_j \left| 16\frac{g^4}{\nu^4}\frac{U}{2}\sum_\alpha b_\alpha^\dagger b_\alpha^\dagger b_\alpha b_\alpha \right| b_i b_j b_i b_j \right\rangle \\
&= \left\langle 0 \left| b_i b_j b_i b_j 16\frac{g^4}{\nu^4}\frac{U}{2}\sum_\alpha (\delta_{\alpha,i} + \delta_{\alpha,j})\, b_\alpha^\dagger b_\alpha^\dagger b_\alpha b_\alpha b_i^\dagger b_j^\dagger b_i^\dagger b_j^\dagger \right| 0 \right\rangle \\
&= \frac{16 g^4 U}{\nu}.
\end{aligned}
\tag{4.6}
$$

As expected the on-site interaction is twice as strong as the nearest and next-nearest neighbour interaction, due to four atoms on two lattice site in Σ_1 are interacting.

At last, we have to determine the hopping rate of the molecules from one lattice site to another. We calculate the matrix-element

$$
\begin{aligned}
\left\langle m_{<i,j>} \left| \hat{\mathrm{H}}_{\mathrm{int}} \right| m_{<i,j>} \right\rangle &= -\sum_{\boldsymbol{k},\boldsymbol{q}} \frac{\left\langle m_{<i,j>} \left| \hat{\mathrm{H}}_{\mathrm{int}} \right| \boldsymbol{k},\boldsymbol{q} \right\rangle \left\langle \boldsymbol{k},\boldsymbol{q} \left| \hat{\mathrm{H}}_{\mathrm{int}} \right| m_{<i,j>} \right\rangle}{E - \nu - \varepsilon(\boldsymbol{k}) - \varepsilon(\boldsymbol{q})} \\
&= -\sum_{\boldsymbol{k},\boldsymbol{q}} \frac{\sum_{\substack{t s \\ t' s'}} \left\langle m_{<i,j>} \left| \hat{\mathrm{H}}_{\mathrm{int}} \right| \boldsymbol{t},\boldsymbol{s} \right\rangle \langle \boldsymbol{t},\boldsymbol{s} | \boldsymbol{k},\boldsymbol{q} \rangle \langle \boldsymbol{k},\boldsymbol{q} | \boldsymbol{t}',\boldsymbol{s}' \rangle \left\langle \boldsymbol{t}',\boldsymbol{s}' \left| \hat{\mathrm{H}}_{\mathrm{int}} \right| m_{<i,j>} \right\rangle}{E - \nu - \varepsilon(\boldsymbol{k}) - \varepsilon(\boldsymbol{q})},
\end{aligned}
\tag{4.7}
$$

where $|\boldsymbol{s},\boldsymbol{t}\rangle = |b_i b_j\rangle$ are two-particle atomic states in the position space, $|\boldsymbol{k},\boldsymbol{q}\rangle = |a_k a_q\rangle$ in the momentum space and $\hat{\mathrm{H}}_{\mathrm{int}} = g\sum_{\alpha\beta}\left(b_\alpha b_\beta m_{<\alpha,\beta>}^\dagger + b_\alpha^\dagger b_\beta^\dagger m_{<\alpha,\beta>}\right)$ is the coupling operator of the system. As only neighbouring atoms are coupled to molecular states $|\boldsymbol{s},\boldsymbol{t}\rangle = |b_i b_j\rangle$ is partially determined by $\boldsymbol{t} = \boldsymbol{s}+1$, from which follows $\boldsymbol{R}_t = \boldsymbol{R}_s + \boldsymbol{a}$, with a the lattice spacing. With the matrix-element

$$
\begin{aligned}
\langle m_{<i,j>} | H_{\mathrm{int}} | \boldsymbol{t},\boldsymbol{s} \rangle &= \langle 0 | \, m_{<i,j>} g\sum_{\alpha\beta}\left(b_\alpha b_\beta m_{<\alpha,\beta>}^\dagger + b_\alpha^\dagger b_\beta^\dagger m_{<\alpha,\beta>}\right) b_t^\dagger b_s^\dagger | 0 \rangle \\
&= \langle 0 | \, g\sum_{\alpha\beta} \delta_{ij,\alpha\beta}\left(\delta_{\alpha,t}\delta_{\beta,s} + \delta_{\alpha,s}\delta_{\beta,t}\right) | 0 \rangle \\
&= 2g,
\end{aligned}
\tag{4.8}
$$

and the second order expansion of the factor $1/[E - \nu - \varepsilon(\boldsymbol{k}) - \varepsilon(\boldsymbol{q})]$ in $\varepsilon(\boldsymbol{k})$ and $\varepsilon(\boldsymbol{q})$

$$
\begin{aligned}
\frac{1}{E - \nu - \varepsilon(\boldsymbol{k}) - \varepsilon(\boldsymbol{q})} \approx\; & \frac{1}{E - \nu - 4J} - \frac{2J\cos(qa)}{(E - \nu - 4J)^2} - \frac{2J\cos(ka)}{(E - \nu - 4J)^2} \\
& + \frac{8J^2\cos(qa)\cos(ka)}{(E - \nu - 4J)^3} + \frac{4J^2\cos^2(qa)}{(E - \nu - 4J)^3} + \frac{4J^2\cos^2(ka)}{(E - \nu - 4J)^3} \\
& + o[\cos(qa),\cos(ka)]^3,
\end{aligned}
\tag{4.9}
$$

4. Many body physics

we obtain

$$
\begin{aligned}
\left\langle m_{<i,j>}\left|\hat{\mathrm{H}}_{\mathrm{int}}\right|m_{<i,j>}\right\rangle &= -\sum_{\boldsymbol{k},\boldsymbol{q}} \frac{\langle m_{<i,j>}|H_{\mathrm{int}}|\boldsymbol{k},\boldsymbol{q}\rangle\,\langle\boldsymbol{k},\boldsymbol{q}|H_{\mathrm{int}}|m_{<i,j>}\rangle}{E-\nu-\varepsilon(\boldsymbol{k})-\varepsilon(\boldsymbol{q})} \\
&= -\sum_{\boldsymbol{k},\boldsymbol{q}} \frac{g^2 \mathrm{e}^{\mathrm{i}(\boldsymbol{k}+\boldsymbol{q})(\boldsymbol{R}_t-\boldsymbol{R}_{t'})}}{E-\nu-\varepsilon(\boldsymbol{k})-\varepsilon(\boldsymbol{q})} \\
&\approx -4g^2\left[\frac{-2J^2\left(\delta_{t-t',0}+\delta_{t-t',a}+\delta_{t-t',-a}\right)}{(4J-E+\nu)^3}-\frac{\delta_{t-t',0}}{4J-E+\nu}\right],
\end{aligned}
$$
$$(4.10)$$

with the self-energy $4g^2/(4J-E+\nu)$ denoting a chemical shift. The three other terms denote nearest and next-nearest neighbour hopping J_{M}, as well as on-site hopping, i.e. the atoms switch their positions only and couple back to the original position of the molecule.

In the limit $g\to\infty$, $\nu\to\infty$ and $g^2/\nu\to\mathrm{const.}$

$$
J_{\mathrm{M}} = \frac{8g^2 J^2}{\nu^3} \tag{4.11}
$$

The parameters of Hamiltonian (4.1) are now fully determined.

$$
\begin{aligned}
\hat{\mathrm{H}} =&\frac{8g^2 J^2}{\nu^3}\sum_{<m,n>}\hat{m}_m^\dagger\hat{m}_n + \frac{8g^2 J^2}{\nu^3}\sum_{<<m,n>>}\hat{m}_m^\dagger\hat{m}_n \\
&+\frac{16g^4 U}{\nu}\sum_m \hat{n}_m\left(\hat{n}_m+1\right)+\frac{8g^4 U}{\nu}\sum_{<m,n>}\hat{n}_m\hat{n}_n+\frac{8g^4 U}{\nu}\sum_{<<m,n>>}\hat{n}_m\hat{n}_n.
\end{aligned}
$$
$$(4.12)$$

Next, the system described by the Hamiltonian (4.12) has to be investigated. We constrain our interest to an integer filled lattice Σ_1 with one atom per lattice site, from which follows a 1/4-filling of molecules in lattice Σ_2. Due to the particular interactions in this system, there are always at least one empty lattice site of Σ_2 between two molecules. Several distribution patterns of molecules are possible [fig 4.6].
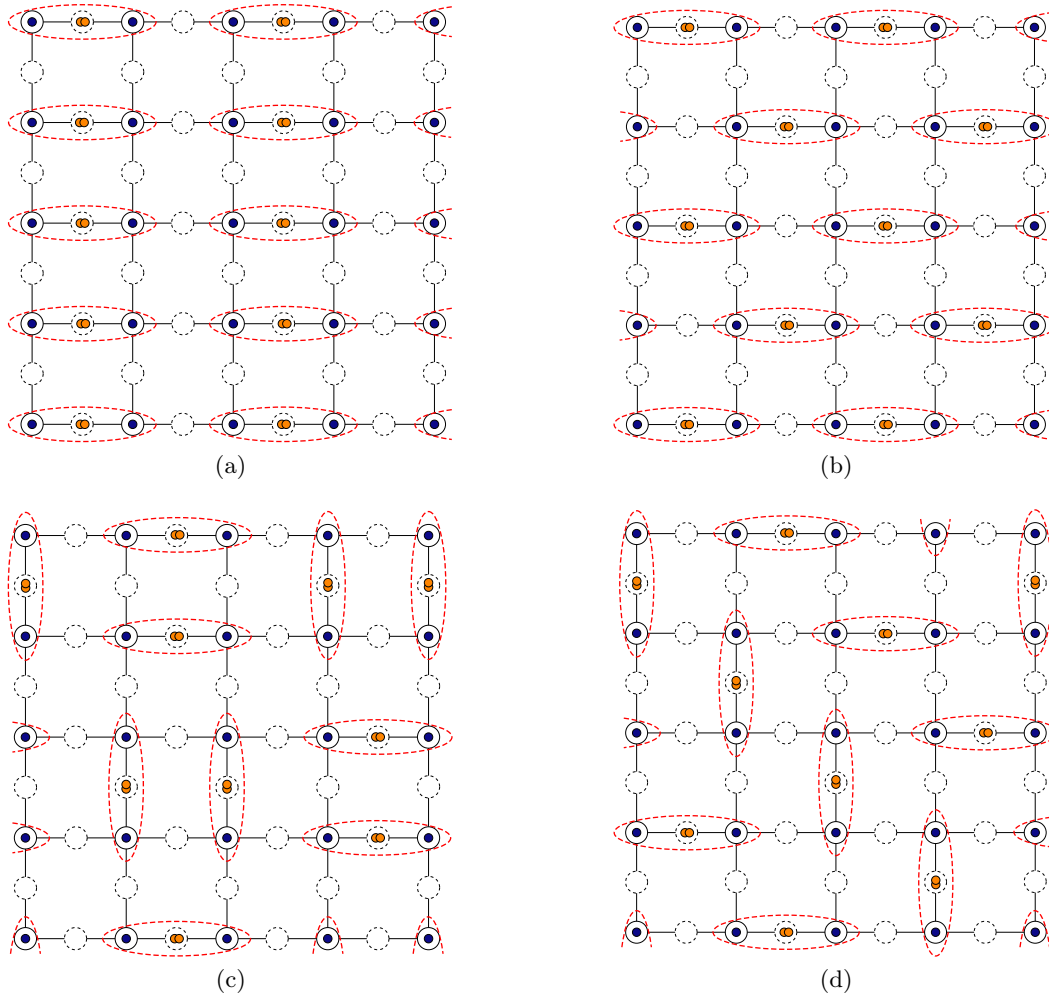
Figure 4.6.: Several distribution patterns of molecules, due to the nearest and next-nearestneighbour interaction.

As all possible distribution patterns are energetically equal, the system has to be describe by a quantum dimer model, due to the particular nearest neighbour interactions of the system.

4.1. Quantum dimer model

As mentioned before, the system behaves like a dimer model. A dimer is associated with the link between two nearest neighbouring particles in a lattice. In our model, the link is occupied by a molecule coupled to two atoms on neighbouring adjacent lattice sites, and

as mentioned before, there a four possibilities, for every atom to couple with a neighbour to a molecule. But there are finite configurations which provide for a covering of the entire lattice.
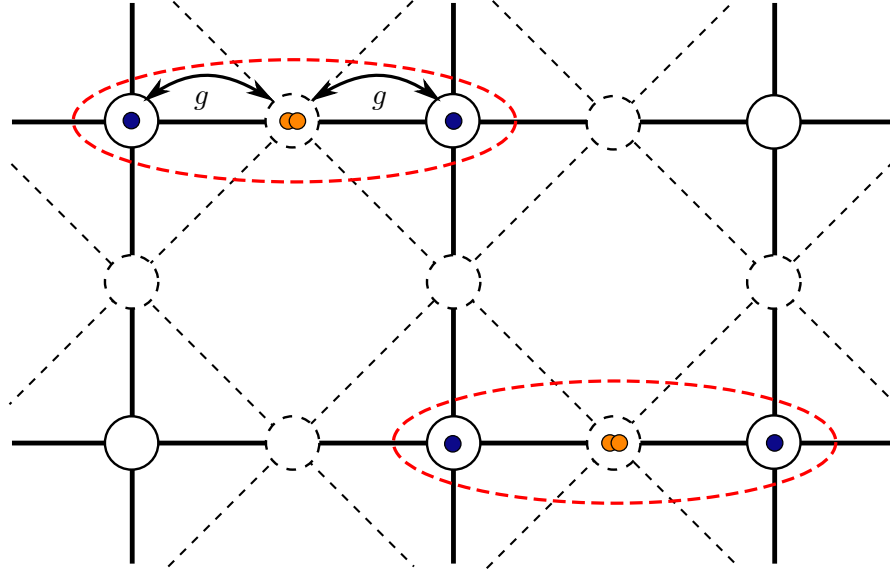

Figure 4.7.: The link between to lattice sites in Σ_1, occupied by a molecule, which is coupled to a two-particle atomic state, is associated with a dimer.

The physics of dimers is captured by quantum dimer model (QDM), e.g. the Rokhsar-Kivelson quantum dimer model (RK-QDM) [15]. The dynamic is described by the RK-Hamiltonian

$$\hat{H}_{RK} = \sum_{\text{plaquettes}} \left[-t \left(|\alpha\rangle \langle\beta| + |\beta\rangle \langle\alpha| \right) + v \left(|\alpha\rangle \langle\alpha| + |\beta\rangle \langle\beta| \right) \right], \tag{4.13}$$

with $|\alpha\rangle$ denoting a state where the B-links of a plaquette are occupied by a molecule an $|\beta\rangle$ the A-links, respectively and t denoting the flipping parameter from one state to the other and v the interaction strength of nearest neighbour dimers.
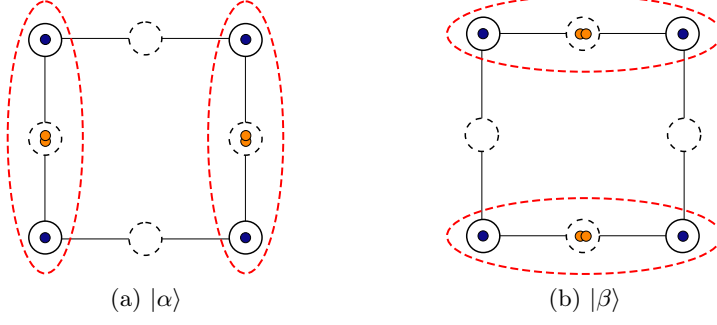
(a) $|\alpha\rangle$ (b) $|\beta\rangle$

Figure 4.8.

The Hamiltonian (4.13) gives rise to a quantum-phase diagram, depending on the parameter v/t. On the two dimensional square lattice appear at least three phases, and critical point. According to new researches a fourth phase might occur [16].

4.1.1. Rokhsar-Kivelson point

In the special case $v = t$ the system is at the Rokhsar-Kivelson point, with the ground state wave function

$$|\phi_{GS}\rangle = \sum_s |c\rangle \,, \tag{4.14}$$

where $|c\rangle$ is a dimer covering and the sum is over a topological sector, i.e. a set of coverings s, which is closed under repeated action of the flip term in (4.13). Such an equal amplitude superposition can be constructed with every such set of coverings and these special wave functions are all energetically degenerate ground states.
At $v = t$ the Hamiltonian (4.13) reduces to a simple sum of projectors

$$\hat{H}_{RK} = \sum_{\text{plaquettes}} \left(|\alpha\rangle - |\beta\rangle\right)\left(\langle\alpha| - \langle\beta|\right), \tag{4.15}$$

and each term of this sum has the eigenvalues 0 or 1, whereby any wave function, annihilated by this Hamiltonian will be a zero energy ground state. A wave function $\phi = \sum_c A_c |c\rangle$, will only be annihilated, if the amplitude A_c of any dimer covering is the same as the amplitude $\{A_{c'}\}$ of all dimer coverings $\{|c'\rangle\}$. Therefore all solutions will have the form of solution (4.14). The kinetic term is believed to be ergodic in each sector on a square lattice, whereby a unique ground state is given for each topological sector by the equal amplitude superposition of all dimer coverings of this sector. As all these states are degenerate, any linear combination of them will also be ground state, including the equal amplitude superposition of all dimer coverings.

4.1.2. Columnar phase

For $v/t \to -\infty$, the system merges into a phase, where the number of flippable plaquettes is maximal. This is accomplished by the columnar state, shown in [fig 4.9a],

which is four-fold degenerate and breaks rotational symmetry and the translation symmetry by one lattice spacing along the direction of the dimer orientation. Actually, the columnar state is only eigenstate in the limit $v/t \to -\infty$, but a state with columnar correlations persists up to a value of $(v/t)_c < 1$, depending on the lattice geometry. On a 2-D square lattice the phase transition to the plaquette phase occur at a critical value $(v/t)_c = 0.60 \pm 0.05$ [17]. Therefore, we call $-\infty < (v/t) < 0.60 \pm 0.05$, the columnar phase.
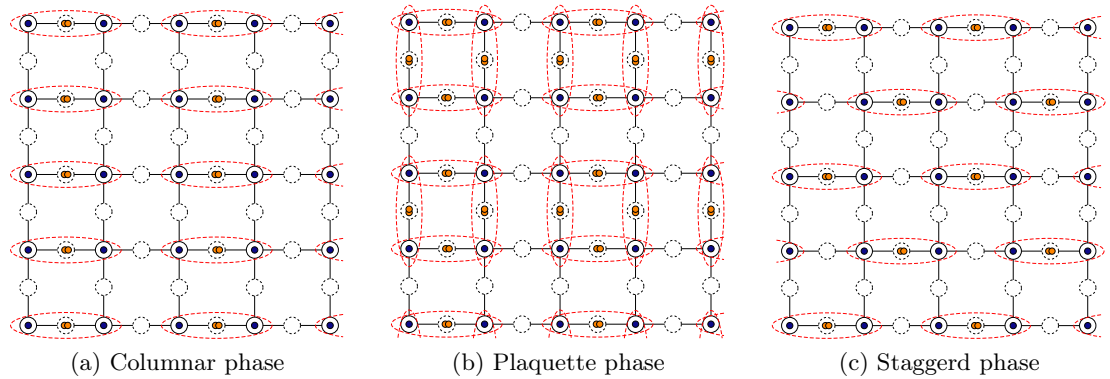

(a) Columnar phase   (b) Plaquette phase   (c) Staggerd phase

Figure 4.9.: Examples of valence bond solids.

4.1.3. Plaquette phase

Figure [fig. 4.9b] shows schematically the plaquette state on 2-D square lattice. The links, where the probability of having a dimer is large, are marked. On the other links the probability is comparatively small. One can imaging a pair of dimers on an elementary plaquette resonating between the horizontal and the vertical configurations. A product of the terms $|\alpha\rangle$ and $|\beta\rangle$ may visualize a variational wave function for this state in zeroth order. So far a plaquette phase has been observed only on 2-D bipartite lattices, particularly the square [17], [18] and [19] and honeycomb [20] lattices. Numerical evidence shows that the onset of plaquette phase begins immediately to the left of the Rokhsar-Kivelson point and persists to certain value $(v/t)_d$. It has been proposed [17] that the plaquette phase gives way to the columnar phase via first order transition, i.e. $(v/t)_d = (v/t)_c$, but there has been recent suggestions that a new "mixed" phase occur on the 2-D square lattice between the columnar and the plaquette phase [16].

4.1.4. Staggered phase

For $v/t \to \infty$, the system merges into a phase, where the number of flippable plaquettes is minimal. If it is possible, the system prefers states with no flippable plaquettes. On a square lattice, there are exponentially many such states. Figure [fig. 4.9c] shows one which is representative. But all other non-flippable states are also called staggered.

The staggered state is of the form (4.14), with only one occupant of its dynamical sector. So the previous discussion of ground states at the Rokhsar-Kivelson point is also consistent here and the staggered state is ground state for all $(v/t) > 1$.

To determine the phase our suggested model is part of, we have to determine the flipping t and interaction parameter v belonging to our model. We have to calculate the matrix-element $t = \left\langle \alpha \middle| \hat{H}_{\text{eff}} \middle| \beta \right\rangle = \left\langle m_{<i,j>} m_{<s,t>} \middle| \hat{H}_{\text{eff}} \middle| m_{<i,s>} m_{<j,t>} \right\rangle$ and $v = \left\langle \alpha \middle| \hat{H}_{\text{eff}} \middle| \alpha \right\rangle = \left\langle m_{<i,j>} m_{<s,t>} \middle| \hat{H}_{\text{eff}} \middle| m_{<i,j>} m_{<s,t>} \right\rangle$, which are fourth order perturbation processes.
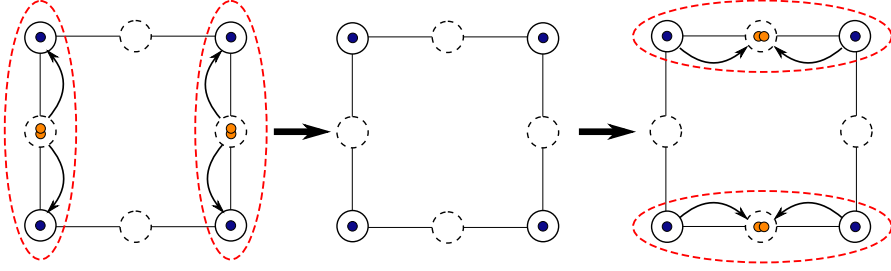
(a) $\left\langle \alpha \middle| \hat{H}_{\text{eff}} \middle| \beta \right\rangle$. The molecules on the vertical links couple to the two particle atomic states. Afterwards the atoms couple to molecular states on the horizontal links.
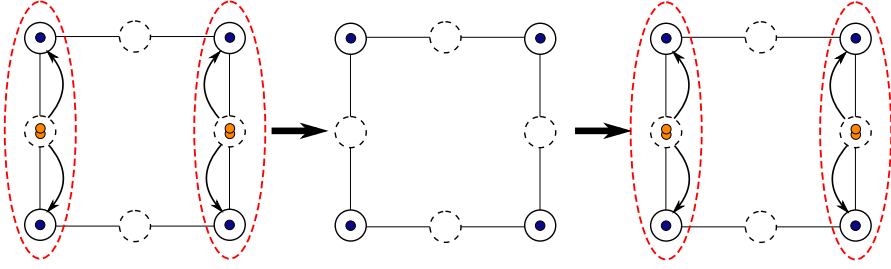
(b) $\left\langle \alpha \middle| \hat{H}_{\text{eff}} \middle| \alpha \right\rangle$. The molecules on the vertical links couple to the two particle atomic states. Afterwards the atoms couple back to molecular states on the vertical links again.

Figure 4.10.

With

$$|\alpha\rangle = m^{\dagger}_{<i,j>} m^{\dagger}_{<s,t>} |0\rangle \tag{4.16}$$

$$|\beta\rangle = m^{\dagger}_{<i,s>} m^{\dagger}_{<j,t>} |0\rangle \tag{4.17}$$

$$|\gamma\rangle = \frac{1}{\sqrt{2}} \left(m^{\dagger}_{<i,j>} b^{\dagger}_s b^{\dagger}_t |0\rangle + m^{\dagger}_{<s,t>} b^{\dagger}_i b^{\dagger}_j |0\rangle \right) \tag{4.18}$$

$$|\delta\rangle = \frac{1}{\sqrt{2}} \left(m^{\dagger}_{<i,s>} b^{\dagger}_j b^{\dagger}_t |0\rangle + m^{\dagger}_{<j,t>} b^{\dagger}_i b^{\dagger}_s |0\rangle \right) \tag{4.19}$$

$$|\tau\rangle = b^{\dagger}_i b^{\dagger}_j b^{\dagger}_s b^{\dagger}_t |0\rangle \tag{4.20}$$

we obtain

$$t = -\left\langle\alpha\left|\hat{H}_{\text{eff}}\right|\beta\right\rangle = \frac{\langle\alpha|g^*|\gamma\rangle\,\langle\gamma|g^*|\tau\rangle\,\langle\tau|g^*|\delta\rangle\,\langle\delta|g^*|\beta\rangle}{(E_\alpha - E_\gamma)\,(E_\alpha - E_\tau)\,(E_\alpha - E_\delta)} = 16\frac{g^4}{\nu^3} \tag{4.21}$$

$$v = \left\langle\alpha\left|\hat{H}_{\text{eff}}\right|\alpha\right\rangle = \frac{\langle\alpha|g^*|\gamma\rangle\,\langle\gamma|g^*|\tau\rangle\,\langle\tau|g^*|\gamma\rangle\,\langle\gamma|g^*|\alpha\rangle}{(E_\alpha - E_\gamma)\,(E_\alpha - E_\tau)\,(E_\alpha - E_\gamma)} = -16\frac{g^4}{\nu^3}, \tag{4.22}$$

with $g^* = g\sum_{<\alpha,\beta>}\left(b_\alpha b_\beta m^\dagger_{<\alpha,\beta>} + b^\dagger_\alpha b^\dagger_\beta m_{<\alpha,\beta>}\right)$. Consequently we obtain for the parameter $v/t = -1$, what gives rise to the columnar phase for our system with artificial interactions between neighbouring atoms in an optical lattice.
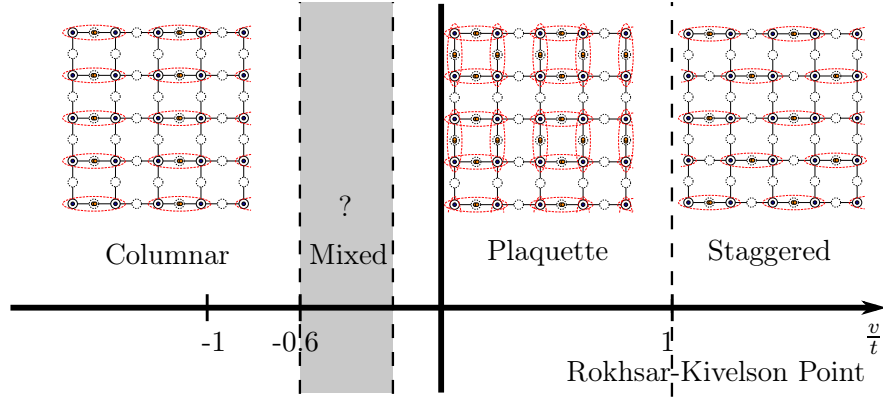

Figure 4.11.: Phase diagram of the Rokhsar-Kivelsion quantum dimer model on a two dimensional square lattice.

5. Summary

In this diploma work the scattering properties of quantum degenerate gases, trapped in optical lattices, with main emphasis on two particle collisions have been investigated. After basic concepts of quantum scattering theory were summarised, we point out the possibilities to tune the s-wave scattering length of two colliding particles with the help of a Feshbach resonance. But the main issues of this thesis are the scattering properties in an optical lattice. The two particle problem of the Bose Hubbard Hamiltonian, first investigated by Winkler *et al.* [8], were analysed. The scattering solutions and the particular effect of the periodic structure of the lattice, bound atom pairs, despite a repulsive interaction potential, have been pointed out. Afterwards the influence of a Feshbach resonance in an optical lattice has been investigated. It has been shown in chapter 3, that if one replaces the on-site interaction parameter by a wide Feshbach resonance with the background scattering length, there are no changes in effects and the results are the same. But an additional Feshbach resonance to tune the on-site interaction strength, gives rise to two additional bound states, whereas one vanishes in the limit of a wide resonance.

The main topic was the proposal of a novel model system, which provides for an artificial nearest neighbour interaction. The coupling of two neighbouring lattices sites to a molecular state, living on a second shifted and rotated optical lattice has been investigated. The scattering solutions and bound states have been again determined. The comparison with the extended Bose Hubbard model with a normal nearest neighbour interaction, gives rise to an effective interaction parameter, due to the coupling. The results have been confirmed by perturbation calculations.

In chapter 4 we investigated the influences of the novel interactions on many body systems. Therefore we calculated the hopping matrix element of the molecules living in the second lattices. The hopping is a second order process, following from the coupling. Besides, we calculated the on-site, nearest and next-nearest interaction matrix element of two molecules on the same or neighbouring lattice site. It was intended to determine the quantum phase diagram of the extend Bose Hubbard Hamiltonian. But it appeared that the system was about a Rokhsar-Kivelson quantum dimer model, where the link between two coupling atoms was defined as a dimer. We concentrated at the two dimensional system with an integer filling with one atom per lattice lattice, which is consistent with a one in four filling of dimers. We determined the matrix elements (flipping and interaction) of the Rokhsar-Kivelson Hamiltonian which were supposed to have the same value, but a different sign, as the interaction parameter is negative and the flipping parameter is always positive. As a consequence, the system is in the Columnar phase of the Rokhsar-Kivelson quantum dimer model.

5. Summary

A. Formal scattering theory and Lippmann-Schwinger equation

$|\phi(t)\rangle$ denotes a state of a particle in the Schrödinger picture.

$$\hat{H} = \hat{H}_0 + \hat{H}_{\text{int}} \tag{A.1}$$

is the Hamilton operator of the system, with $\hat{H}_0$ the free Hamiltonian and $\hat{H}_{\text{int}}$ describing the interaction between the particle and a target. The eigenstates of $\hat{H}_0$ are $\left|E_n^{(0)}\right\rangle$ and its eigenvalues are $E_n^{(0)}$, with n a set of quantum numbers.

$$\hat{H}_0 \left|E_n^{(0)}\right\rangle = E_n^{(0)} \left|E_n^{(0)}\right\rangle. \tag{A.2}$$

The eigenstates form a complete orthonormal basis, i.e.

$$\int dn \left|E_n^{(0)}\right\rangle \left\langle E_n^{(0)}\right| = \mathbb{1} \tag{A.3}$$

$$\left\langle E_n^{(0)} \middle| E_m^{(0)} \right\rangle = \delta(n-m) \tag{A.4}$$

Long before the scattering and in large distance to the target, the particle's wave packet can be expanded in the basis of the free problem

$$|\phi_0(0)\rangle = \int dn\ \alpha_n \left|E_n^{(0)}\right\rangle, \tag{A.5}$$

with α_n the expansion coefficients ($\int dn\ |\alpha_n|^2 = 1$). The time evolution is given by

$$|\phi_0(t)\rangle = e^{-\frac{i}{\hbar}\hat{H}_0 t} \int dn\ \alpha_n \left|E_n^{(0)}\right\rangle = \int dn\ \alpha_n e^{-\frac{i}{\hbar}E_n^{(0)}t} \left|E_n^{(0)}\right\rangle. \tag{A.6}$$

In large distance to the target, i.e. in the limit $t \to -\infty$, thus long before the scattering act, the solution (A.6) have also to be eigenstate to $\hat{H}$. With the Schrödinger time evolution operator a relation between $|\phi_0(t \to -\infty)\rangle$ and the general scattering states $|\phi(t)\rangle$ can be found.

$$|\phi(t)\rangle = \lim_{t' \to -\infty} e^{-\frac{i}{\hbar}\hat{H}(t-t')} |\phi_0(t')\rangle \tag{A.7}$$

$$= e^{-\frac{i}{\hbar}\hat{H}t} \lim_{t' \to -\infty} \int dn\ \alpha_n e^{-\frac{i}{\hbar}\left(E_n^{(0)}-\hat{H}\right)t'} \left|E_n^{(0)}\right\rangle. \tag{A.8}$$

A. Formal scattering theory and Lippmann-Schwinger equation

Such a limit does not always exist, but for reasonable scattering potentials it should always exist and can be calculated with

$$f(-\infty) = f(-\infty) \int_{-\infty}^{0} dx \, e^{x} = \lim_{\eta \to 0^+} \int_{-\infty}^{0} dx \, e^{x} f\left(\frac{x}{\eta}\right) \tag{A.9}$$

$$= \lim_{\eta \to 0^+} \eta \int_{-\infty}^{0} dt \, e^{\eta t} f(t). \tag{A.10}$$

Applying equation (A.9) on (A.8) yields

$$\lim_{\eta \to 0^+} \eta \int_{-\infty}^{0} dt \, e^{-\frac{i}{\hbar}\left(E_n^{(0)} - \hat{H} + i\eta\hbar\right)t} \left|E_n^{(0)}\right\rangle = \lim_{\eta \to 0^+} \eta \frac{1}{-i/\hbar\left(E_n^{(0)} - \hat{H} + i0^+\right)} \left|E_n^{(0)}\right\rangle$$

$$= \frac{i0^+}{E_n^{(0)} - \hat{H} + i0^+} \left|E_n^{(0)}\right\rangle$$

$$=: \left|E_n^{(+)}\right\rangle. \tag{A.11}$$

Inserting (A.11) in (A.8) yields

$$|\phi(t)\rangle = e^{-\frac{i}{\hbar}\hat{H}t} \int dn \, \alpha_n \left|E_n^{(+)}\right\rangle. \tag{A.12}$$

It can also be shown that $\left|E_n^{(+)}\right\rangle$ is an eigenstate to $\hat{H}$ with the eigenvalue $E_n^{(0)}$:

$$\left(E_n^{(0)} - \hat{H} + i0^+\right)|E_n^+\rangle = i0^+ |E_n^+\rangle \Rightarrow \left(E_n^{(0)} - \hat{H}\right)|E_n^+\rangle = 0, \tag{A.13}$$

which applied to (A.12):

$$|\phi(t)\rangle = e^{-\frac{i}{\hbar}E_n^{(0)}t} \int dn \, \alpha_n \left|E_n^{(+)}\right\rangle. \tag{A.14}$$

The next step is to determine $\left|E_n^{(+)}\right\rangle$.

$$\left|E_n^{(+)}\right\rangle = \frac{1}{E_n^{(0)} - \hat{H}_0 + i0^+} \left[i0^+ + \underbrace{\left(E_n^{(0)} - \hat{H}_0\right)}\right] \left|E_n^{(0)}\right\rangle \tag{A.15}$$

$$\underbrace{\phantom{\left(E_n^{(0)} - \hat{H}_0\right)}}_{=0}$$

$$\Longleftrightarrow \frac{E_n^{(0)} - \hat{H} + i0^+}{E_n^{(0)} - \hat{H}_0 + i0^+} \left|E_n^{(+)}\right\rangle = \left(\mathbb{1} - \frac{1}{E_n^{(0)} - \hat{H}_0 + i0^+}\hat{H}_{\text{int}}\right)\left|E_n^{(+)}\right\rangle$$

$$= \left|E_n^{(0)}\right\rangle \tag{A.16}$$

The result is a self-consistent equation, called the **Lippmann-Schwinger equation**:

$$\left|E_n^{(+)}\right\rangle = \left|E_n^{(0)}\right\rangle + \frac{1}{E_n^{(0)} - \hat{H}_0 + i0^+}\hat{H}_{\text{int}}\left|E_n^{(+)}\right\rangle, \tag{A.17}$$

II

with

$$G_n^+ = \frac{1}{E_n^{(0)} - \hat{H}_0 + i0^+} \tag{A.18}$$

the Green's operator. Equation (A.17) can be expressed in any orthonormal basis of the Hilbert space. For the position space, e.g, the Lippmann-Schwinger equation is

$$\left\langle \boldsymbol{r} \middle| E_n^{(+)} \right\rangle = \left| E_n^{(0)} \right\rangle + \iint d\boldsymbol{r}' d\boldsymbol{r}'' \left\langle \boldsymbol{r} \middle| G_n^+ \middle| \boldsymbol{r}' \right\rangle \left\langle \boldsymbol{r}' \middle| \hat{H}_{\text{int}} \middle| \boldsymbol{r}'' \right\rangle \left\langle \boldsymbol{r}'' \middle| E_n^{(+)} \right\rangle$$

$$\Longleftrightarrow \phi(\boldsymbol{r}) \quad = \phi_0(\boldsymbol{r}) + \int d^3\boldsymbol{r} \; G^+(\boldsymbol{r} - \boldsymbol{r}') V(\boldsymbol{r}') \phi(\boldsymbol{r}'), \tag{A.19}$$

with $\hat{H}_{\text{int}} = V(\boldsymbol{r}')$.

A. *Formal scattering theory and Lippmann-Schwinger equation*

B. Two particle scattering in an optical lattice

In the following we present the bare calculations for scattering properties of two particles in an optical lattice with on-site and nearest neighbour interaction. For a better overview the explanation are kept short. The system's dynamics can be described with the Bose Hubbard Hamiltonian in second quantization

$$\hat{H} - J \sum_{<i,j>} \left(b_i^\dagger b_j + b_j^\dagger b_i \right) + \frac{U}{2} \sum_i \hat{n}_i \left(\hat{n}_i - 1 \right) + \frac{V}{2} \sum_{<i,j>} \hat{n}_i \hat{n}_j. \tag{B.1}$$

The calculations are established successively, therefore not all terms in the Hamiltonian (B.1) are considered in all calculation. For the two particle problem it is convenient to perform the calculations in the first quantization formalism. The starting point for all cases will be the Schrödinger equation with relative coordinates only, which is valid, since the center of mass energy is a constant, which can be separate. First steps of the calculations are shown in detail for the case of on-site interaction only. Later resonant coupling to a molecular state, living on the or between the lattice is implemented. The coupling can be associated with a artificial Feshbach resonance, where two particle atomic state represents the open channel and the molecular state represents the closed channel.

B.1. on-site interaction U:

The Hamiltonian describing the dynamics of atom in an optical lattice with only on-site interaction is the Bose Hubbard Hamiltonian

$$\hat{H} - J \sum_{<i,j>} \left(b_i^\dagger b_j + b_j^\dagger b_i \right) + \frac{U}{2} \sum_i \hat{n}_i \left(\hat{n}_i - 1 \right). \tag{B.2}$$

The Hamiltonian in first quantization is

$$\hat{H}_{\text{TP}} = \hat{H}_{\text{kin}} + \hat{H}_{\text{int}} = -J \left[\tilde{\Delta}_{\boldsymbol{x}}^0 + \tilde{\Delta}_{\boldsymbol{y}}^0 \right] + U \delta_{\boldsymbol{x},\boldsymbol{y}}$$

$$= -2J \tilde{\Delta}_{\boldsymbol{r}}^{\boldsymbol{Q}} + 4J \sum_{i=1}^d \left(1 - \cos \frac{Q_i a}{2} \right) + U \delta_{\boldsymbol{r},\boldsymbol{0}}, \tag{B.3}$$

with the discrete lattice derivation

$$\tilde{\Delta}_{\boldsymbol{x}}^{\boldsymbol{Q}} \psi \left(\boldsymbol{x} \right) = \sum_{i=1}^d \cos \frac{Q_i a}{2} \left[\psi(\boldsymbol{x} + \boldsymbol{a}_i) + \psi(\boldsymbol{x} - \boldsymbol{a}_i) - 2\psi(\boldsymbol{x}) \right] \tag{B.4}$$

B. Two particle scattering in an optical lattice

where $\boldsymbol{Q}$ is an arbitrary vector. The particles position is denoted by the vectors $\boldsymbol{x} = \sum_i x_i \boldsymbol{a}_i$ and $\boldsymbol{y} = \sum_i y_i \boldsymbol{a}_i$, with $\boldsymbol{a}_i$ the primitive vector of the unit cell of the optical lattice. Introducing relative and center of mass coordinates

$$\boldsymbol{r} := \boldsymbol{r}_2 - \boldsymbol{r}_1 \tag{B.5}$$

$$\boldsymbol{R} := \frac{m_1 \boldsymbol{r}_1 + m_2 \boldsymbol{r}_2}{m_1 + m_2}, \tag{B.6}$$

gives rise to the Schödinger equation

$$\left[-2J\tilde{\Delta}_{\boldsymbol{r}}^{\boldsymbol{Q}} + U\delta_{\boldsymbol{r},\boldsymbol{0}} \right] \psi(\boldsymbol{r}) = E\psi(\boldsymbol{r}). \tag{B.7}$$

It can be solved with the Green's function formalism. The Green's function is defined by the equation

$$\left[E + 2J\tilde{\Delta}_{\boldsymbol{r}}^{\boldsymbol{Q}} \right] G_{\boldsymbol{Q}}(E,\boldsymbol{r}) = \delta_{\boldsymbol{r},\boldsymbol{0}}. \tag{B.8}$$

Performing Fourier transformation for $G_{\boldsymbol{Q}}(E,\boldsymbol{r})$ and $\delta_{\boldsymbol{r},\boldsymbol{0}}$ and inserting in equation (B.8) yields

$$\frac{1}{v_0} \sum_{\boldsymbol{q} \in K} e^{i\boldsymbol{q}\cdot\boldsymbol{r}} \left\{ G_{\boldsymbol{Q}} \left[E - \varepsilon_{\boldsymbol{Q}}(\boldsymbol{q}) \right] - 1 \right\} = 0. \tag{B.9}$$

from which follows

$$G_{\boldsymbol{Q}}(E,\boldsymbol{q}) = \frac{1}{E - \varepsilon_{\boldsymbol{Q}}(\boldsymbol{q}) + i\eta}, \tag{B.10}$$

or

$$G_{\boldsymbol{Q}}(E,\boldsymbol{r}) = \int \frac{d\boldsymbol{q}}{v_0} \frac{e^{i\boldsymbol{q}\cdot\boldsymbol{r}}}{E - \varepsilon_{\boldsymbol{Q}}(\boldsymbol{q}) + i\eta} \tag{B.11}$$

respectivley, where $\varepsilon_{\boldsymbol{Q}}(\boldsymbol{q})$ is the dispersion relation for a particle in an optical lattice

$$\varepsilon_{\boldsymbol{Q}}(\boldsymbol{q}) = 4J \sum_{i=1}^{d} \cos \frac{Q_i a}{2} \left[1 - \cos(q_i a) \right]. \tag{B.12}$$

The solution of $\psi(\boldsymbol{r})$ can be found with the help of the Lippmann-Schwinger equation.

$$\psi(\boldsymbol{r}) = \psi_0(\boldsymbol{r}) + \sum_{\boldsymbol{r}'} G_{\boldsymbol{Q}}(E, \boldsymbol{r} - \boldsymbol{r}')V(\boldsymbol{r}')\psi(\boldsymbol{r}'), \tag{B.13}$$

with $\psi_0(\boldsymbol{r}) = \exp(i\boldsymbol{q}_0 \cdot \boldsymbol{r})$ the incoming plane wave. With the short-range potential $V(\boldsymbol{r}') = U\delta_{\boldsymbol{r},\boldsymbol{0}}$ one obtains

$$\psi(\boldsymbol{r}) = e^{i\boldsymbol{q}_0\cdot\boldsymbol{r}} + G_{\boldsymbol{Q}}(E,\boldsymbol{r})U\psi(\boldsymbol{0}). \tag{B.14}$$

Equation (B.14) gives rise to a self-consistency equation for $\psi(\boldsymbol{0})$

$$\psi(\boldsymbol{0}) = 1 + G_{\boldsymbol{Q}}(E,\boldsymbol{0})U\psi(\boldsymbol{0}) = \frac{1}{1 - G_{\boldsymbol{Q}}(E,\boldsymbol{0})U}. \tag{B.15}$$

VI

Inserting equation (B.15) in (B.14) leads to

$$\psi\left(\boldsymbol{r}\right) = \mathrm{e}^{\mathrm{i}\boldsymbol{q}_0 \cdot \boldsymbol{r}} + \frac{U}{1 - G_{\boldsymbol{Q}}(E, \boldsymbol{0})U} G_{\boldsymbol{Q}}(E, \boldsymbol{r}) \tag{B.16}$$

where the scattering amplitude $f(\boldsymbol{q}, \boldsymbol{q}')$ can be identified as

$$f(\boldsymbol{q}, \boldsymbol{q}') = \frac{U}{1 - G_{\boldsymbol{Q}}(E, \boldsymbol{0})U}. \tag{B.17}$$

Further analysis are performed in [sec. 3.1]

B.2. coupling to a molecular state on the lattice sites:

Two particle interaction in an optical lattice with a resonant coupling to a closed channel living on the lattice, i.e. a Feshbach resonance, can be described by the Hamiltonian

$$\hat{\mathrm{H}} = -J \sum_{<i,j>} \left(b_i^\dagger b_j + b_j^\dagger b_i \right) + g \sum_i \left(\hat{b}_i \hat{b}_i \hat{m}_i^\dagger + \hat{b}_i^\dagger \hat{b}_i^\dagger \hat{m}_i \right) - \nu \sum_i \hat{m}_i^\dagger \hat{m}_i. \tag{B.18}$$

In first quantization the system is captured by a two-channel Schrödinger equation system.

$$\left[E + 2J\tilde{\Delta}_{\boldsymbol{r}}\right]\psi(\boldsymbol{r}) = g\chi\delta_{\boldsymbol{r},\boldsymbol{0}} \tag{B.19}$$

$$[E - \nu]\chi = g\delta_{\boldsymbol{r},0}\psi(\boldsymbol{r}) = g\psi(0) \tag{B.20}$$

with $\psi(\boldsymbol{r})$ describing the two particle atomic state, with the relative coordinate $\boldsymbol{r}$ between the particle and χ describing the molecular state living on the lattice sites. The general solution of the differential equation (B.19) is

$$\psi(\boldsymbol{r}) = \psi_0(\boldsymbol{r}) + g\chi G(\boldsymbol{r}), \tag{B.21}$$

where $\psi_0(\boldsymbol{r}) = \exp\left(\mathrm{i}\boldsymbol{q}_0 \cdot \boldsymbol{r}\right)$ is the solution of the homogeneous equation and $g\chi G(\boldsymbol{r})$ of the inhomogeneous equation. Equation (B.21) gives rise to a self-consistency equation for $\psi(\boldsymbol{0})$

$$\psi(\boldsymbol{0}) = 1 + g\chi G(\boldsymbol{0}). \tag{B.22}$$

Inserting this in equation (B.19) yields

$$[E - \nu]\chi = g + g^2 \chi G(\boldsymbol{0}), \tag{B.23}$$

from which follows

$$\chi = \frac{g}{E - \nu - g^2 G(\boldsymbol{0})}. \tag{B.24}$$

The final result for $\psi(\boldsymbol{r})$ is

$$\psi(\boldsymbol{r}) = \mathrm{e}^{\mathrm{i}\boldsymbol{q}_0 \cdot \boldsymbol{r}} + \frac{g^2}{E - \nu - g^2 G(\boldsymbol{0})} G(\boldsymbol{r}), \tag{B.25}$$

B. Two particle scattering in an optical lattice

where the scattering amplitude $f(\boldsymbol{q}, \boldsymbol{q}')$ can be identified

$$f(\boldsymbol{q}, \boldsymbol{q}') = \frac{g^2}{E - \nu - g^2 G(\boldsymbol{0})}. \tag{B.26}$$

In the limit of a wide Feshbach resonance, i.e. $g \to \infty$, $\nu \to \infty$ and $g^2/\nu \to$ const. one obtains

$$\psi(\boldsymbol{r}) = e^{i\boldsymbol{q}_0 \cdot \boldsymbol{r}} + \frac{-\frac{g^2}{\nu}}{1 + \frac{g^2}{\nu} G(\boldsymbol{0})} G(\boldsymbol{r}) \tag{B.27}$$

with the scattering amplitude

$$f(\boldsymbol{q}, \boldsymbol{q}') = \frac{-\frac{g^2}{\nu}}{1 + \frac{g^2}{\nu} G(\boldsymbol{0})} \tag{B.28}$$

The comparison with equation (B.17) leads to an effective on-site interaction parameter

$$U_{\text{eff}} = -\frac{g^2}{\nu} \tag{B.29}$$

B.3. nearest neighbour interaction V:

The two particle problem in an optical lattice with nearest neighbour interaction is in second quantization described by

$$\hat{H} - J \sum_{<i,j>} \left(b_i^\dagger b_j + b_j^\dagger b_i \right) + \frac{V}{2} \sum_{<i,j>} \hat{n}_i \hat{n}_j. \tag{B.30}$$

In first quantization the problem is described by the Schrödinger equation

$$\left[E + 2J \tilde{\Delta}_{\boldsymbol{r}}^{\boldsymbol{Q}} \right] \psi(\boldsymbol{r}) = \frac{V}{2} \left(\delta_{\boldsymbol{r},\boldsymbol{a}} + \delta_{\boldsymbol{r},-\boldsymbol{a}} \right) \psi(\boldsymbol{r}). \tag{B.31}$$

The solution of $\psi(\boldsymbol{r})$ can be found with the help of the Lippmann-Schwinger equation

$$\begin{aligned}
\psi(\boldsymbol{r}) &= \psi_0(\boldsymbol{r}) + \sum_{\boldsymbol{r}'} G(E, \boldsymbol{r} - \boldsymbol{r}') \frac{V}{2} \left(\delta_{\boldsymbol{r},\boldsymbol{a}} + \delta_{\boldsymbol{r},-\boldsymbol{a}} \right) \psi(\boldsymbol{r}') \\
&= \psi_0(\boldsymbol{r}) + \frac{V}{2} \left[G(\boldsymbol{r} - \boldsymbol{a})\psi(\boldsymbol{a}) + G(\boldsymbol{r} + \boldsymbol{a})\psi(-\boldsymbol{a}) \right].
\end{aligned} \tag{B.32}$$

It is necessary to solve the to self-consistency equations for $\psi(\boldsymbol{a})$ and $\psi(-\boldsymbol{a})$

$$\psi(\boldsymbol{a}) = e^{i\boldsymbol{q}_0 \cdot \boldsymbol{a}} + \frac{V}{2} \left[G(\boldsymbol{0})\psi(\boldsymbol{a}) + G(2\boldsymbol{a})\psi(-\boldsymbol{a}) \right] \tag{B.33}$$

$$\psi(-\boldsymbol{a}) = e^{-i\boldsymbol{q}_0 \cdot \boldsymbol{a}} + \frac{V}{2} \left[G(2\boldsymbol{a})\psi(\boldsymbol{a}) + G(\boldsymbol{0})\psi(-\boldsymbol{a}) \right]. \tag{B.34}$$

VIII

One obtains

$$\psi(\boldsymbol{a}) + \psi(-\boldsymbol{a}) = 2 \sum_i^d \cos(q_{0i}a) + \frac{V}{2} \left[G(\boldsymbol{0}) + G(2\boldsymbol{a}) \right] \left[\psi(\boldsymbol{a}) + \psi(-\boldsymbol{a}) \right]$$

$$= \frac{2 \sum_i^d \cos(q_{0i}a)}{1 - \frac{V}{2} \left[G(\boldsymbol{0}) + G(2\boldsymbol{a}) \right]}$$

(B.35)

In the large distance limit the two Green's function reduce to

$$G(\boldsymbol{r} \pm \boldsymbol{a}) \xrightarrow[\boldsymbol{r} \to \infty]{} G(\boldsymbol{r})$$

(B.36)

Inserting equation (B.35) in equation (B.32) leads to

$$\psi(\boldsymbol{r}) = \mathrm{e}^{\mathrm{i}\boldsymbol{q}_0 \cdot \boldsymbol{r}} + \frac{V \sum_i^d \cos(q_{0i}a)}{1 - \frac{V}{2} \left[G(\boldsymbol{0}) + G(2\boldsymbol{a}) \right]} G(\boldsymbol{r}),$$

(B.37)

where the scattering amplitude $f(\boldsymbol{q}, \boldsymbol{q}')$ can be identified as

$$f(\boldsymbol{q}, \boldsymbol{q}') = \frac{V \sum_i^d \cos(q_{0i}a)}{1 - \frac{V}{2} \left[G(\boldsymbol{0}) + G(2\boldsymbol{a}) \right]}.$$

(B.38)

B.4. coupling to a molecular state between the lattice sites:

Two particle interaction in an optical lattice with a resonant coupling to a closed channel, living between the lattice, can be described by the Hamiltonian

$$\hat{\mathrm{H}} = - J \sum_{<i,j>} \left(b_i^\dagger b_j + b_j^\dagger b_i \right)$$

$$+ g \sum_{<i,j>} \left(\hat{b}_i \hat{b}_j \hat{m}_{<i,j>}^\dagger + \hat{b}_i^\dagger \hat{b}_j^\dagger \hat{m}_{<i,j>} \right) - \nu \sum_{<i,j>} \hat{m}_{<i,j>}^\dagger \hat{m}_{<i,j>}$$

(B.39)

In first quantization the problem is captured by a two-channel system, described by a Schrödinger equation system

$$\left[E + 2J\tilde{\Delta}_{\boldsymbol{r}} \right] \psi(\boldsymbol{r}) = g\chi \left(\delta_{\boldsymbol{r},\boldsymbol{a}} + \delta_{\boldsymbol{r},-\boldsymbol{a}} \right)$$

(B.40)

$$\left[E - \nu \right] \chi = g \left(\delta_{\boldsymbol{r},\boldsymbol{a}} + \delta_{\boldsymbol{r},-\boldsymbol{a}} \right) \psi(\boldsymbol{r})$$

(B.41)

with $\psi(\boldsymbol{r})$ describing the two particle atomic state, with the relative coordinate $\boldsymbol{r}$ between the particle and χ describing the molecular state living between the lattice sites. The general solution of the differential equation (B.40) is

$$\psi(\boldsymbol{r}) = \psi_0(\boldsymbol{r}) + g\chi \left[G(\boldsymbol{r} - \boldsymbol{a}) + G(\boldsymbol{r} + \boldsymbol{a}) \right]$$

(B.42)

where $\psi_0(\boldsymbol{r}) = \exp(\mathrm{i}\boldsymbol{q}_0 \cdot \boldsymbol{a})$ is the homogeneous and $g\chi \left[G(\boldsymbol{r} - \boldsymbol{a}) + G(\boldsymbol{r} + \boldsymbol{a}) \right]$ the inhomogeneous solution. Equation (B.42) gives rise to self-consistency equations for $\psi(\boldsymbol{a})$ and $\psi(-\boldsymbol{a})$

$$\psi(\boldsymbol{a}) = \mathrm{e}^{\mathrm{i}\boldsymbol{q}_0 \cdot \boldsymbol{a}} + g\chi \left[G(\boldsymbol{0}) + G(2\boldsymbol{a}) \right]$$

(B.43)

$$\psi(-\boldsymbol{a}) = \mathrm{e}^{-\mathrm{i}\boldsymbol{q}_0 \cdot \boldsymbol{a}} + g\chi \left[G(2\boldsymbol{a}) + G(\boldsymbol{0}) \right],$$

(B.44)

from which follows

$$\psi(\boldsymbol{a}) + \psi(-\boldsymbol{a}) = 2\sum_i^d \cos(q_{0i}a) + 2g\chi\left[G(\boldsymbol{0}) + G(2\boldsymbol{a})\right]. \tag{B.45}$$

Inserting this in equation (B.41) yields

$$\left[E - \nu\right]\chi = 2g\sum_i^d \cos(q_{0i}a) + 2g^2\chi\left[G(\boldsymbol{0}) + G(2\boldsymbol{a})\right]. \tag{B.46}$$

The solution of this self-consistency equation is

$$\chi = \frac{2g\sum_i^d \cos(q_{0i}a)}{E - \nu - 2g^2\left[G(\boldsymbol{0}) + G(2\boldsymbol{a})\right]}. \tag{B.47}$$

The final result for $\psi(\boldsymbol{r})$

$$\psi(\boldsymbol{r}) = e^{i\boldsymbol{q}_0\cdot\boldsymbol{r}} + \frac{4g^2\sum_i^d \cos(q_{0i}a)}{E - \nu - 2g^2\left[G(\boldsymbol{0}) + G(2\boldsymbol{a})\right]}G(\boldsymbol{r}). \tag{B.48}$$

In the limit of a wide resonant coupling, i.e. $g \to \infty$, $\nu \to \infty$ and $g^2/\nu \to$ const. one obtains

$$\psi(\boldsymbol{r}) = e^{i\boldsymbol{q}_0\cdot\boldsymbol{r}} + \frac{-\frac{4g^2}{\nu}\sum_i^d \cos(q_{0i}a)}{1 + \frac{2g^2}{\nu}\left[G(\boldsymbol{0}) + G(2\boldsymbol{a})\right]}G(\boldsymbol{r}), \tag{B.49}$$

with the scattering amplitude

$$f(\boldsymbol{q}, \boldsymbol{q}') = \frac{-\frac{4g^2}{\nu}\sum_i^d \cos(q_{0i}a)}{1 + \frac{2g^2}{\nu}\left[G(\boldsymbol{0}) + G(2\boldsymbol{a})\right]}. \tag{B.50}$$

The Comparison with equation (B.38) leads to an effective nearest neighbour interaction parameter

$$V_{\text{eff}} = -\frac{4g^2}{\nu} \tag{B.51}$$

B.5. on-site and nearest neighbour interaction:

The two particle problem with on-site and nearest neighbour interaction in an optical lattice is in second quantization described by the extended Bose Hubbard Hamiltonian

$$\hat{H} - J\sum_{<i,j>}\left(b_i^\dagger b_j + b_j^\dagger b_i\right) + \frac{U}{2}\sum_i \hat{n}_i\left(\hat{n}_i - 1\right) + \frac{V}{2}\sum_{<i,j>}\hat{n}_i\hat{n}_j. \tag{B.52}$$

The problem is described in frist quantization by the Schrödinger equation

$$\left[E + 2J\tilde{\Delta}_{\boldsymbol{r}}^{\boldsymbol{Q}}\right]\psi(\boldsymbol{r}) = \left[U\delta_{\boldsymbol{r},\boldsymbol{0}} + \frac{V}{2}\left(\delta_{\boldsymbol{r},\boldsymbol{a}} + \delta_{\boldsymbol{r},-\boldsymbol{a}}\right)\right]\psi(\boldsymbol{r}). \tag{B.53}$$

X

B.6. on-site interaction and coupling to a molecular state on the lattice sites:

The solution of $\psi(\boldsymbol{r})$ can be found with the help of the Lippmann-Schwinger equation

$$
\begin{aligned}
\psi\left(\boldsymbol{r}\right) &= \mathrm{e}^{\mathrm{i}\boldsymbol{q}_0\cdot\boldsymbol{r}} + \sum_{\boldsymbol{r}'} G(\boldsymbol{r}-\boldsymbol{r}') \left[U\delta_{\boldsymbol{r},\boldsymbol{0}} + \frac{V}{2}\left(\delta_{\boldsymbol{r},\boldsymbol{a}}+\delta_{\boldsymbol{r},-\boldsymbol{a}}\right)\right]\psi(\boldsymbol{r}') \\
&= \mathrm{e}^{\mathrm{i}\boldsymbol{q}_0\cdot\boldsymbol{r}} + G(\boldsymbol{r})U\psi(\boldsymbol{0}) + \frac{V}{2}\left[G(\boldsymbol{r}-\boldsymbol{a})\psi(\boldsymbol{a})+G(\boldsymbol{r}+\boldsymbol{a})\psi(-\boldsymbol{a})\right].
\end{aligned}
\tag{B.54}
$$

It is necessary to solve the self-consistency equations for $\psi(\boldsymbol{0})$, $\psi(\boldsymbol{a})$ and $\psi(-\boldsymbol{a})$

$$
\psi(\boldsymbol{0}) = 1 + G(\boldsymbol{0})U\psi(\boldsymbol{0}) + \frac{V}{2}G(\boldsymbol{a})\left[\psi(\boldsymbol{a})+\psi(-\boldsymbol{a})\right]
\tag{B.55}
$$

$$
\psi(\boldsymbol{a}) = \mathrm{e}^{\mathrm{i}\boldsymbol{q}_0\cdot\boldsymbol{a}} + G(\boldsymbol{a})U\psi(\boldsymbol{0}) + \frac{V}{2}\left[G(\boldsymbol{0})\psi(\boldsymbol{a})+G(2\boldsymbol{a})\psi(-\boldsymbol{a})\right]
\tag{B.56}
$$

$$
\psi(-\boldsymbol{a}) = \mathrm{e}^{-\mathrm{i}\boldsymbol{q}_0\cdot\boldsymbol{a}} + G(\boldsymbol{a})U\psi(\boldsymbol{0}) + \frac{V}{2}\left[G(2\boldsymbol{a})\psi(\boldsymbol{a})+G(\boldsymbol{0})\psi(-\boldsymbol{a})\right].
\tag{B.57}
$$

One obtains

$$
\psi(\boldsymbol{0}) = \frac{1}{1-UG(\boldsymbol{0})} + \frac{1}{2}\frac{VG(\boldsymbol{a})\left[\psi(\boldsymbol{a})+\psi(-\boldsymbol{a})\right]}{1-UG(\boldsymbol{0})}
\tag{B.58}
$$

and

$$
\begin{aligned}
\psi(\boldsymbol{a})+\psi(-\boldsymbol{a}) &= 2\sum_i^d \cos\left(q_{0i}a\right) + 2G(\boldsymbol{a})U\psi(\boldsymbol{0}) + \frac{V}{2}\left[G(\boldsymbol{0})+G(2\boldsymbol{a})\right]\left[\psi(\boldsymbol{a})+\psi(-\boldsymbol{a})\right] \\
&= 2\sum_i^d \cos\left(q_{0i}a\right) + \frac{2G(\boldsymbol{a})U}{1-UG(\boldsymbol{0})} + \frac{UVG^2(\boldsymbol{a})\left[\psi(\boldsymbol{a})+\psi(-\boldsymbol{a})\right]}{1-UG(\boldsymbol{0})} \\
&\quad + \frac{V}{2}\left[G(\boldsymbol{0})+G(2\boldsymbol{a})\right]\left[\psi(\boldsymbol{a})+\psi(-\boldsymbol{a})\right] \\
&= \frac{2\sum_i^d \cos\left(q_{0i}a\right) + \frac{2G(\boldsymbol{a})U}{1-UG(\boldsymbol{0})}}{1 - \frac{UVG^2(\boldsymbol{a})}{1-UG(\boldsymbol{0})} - \frac{V}{2}\left[G(\boldsymbol{0})+G(2\boldsymbol{a})\right]}.
\end{aligned}
\tag{B.59}
$$

The final result for $\psi(\boldsymbol{r})$ is

$$
\begin{aligned}
\psi\left(\boldsymbol{r}\right) &= \mathrm{e}^{\mathrm{i}\boldsymbol{q}_0\cdot\boldsymbol{r}} + \frac{U}{1-UG(\boldsymbol{0})}G(\boldsymbol{r}) \\
&\quad + \left[\frac{UG(\boldsymbol{a})}{1-UG(\boldsymbol{0})}+1\right]\frac{V\sum_i^d \cos\left(q_{0i}a\right) + \frac{G(\boldsymbol{a})UV}{1-UG(\boldsymbol{0})}}{1 - \frac{UVG^2(\boldsymbol{a})}{1-UG(\boldsymbol{0})} - \frac{V}{2}\left[G(\boldsymbol{0})+G(2\boldsymbol{a})\right]}G(\boldsymbol{r})
\end{aligned}
\tag{B.60}
$$

B.6. on-site interaction and coupling to a molecular state on the lattice sites:

The two particle scattering problem in an optical lattice with on-site interaction and additional Feshbach resonance with a molecular state, living on the lattice sites, can be

B. Two particle scattering in an optical lattice

described in second quantization with the Hamiltonian

$$\hat{H} = -J \sum_{<i,j>} \left(b_i^\dagger b_j + b_j^\dagger b_i \right) + \frac{U}{2} \sum_i \hat{n}_i \left(\hat{n}_i - 1 \right)$$
$$+ g \sum_i \left(\hat{b}_i \hat{b}_i \hat{m}_i^\dagger + \hat{b}_i^\dagger \hat{b}_i^\dagger \hat{m}_i \right) - \nu \sum_i \hat{m}_i^\dagger \hat{m}_i. \tag{B.61}$$

In first quantization the problem is captured by a two channel system, described by the Schrödinger equation system

$$\left[E + 2J\tilde{\Delta}_{\boldsymbol{r}} \right] \psi(\boldsymbol{r}) = U\delta_{\boldsymbol{r},\boldsymbol{0}} + g\chi\delta_{\boldsymbol{r},\boldsymbol{0}} \tag{B.62}$$

$$[E - \nu]\chi = g\psi(\boldsymbol{r})\delta_{\boldsymbol{r},\boldsymbol{0}}, \tag{B.63}$$

with $\psi(\boldsymbol{r})$ describing the two particle atomic state, with the relative coordinate $\boldsymbol{r}$ between the particle and χ describing the molecular state living on the lattice sites. The general solution of the differential equation (B.62) is

$$\psi(\boldsymbol{r}) = \psi_0(\boldsymbol{r}) + G(\boldsymbol{r})U\psi(\boldsymbol{0}) + g\chi G(\boldsymbol{r}) \tag{B.64}$$

where $\psi_0(\boldsymbol{r}) = \exp\left(\mathrm{i}\boldsymbol{q}_0 \cdot \boldsymbol{a}\right)$ is the homogeneous and $G(\boldsymbol{r})U\psi(\boldsymbol{0}) + g\chi G(\boldsymbol{r})$ the inhomogeneous solution. Equation (B.64) gives rise to self-consistency equations for $\psi(\boldsymbol{0})$.

$$\psi(\boldsymbol{0}) = 1 + G(\boldsymbol{0})U\psi(\boldsymbol{0}) + g\chi G(\boldsymbol{0})$$
$$= \frac{1 + g\chi G(\boldsymbol{0})}{1 - G(\boldsymbol{0})U} \tag{B.65}$$

Inserting this in equation (B.63) gives rise to a self-consistency equation for the molecular state χ.

$$[E - \nu]\chi = \frac{g + g^2\chi G(\boldsymbol{0})}{1 - G(\boldsymbol{0})U}. \tag{B.66}$$

Rewritting leads to

$$\chi = \frac{\frac{g}{1 - G(\boldsymbol{0})U}}{E - \nu - \frac{g^2 G(\boldsymbol{0})}{1 - G(\boldsymbol{0})U}}. \tag{B.67}$$

The final result for $\psi(\boldsymbol{r})$ is

$$\psi(\boldsymbol{r}) = \mathrm{e}^{\mathrm{i}\boldsymbol{q}_0 \cdot \boldsymbol{r}} + \frac{U}{1 - G(\boldsymbol{0})U}G(\boldsymbol{r}) + g\chi \frac{UG(\boldsymbol{0})}{1 - G(\boldsymbol{0})U}G(\boldsymbol{r}) + g\chi G(\boldsymbol{r})$$

$$= \mathrm{e}^{\mathrm{i}\boldsymbol{q}_0 \cdot \boldsymbol{r}} + \frac{U}{1 - G(\boldsymbol{0})U}G(\boldsymbol{r}) + \left[\frac{UG(\boldsymbol{0})}{1 - G(\boldsymbol{0})U} + 1 \right] \frac{\frac{g^2}{1 - G(\boldsymbol{0})U}}{E - \nu - \frac{g^2 G(\boldsymbol{0})}{1 - G(\boldsymbol{0})U}}G(\boldsymbol{r}) \tag{B.68}$$

$$= \mathrm{e}^{\mathrm{i}\boldsymbol{q}_0 \cdot \boldsymbol{r}} + \frac{U}{1 - G(\boldsymbol{0})U}G(\boldsymbol{r}) + \frac{\frac{g^2}{(1 - G(\boldsymbol{0})U)^2}}{E - \nu - \frac{g^2 G(\boldsymbol{0})}{1 - G(\boldsymbol{0})U}}G(\boldsymbol{r}).$$

B.7. on-site interaction and coupling to a molecular state between the lattice sites:

The two particle scattering problem in an optical lattice with on-site interaction and additional Feshbach resonance with a molecular state, living between the lattice sites, can be described in second quantization with the Hamiltonian

$$
\hat{H} = - J \sum_{<i,j>} \left(b_i^\dagger b_j + b_j^\dagger b_i \right) + \frac{U}{2} \sum_i \hat{n}_i \left(\hat{n}_i - 1 \right)
$$
$$
+ g \sum_{<i,j>} \left(\hat{b}_i \hat{b}_j \hat{m}_{<i,j>}^\dagger + \hat{b}_i^\dagger \hat{b}_j^\dagger \hat{m}_{<i,j>} \right) - \nu \sum_{<i,j>} \hat{m}_{<i,j>}^\dagger \hat{m}_{<i,j>}
\tag{B.69}
$$

In first quantization the problem is captured by a two channel system, described by the Schrödinger equation system

$$
\left[E + 2J \tilde{\Delta}_{\boldsymbol{r}} \right] \psi(\boldsymbol{r}) = U \delta_{\boldsymbol{r},\boldsymbol{0}} + g\chi \left(\delta_{\boldsymbol{r},\boldsymbol{a}} + \delta_{\boldsymbol{r},-\boldsymbol{a}} \right)
\tag{B.70}
$$
$$
\left[E - \nu \right] \chi = g\psi(\boldsymbol{r}) \left(\delta_{\boldsymbol{r},\boldsymbol{a}} + \delta_{\boldsymbol{r},-\boldsymbol{a}} \right) .
\tag{B.71}
$$

with $\psi(\boldsymbol{r})$ describing the two particle atomic state, with the relative coordinate $\boldsymbol{r}$ between the particle and χ describing the molecular state, living between the lattice sites. The general solution of the differential equation (B.62) is

$$
\psi(\boldsymbol{r}) = \psi_0(\boldsymbol{r}) + G(\boldsymbol{r})U\psi(\boldsymbol{0}) + g\chi \left[G(\boldsymbol{r} - \boldsymbol{a}) + G(\boldsymbol{r} + \boldsymbol{a}) \right]
\tag{B.72}
$$

where $\psi_0(\boldsymbol{r}) = \exp\left(i\boldsymbol{q}_0 \cdot \boldsymbol{a} \right)$ is the homogeneous and
$G(\boldsymbol{r})U\psi(\boldsymbol{0}) + g\chi \left[G(\boldsymbol{r} - \boldsymbol{a}) + G(\boldsymbol{r} + \boldsymbol{a}) \right]$ the inhomogeneous solution. Equation (B.72) gives rise to self-consistency equations for $\psi(\boldsymbol{0})$, $\psi(\boldsymbol{a})$ and $\psi(-\boldsymbol{a})$.

$$
\psi(\boldsymbol{0}) = 1 + G(\boldsymbol{0})U\psi(\boldsymbol{0}) + 2g\chi G(\boldsymbol{a})
\tag{B.73}
$$
$$
\psi(\boldsymbol{a}) = e^{i\boldsymbol{q}_0 \cdot \boldsymbol{a}} + G(\boldsymbol{0})U\psi(\boldsymbol{0}) + g\chi \left[G(\boldsymbol{0}) + G(2\boldsymbol{a}) \right]
\tag{B.74}
$$
$$
\psi(-\boldsymbol{a}) = e^{-i\boldsymbol{q}_0 \cdot \boldsymbol{a}} + G(\boldsymbol{0})U\psi(\boldsymbol{0}) + g\chi \left[G(2\boldsymbol{a}) + G(\boldsymbol{0}) \right] .
\tag{B.75}
$$

One obtains

$$
\psi(\boldsymbol{0}) = \frac{1 + 2g\chi G(\boldsymbol{a})}{1 - G(\boldsymbol{0})U}
\tag{B.76}
$$

and

$$
\psi(\boldsymbol{a}) + \psi(-\boldsymbol{a}) = 2 \sum_i^d \cos\left(q_{0i}a \right) + 2G(\boldsymbol{0})U \frac{1 + 2g\chi G(\boldsymbol{a})}{1 - G(\boldsymbol{0})U} + 2g\chi \left[G(2\boldsymbol{a}) + G(\boldsymbol{0}) \right]
\tag{B.77}
$$

Inserting this in equation (B.71) gives rise to a self-consistency equation for the molecular state χ

$$
\left[E - \nu \right] \chi = 2g \sum_i^d \cos\left(q_{0i}a \right) + 2G(\boldsymbol{0})U \frac{g + 2g^2\chi G(\boldsymbol{a})}{1 - G(\boldsymbol{0})U} + 2g^2\chi \left[G(2\boldsymbol{a}) + G(\boldsymbol{0}) \right] .
\tag{B.78}
$$

B. Two particle scattering in an optical lattice

Rewritting equation (B.78) leads to

$$\chi = \frac{2g \sum_i^d \cos(q_{0i}a) + \frac{2gG(\mathbf{0})U}{1-G(\mathbf{0})U}}{E - \nu - 2g^2 [G(2\mathbf{a}) + G(\mathbf{0})] - \frac{2g^2 G(\mathbf{a})}{1-G(\mathbf{0})U}}. \tag{B.79}$$

The final result for $\psi(\mathbf{r})$ is

$$\psi(\mathbf{r}) = \mathrm{e}^{\mathrm{i}\mathbf{q}_0 \cdot \mathbf{r}} + \frac{U}{1 - G(\mathbf{0})U}G(\mathbf{r}) +$$

$$+ \left[\frac{UG(\mathbf{a})}{1 - G(\mathbf{0})U} + 1\right] \frac{4g^2 \sum_i^d \cos(q_{0i}a) + \frac{4g^2 G(\mathbf{0})U}{1-G(\mathbf{0})U}}{E - \nu - 2g^2 [G(2\mathbf{a}) + G(\mathbf{0})] - \frac{2g^2 G(\mathbf{a})}{1-G(\mathbf{0})U}}G(\mathbf{r}). \tag{B.80}$$

C. The behaviour of reciprocal Green's function

As shown in figure [fig. C.1] and [fig. C.2] the reciprocal Green's function $1/G(E,0)$ can be approximated by $E - 12J + \xi$. For a center of mass quasi-momentum $\boldsymbol{Q} = 0$ the error ξ takes its largest value and gets better with increasing $\boldsymbol{Q} \to \pi/a$.
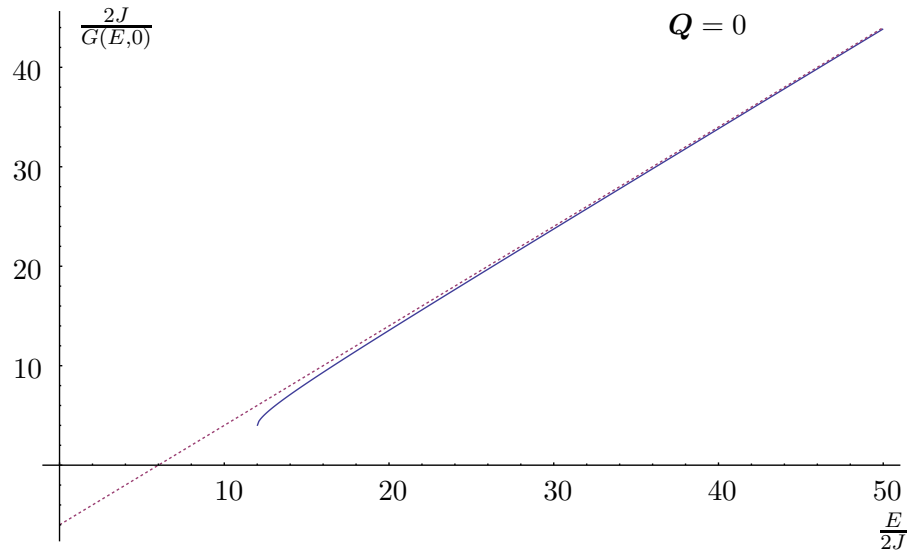
Figure C.1.: This figure shows the course of the reduced reciprocal Green's function $2J/G(E,0)$ with the reduced energy $E/2J$ for a center of mass quasimomentum $\mathbf{Q} = 0$. The function $E/2J - 6$ (dashed line) is a very good approximation for energies $E/2J > 12$. The error ξ for energies $E/2J < 30$ is marginal.
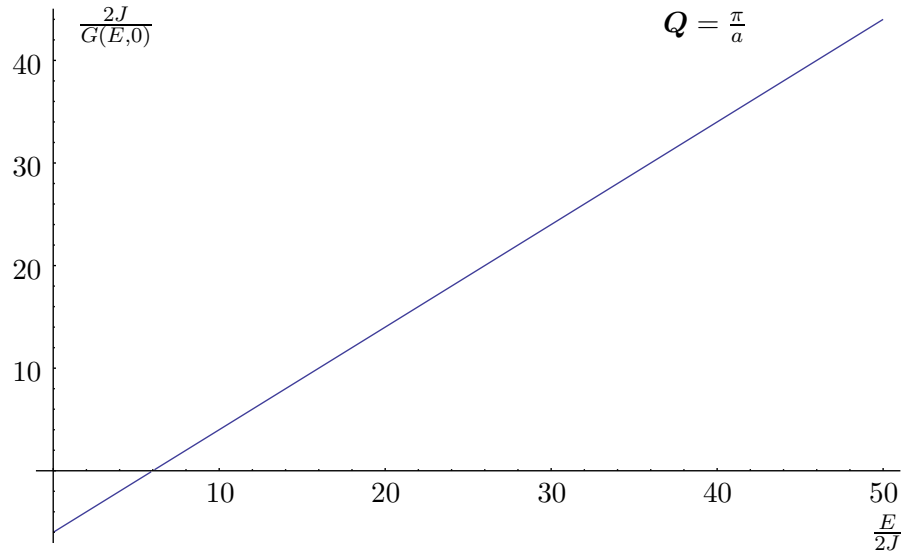

Figure C.2.: This figure shows the course of the reduced reciprocal Green's function $2J/G(E,0)$ with the reduced energy $E/2J$ for a center of mass quasimomentum $\mathbf{Q} = \pi/a$. It is exact $E/2J - 6$ and defined for all energies $E/2J$.1

Bibliography

[1] Matthew P. A. Fisher, Peter B. Weichman, G. Grinstein, and Daniel S. Fisher. Boson localization and the superfluid-insulator transition. *Phys. Rev. B*, 40(1):546–570, Jul 1989.

[2] Werner Krauth, Michel Caffarel, and Jean-Philippe Bouchaud. Gutzwiller wave function for a model of strongly interacting bosons. *Phys. Rev. B*, 45(6):3137–3140, Feb 1992.

[3] Arno P. Kampf and Gergely T. Zimanyi. Superconductor-insulator phase transition in the boson hubbard model. *Phys. Rev. B*, 47(1):279–286, Jan 1993.

[4] C. Bruder, Rosario Fazio, and Gerd Schön. Superconductor–mott-insulator transition in bose systems with finite-range interactions. *Phys. Rev. B*, 47(1):342–347, Jan 1993.

[5] D. Jaksch, C. Bruder, J. I. Cirac, C. W. Gardiner, and P. Zoller. Cold bosonic atoms in optical lattices. *Phys. Rev. Lett.*, 81(15):3108–3111, Oct 1998.

[6] F. A. van Abeelen and B. J. Verhaar. Time-dependent feshbach resonance scattering and anomalous decay of a na bose-einstein condensate. *Phys. Rev. Lett.*, 83(8):1550–1553, Aug 1999.

[7] G. Raithel, G. Birkl, A. Kastberg, W. D. Phillips, and S. L. Rolston. Cooling and localization dynamics in optical lattices. *Phys. Rev. Lett.*, 78(4):630–633, Jan 1997.

[8] K. Winkler, G. Thalhammer, F. Lang, R. Grimm, J. Hecker Denschlag, A. J. Daley, A. Kantian, H. P. Büchler, and P. Zoller. Repulsively bound atom pairs in an optical lattice. *Nature*, 441:853–856, June 2006.

[9] L. Dang, M. Boninsegni, and L. Pollet. Vacancy supersolid of hard-core bosons on the square lattice. *Physical Review B (Condensed Matter and Materials Physics)*, 78(13):132512, 2008.

[10] S. Inouye, M. R. Andrews, J. Stenger, H.-J. Miesner, D. M. Stamper-Kurn, and W. Ketterle. Observation of feshbach resonances in a bose‚Äìeinstein condensate. *Nature*, 392:151–154, March 1998.

[11] E. A. Donley, N. R. Claussen, S. T. Thompson, and C. E. Wieman. Atom‚Äìmolecule coherence in a bose‚Äìeinstein condensate. *Nature*, 417:529–533, May 2002.

Bibliography

[12] K. Dieckmann, C. A. Stan, S. Gupta, Z. Hadzibabic, C. H. Schunck, and W. Ketterle. Decay of an ultracold fermionic lithium gas near a feshbach resonance. *Phys. Rev. Lett.*, 89(20):203201, Oct 2002.

[13] P. O. Fedichev, M. J. Bijlsma, and P. Zoller. Extended molecules and geometric scattering resonances in optical lattices. *Phys. Rev. Lett.*, 92(8):080401, Feb 2004.

[14] Pinaki Sengupta, Leonid P. Pryadko, Fabien Alet, Matthias Troyer, and Guido Schmid. Supersolids versus phase separation in two-dimensional lattice bosons. *Phys. Rev. Lett.*, 94(20):207202, May 2005.

[15] Daniel S. Rokhsar and Steven A. Kivelson. Superconductivity and the quantum hard-core dimer gas. *Phys. Rev. Lett.*, 61(20):2376–2379, Nov 1988.

[16] A. Ralko, D. Poilblanc, and R. Moessner. Generic mixed columnar-plaquette phases in rokhsar-kivelson models. *Physical Review Letters*, 100(3):037201, 2008.

[17] Olav F. Syljuåsen. Plaquette phase of the square-lattice quantum dimer model: Quantum monte carlo calculations. *Physical Review B (Condensed Matter and Materials Physics)*, 73(24):245105, 2006.

[18] Subir Sachdev. Spin-peierls ground states of the quantum dimer model: A finite-size study. *Phys. Rev. B*, 40(7):5204–5207, Sep 1989.

[19] P. W. Leung, K. C. Chiu, and Karl J. Runge. Columnar dimer and plaquette resonating-valence-bond orders in the quantum dimer model. *Phys. Rev. B*, 54(18):12938–12945, Nov 1996.

[20] R. Moessner, S. L. Sondhi, and P. Chandra. Phase diagram of the hexagonal lattice quantum dimer model. *Phys. Rev. B*, 64(14):144416, Sep 2001.

Acknowledgements

First of all, I want to thank Prof. Dr. Büchler, who gave me the opportunity to join is group and write this thesis. In addition, I want to thank him for having an open ear all time, his help for problems and his patience. I enjoyed the working atmosphere very much.

I would like to thank Prof. Dr. Weiß for writing the second report on my thesis.

Furthermore I have to thank Prof. Dr. Muramatsu for accepting me and providing good working conditions at his institute. A special thanks goes to Torsten Schwidder, who helped me a lot during my studies at the university and especially at the lab courses.

My room mate Steffen Müller had to sustain lots of question and he always tried to answer them. Thank you for that.

I am also very grateful to my parents Herbert and Sigrun Janisch to allowing me do my studies in the past years. It would not have been possible, without their support.

Of course, I have to thank all other members of the Third Institut of Theoretical Physics: Thorsten Beck, Lars Bonnes, Adam Bühler, Jürgen Falb, Jan Gukelberger, Andreas Hehn, Zi Yang Meng, Alexander Moreno, Ildiko Poljak, Hendrik Weimer and PD Dr. Stefan Wessel, and the former members Ferdinand Albrecht, Prof. Dr. Marcello Barbosa da Silva Neto and Thomas Fabritius.

Last but not least, i am very grateful to my love Andreea. Thank you for your love, care and support. I'm so glad, that you exist.